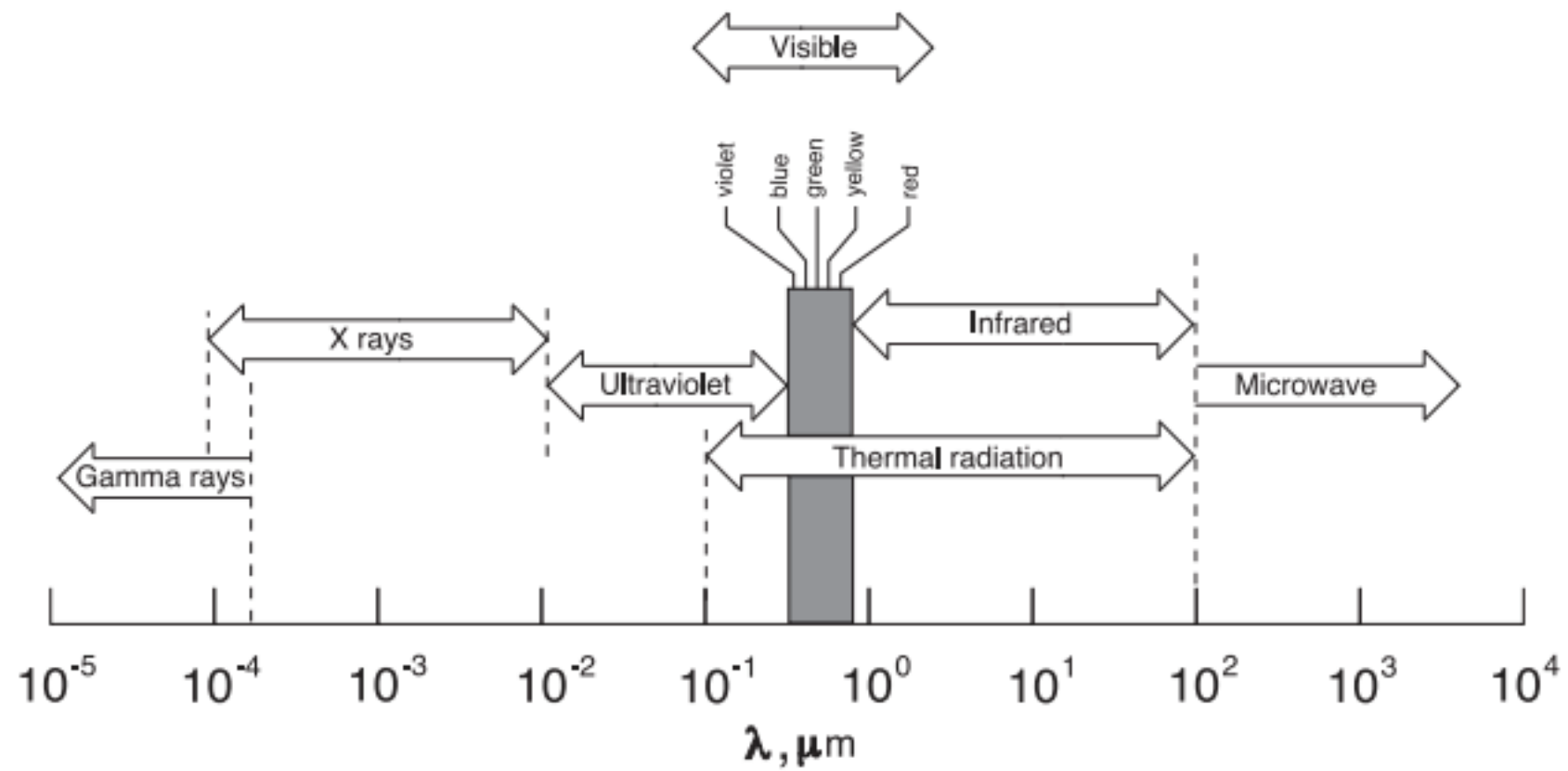


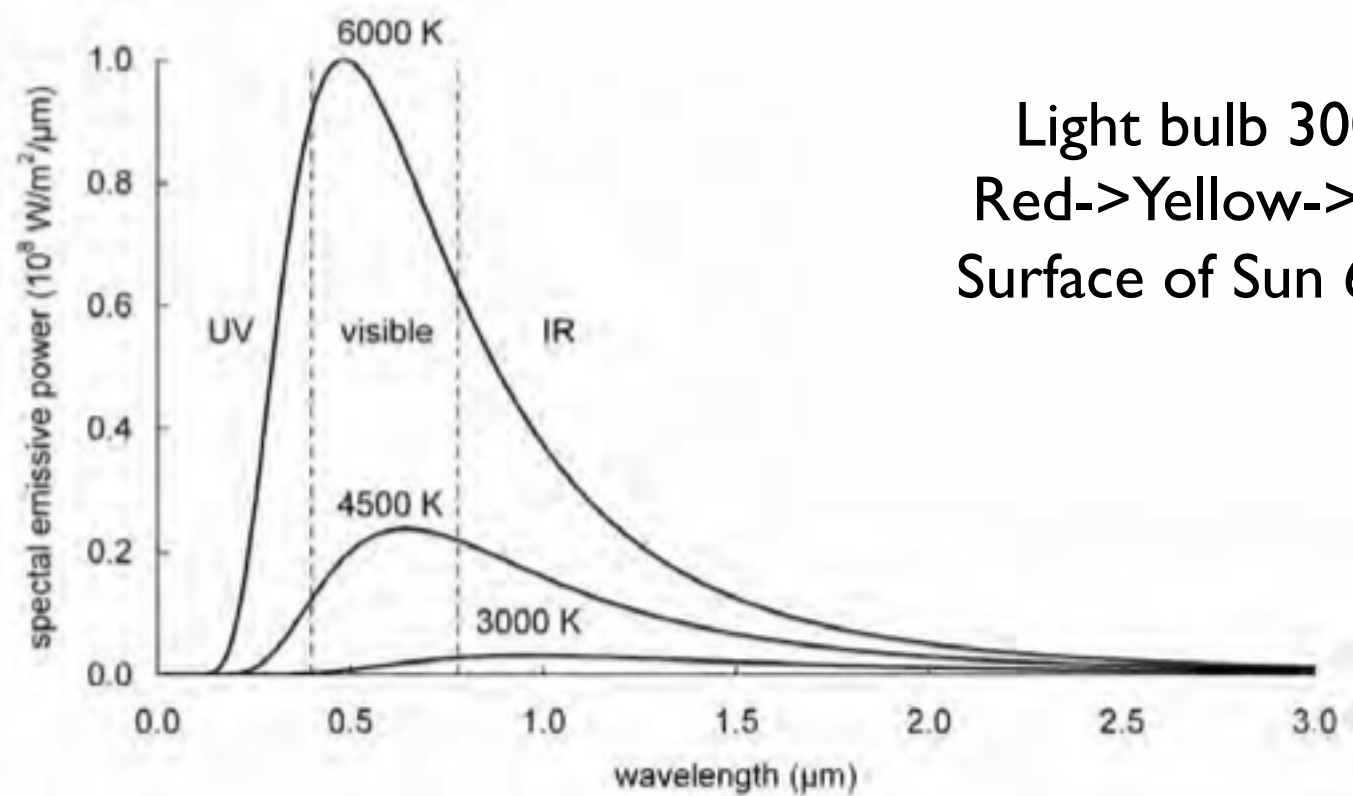
Solar Spectrum



Solar Spectrum

-Black body radiation

$$E(\lambda, T) = \frac{2\pi hc^2}{\lambda^5 [\exp(hc/(\lambda kT)) - 1]}$$



Light bulb 3000°K
Red->Yellow->White
Surface of Sun 6000°K

Figure 1.1. Radiation distributions from perfect blackbodies at three different temperatures, as would be observed at the surface of the blackbodies.

Solar Spectrum

$$E_b = \sigma T^4 \quad [W/m^2] \quad \Leftarrow \text{Stefan-Boltzmann law}$$

where

$$\sigma = \text{Stefan-Boltzmann constant} = 5.67 \times 10^{-8} \text{ W}/(m^2 \cdot K^4)$$

and the temperature T is given in K .

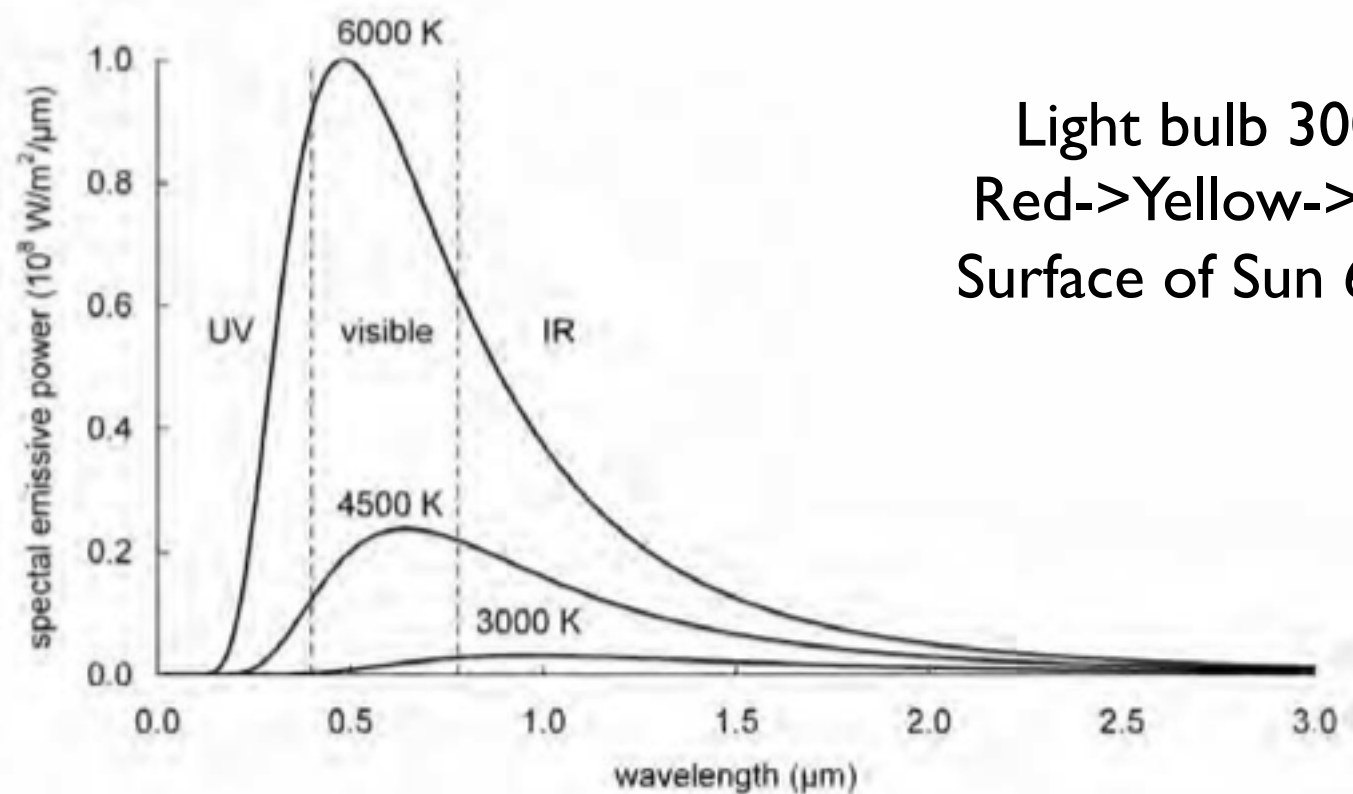
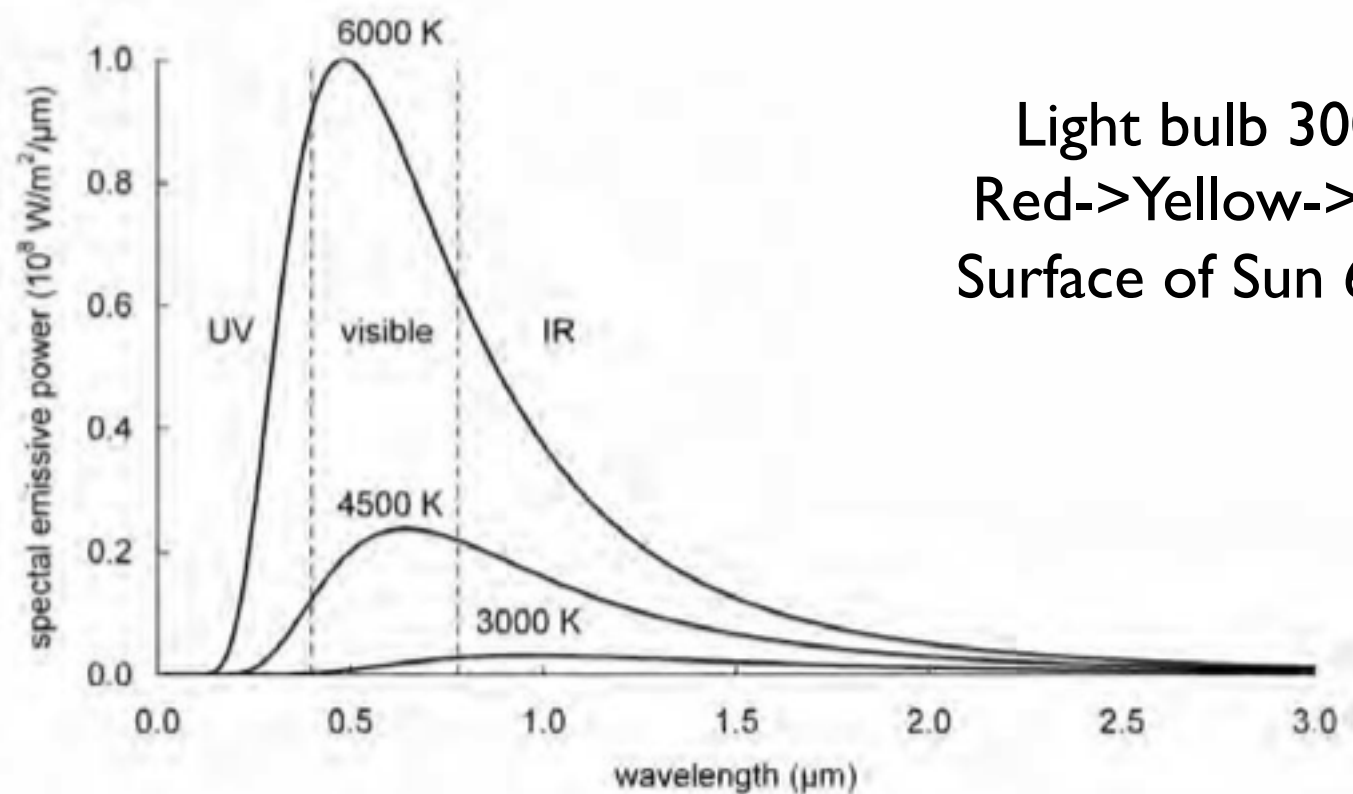


Figure 1.1. Radiation distributions from perfect blackbodies at three different temperatures, as would be observed at the surface of the blackbodies.

Solar Spectrum

The wavelength at which the peak emissive power occurs for a given temperature can be obtained from *Wien's displacement law*

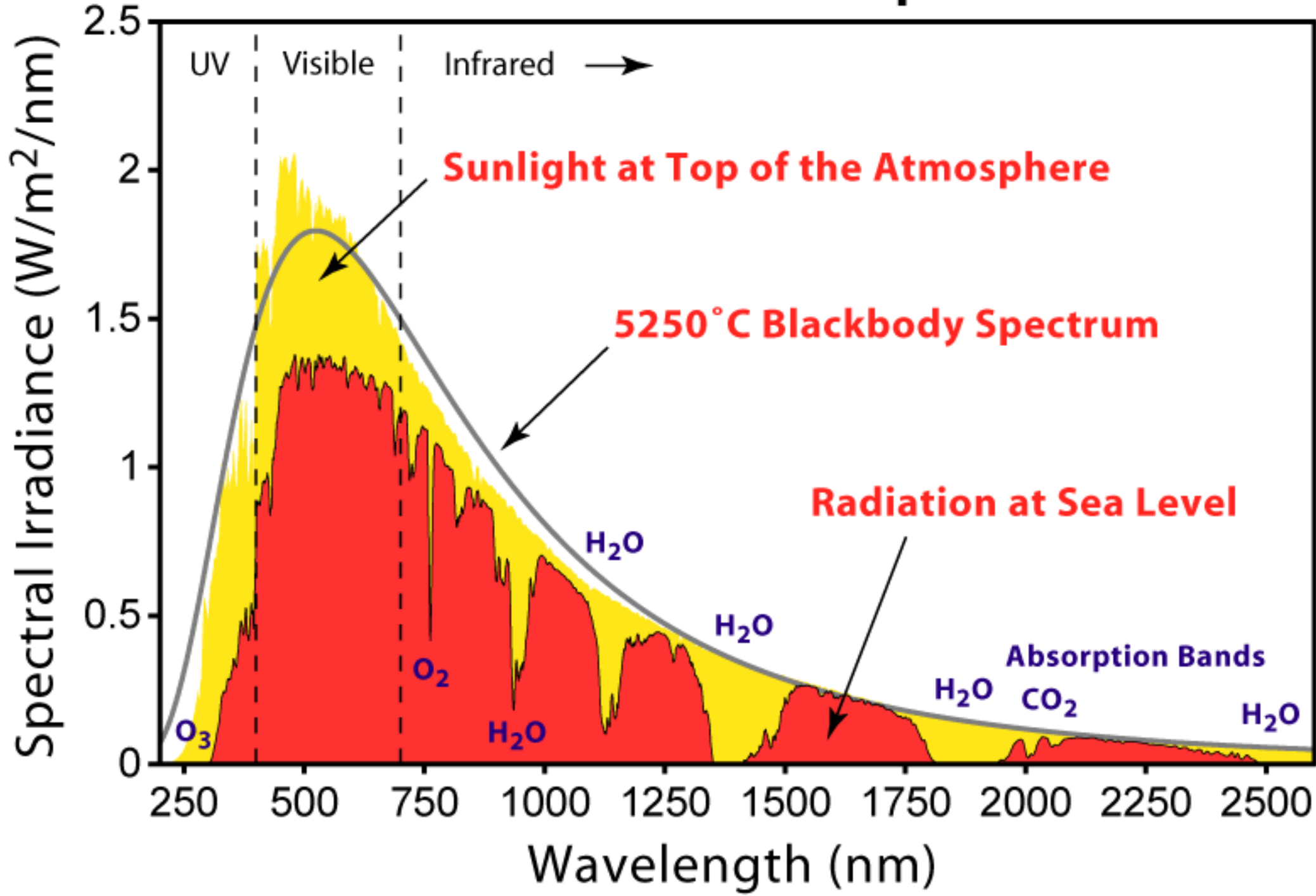
$$(\lambda T)_{max\ power} = 2897.8\ \mu m \cdot K$$



Light bulb 3000°K
Red->Yellow->White
Surface of Sun 6000°K

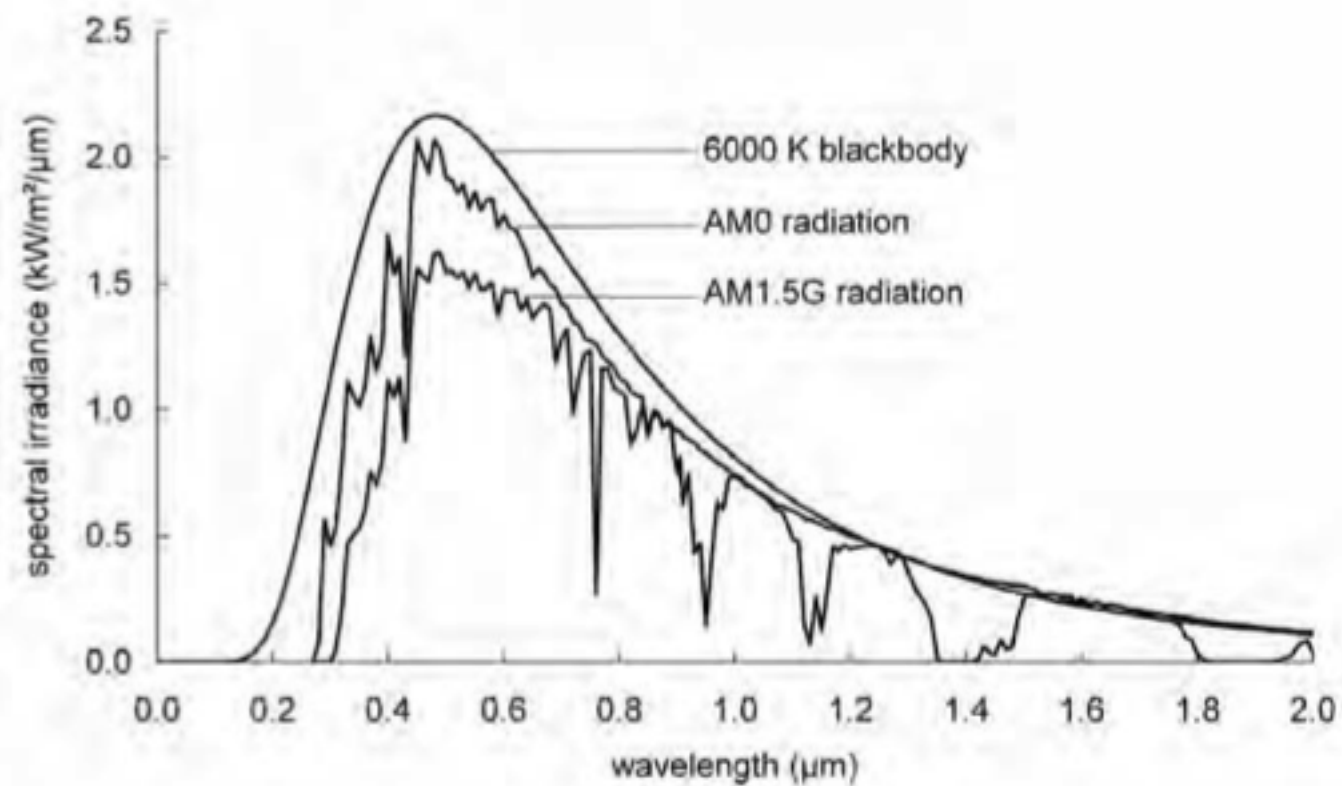
Figure 1.1. Radiation distributions from perfect blackbodies at three different temperatures, as would be observed at the surface of the blackbodies.

Solar Radiation Spectrum



Solar Spectrum

-Atmospheric Absorption and Scattering



Light bulb 3000°K
Red->Yellow->White
Surface of Sun 6000°K

Figure 1.3. The spectral irradiance from a blackbody at 6000 K (at the same apparent diameter as the sun when viewed from earth); from the sun's photosphere as observed just outside earth's atmosphere (AM0); and from the sun's photosphere after having passed through 1.5 times the thickness of earth's atmosphere (AM1.5G).

Solar Spectrum

-Atmospheric Absorption and Scattering

Air Mass through which solar radiation passes

$$AM = 1/\cos \varphi$$

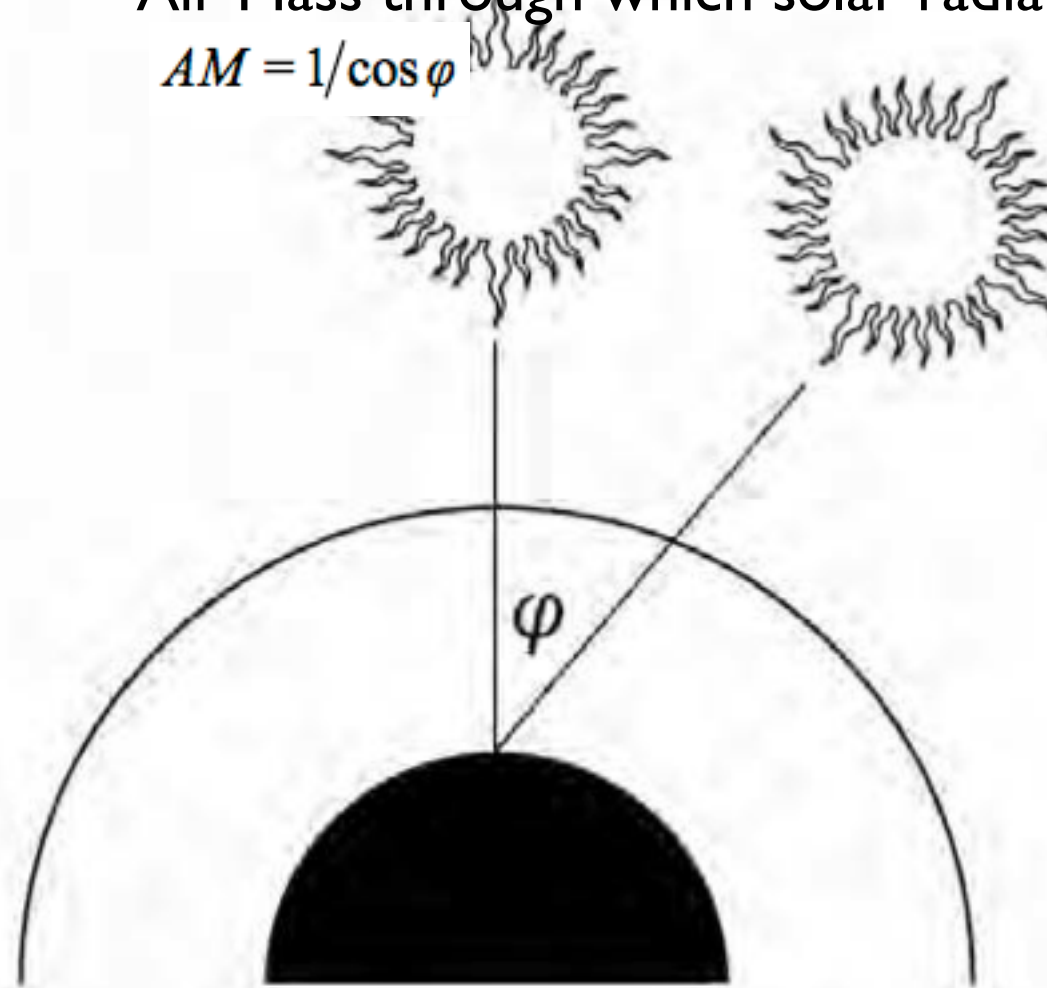


Figure 1.4. The amount of atmosphere (air mass) through which radiation from the sun must pass to reach the earth's surface depends on the sun's position.

Solar Spectrum

When $\varphi = 0$, the Air Mass equals 1 or 'AM1' radiation is being received; when $\varphi = 60^\circ$, the Air Mass equals 2 or 'AM2' conditions prevail. AM1.5 (equivalent to a sun angle of 48.2° from overhead) has become the standard for photovoltaic work.

-Atmospheric Absorption and Scattering

Air Mass through which solar radiation passes

$$AM = 1/\cos \varphi$$

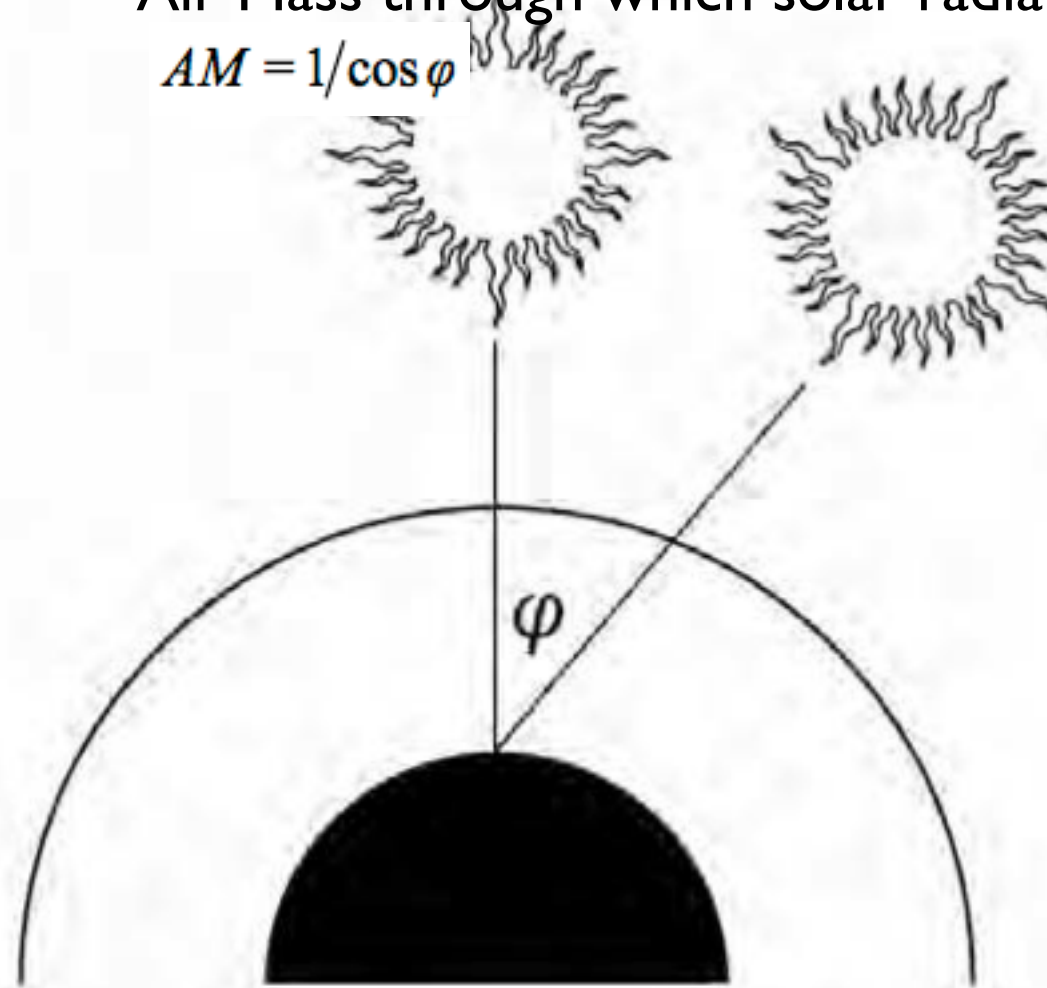


Figure 1.4. The amount of atmosphere (air mass) through which radiation from the sun must pass to reach the earth's surface depends on the sun's position.

The Air Mass (AM) can be estimated at any location using the following formula:

$$AM = \sqrt{1 + (s/h)^2} \quad (1.4)$$

where s is the length of the shadow cast by a vertical post of height h , as shown in

$$\gamma = 1.3661 \text{ kW/m}^2 \quad (1.5)$$

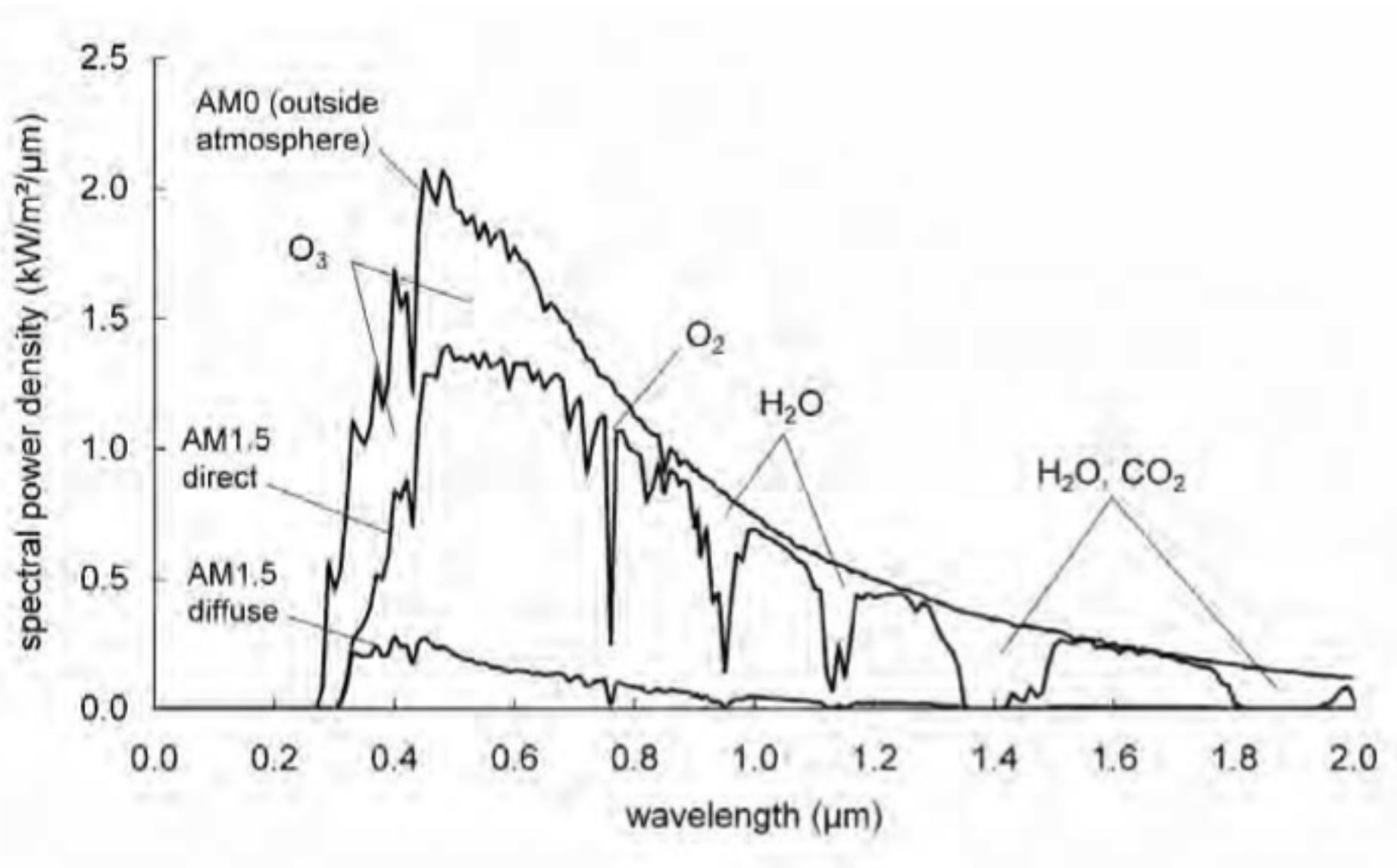


Figure 1.6. The spectral power density of sunlight, outside the atmosphere (AM0) and at the earth's surface (AM1.5), showing absorption from various atmospheric components.

The Air Mass (AM) can be estimated at any location using the following formula:

$$AM = \sqrt{1 + (s/h)^2} \quad (1.4)$$

where s is the length of the shadow cast by a vertical post of height h , as shown in Fig. 1.5.

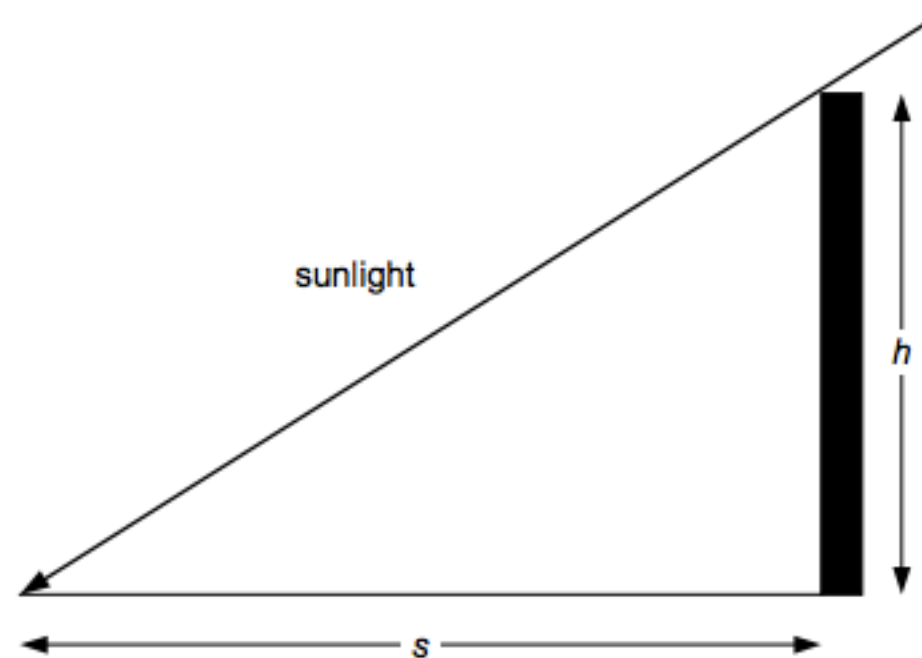


Figure 1.5. Calculation of Air Mass using the shadow of an object of known height.

where k is Boltzmann's constant and E has dimensions of power per unit area per unit wavelength. The total emissive power, expressed in power per unit area, may be found by integration of Eqn. (1.2) over all possible wavelengths from zero to infinity, yielding $E = \sigma T^4$, where σ is the Stefan-Boltzmann constant (Incropera & DeWitt, 2002).

$$\gamma = 1.3661 \text{ kW/m}^2 \quad (1.5)$$

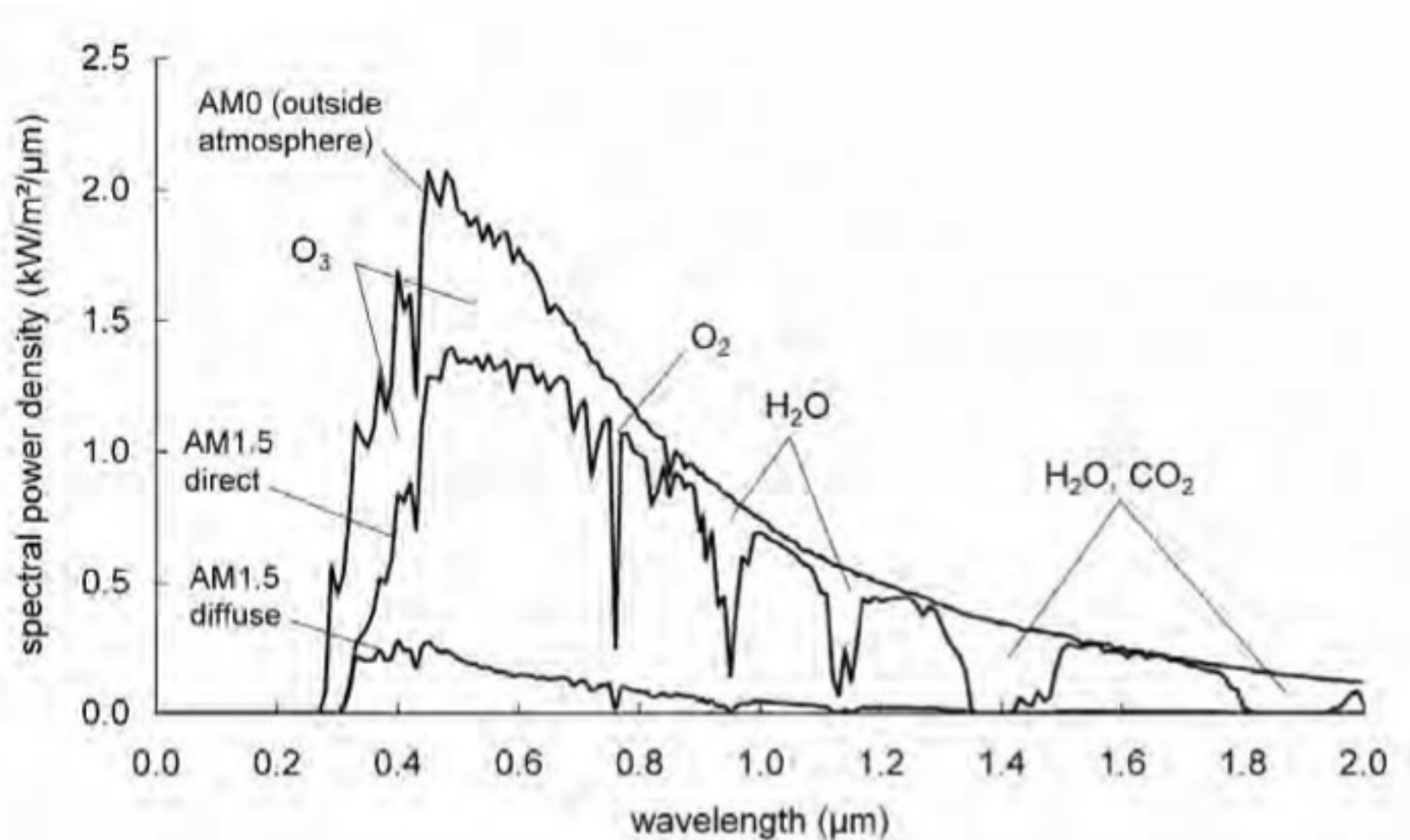


Figure 1.6. The spectral power density of sunlight, outside the atmosphere (AM0) and at the earth's surface (AM1.5), showing absorption from various atmospheric components.

30% lost to Rayleigh Scattering λ^{-4} (blue sky/orange sunset)
Scattering by aerosols (Smoke, Dust and Haze S.K. Friedlander)
Absorption: Ozone all below 0.3 μm , CO_2 , O_2 , H_2O

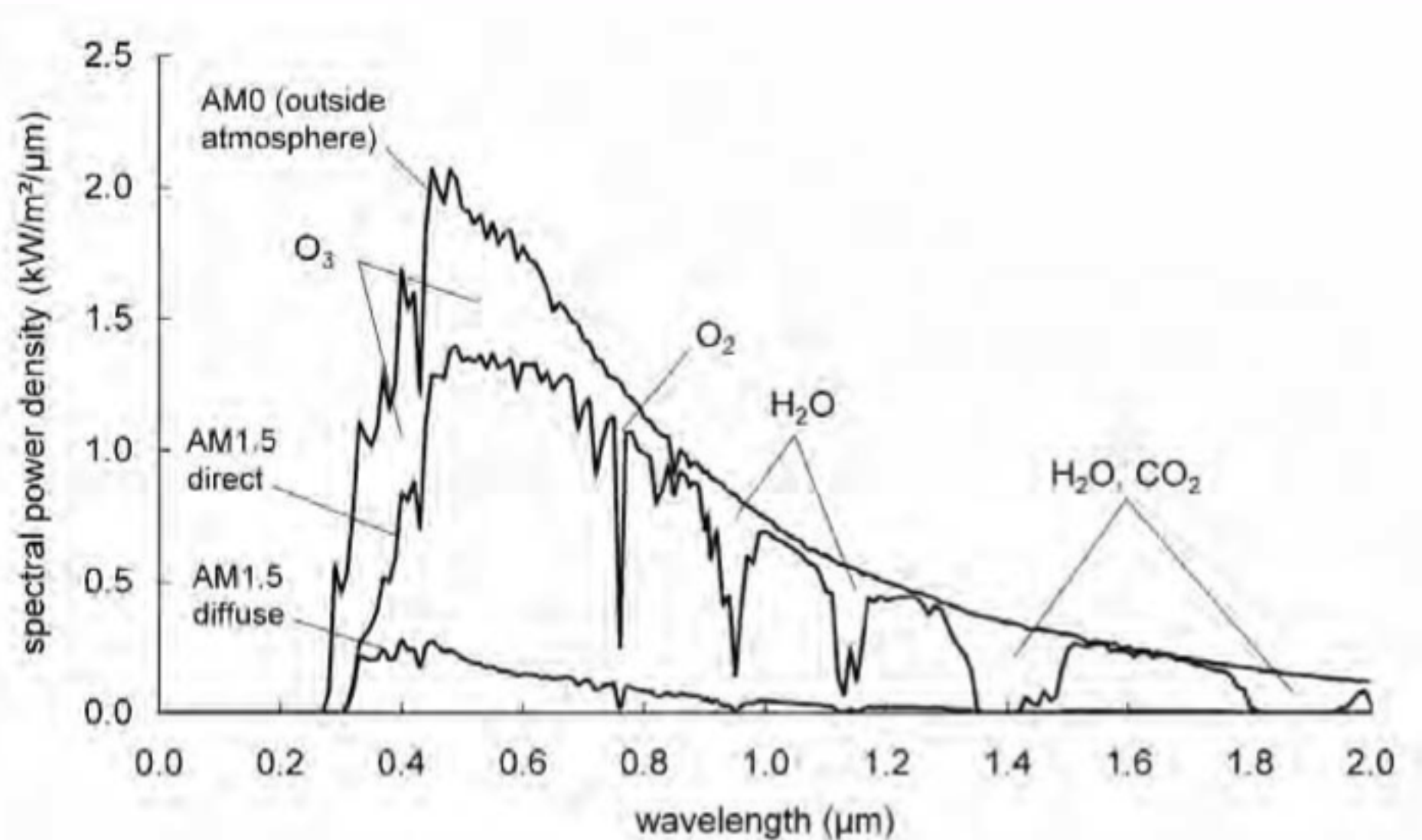


Figure 1.6. The spectral power density of sunlight, outside the atmosphere (AM0) and at the earth's surface (AM1.5), showing absorption from various atmospheric components.

10% added to AMI for clear skies by diffuse component
Increases with cloud cover
 $\frac{1}{2}$ lost to clouds is recovered in diffuse radiation

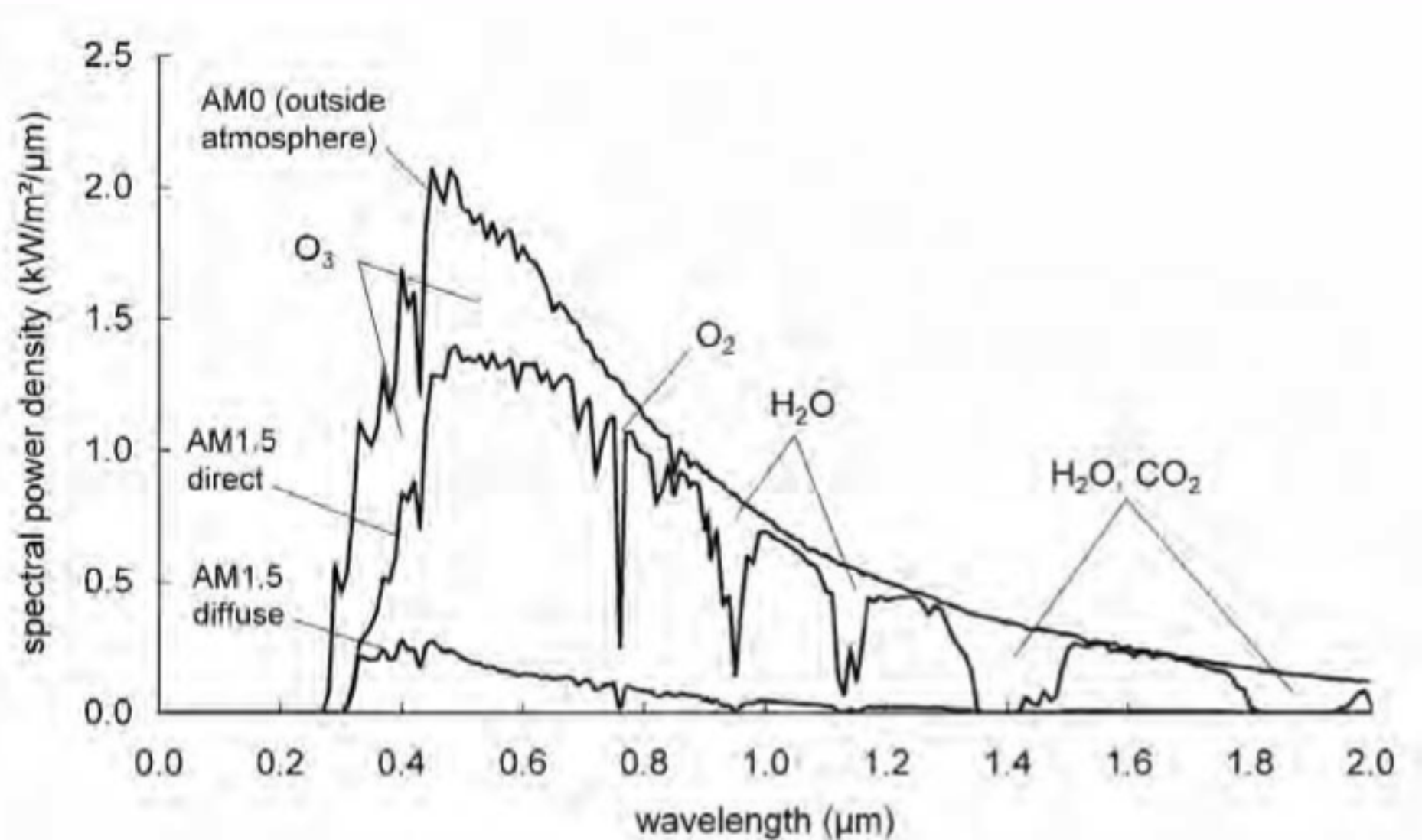


Figure 1.6. The spectral power density of sunlight, outside the atmosphere (AM0) and at the earth's surface (AM1.5), showing absorption from various atmospheric components.

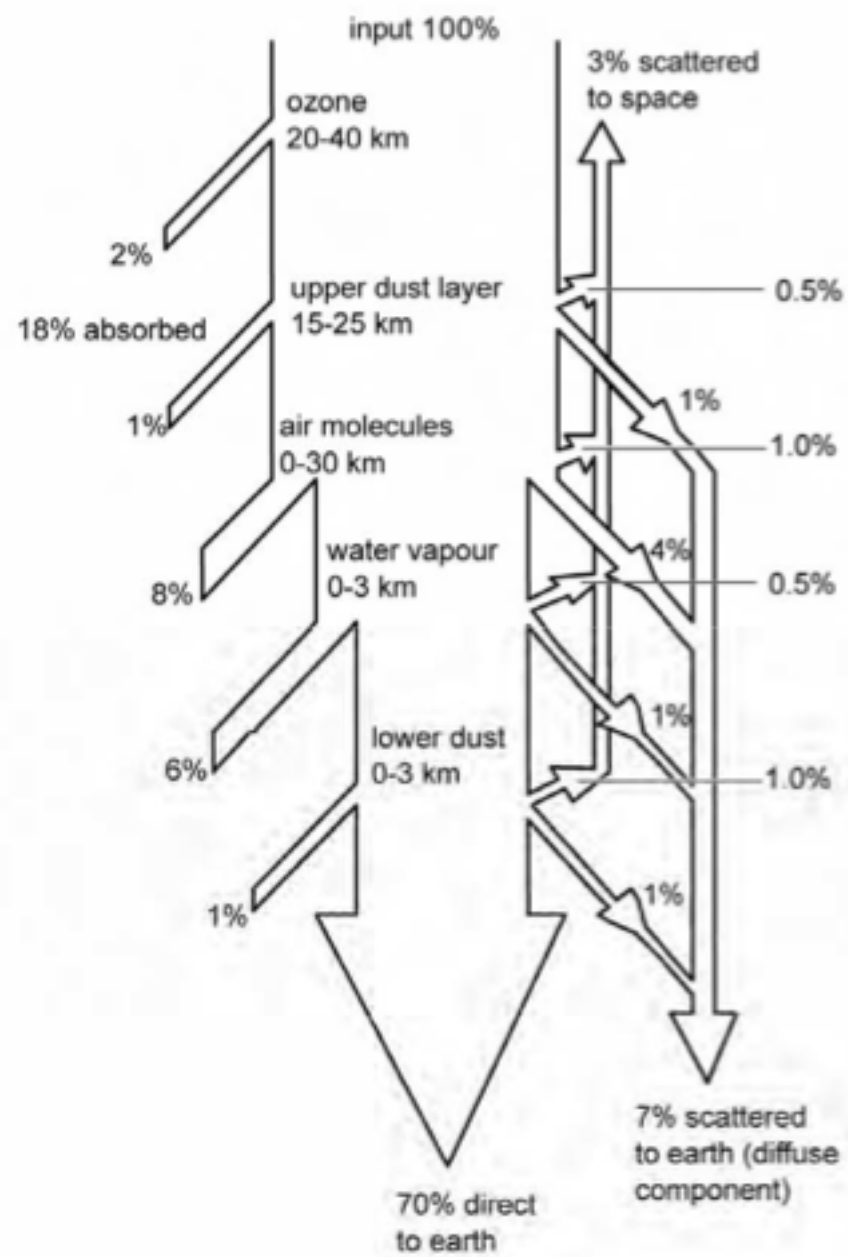
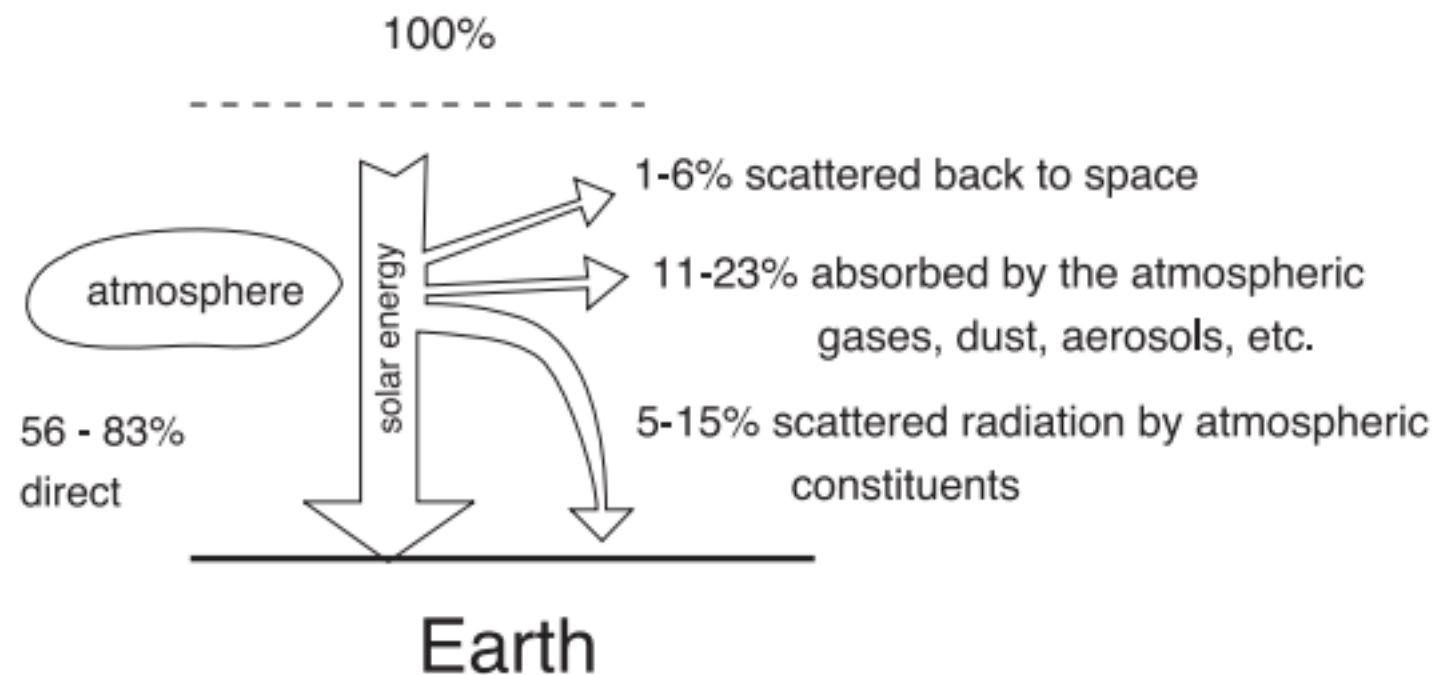


Figure 1.14. Typical AM1 clear sky absorption and scattering of incident sunlight (Used with permission of McGraw-Hill Companies, Hu, C. & White, R.M. (1983), Solar Cells: From Basic to Advanced Systems, McGraw-Hill, New York.).

The incident radiation energy reaching the earth's atmosphere is known as the solar constant, G_s and has a value of

$$G_s = 1353 \text{ W/m}^2$$

While this value can change by about $\pm 3.4\%$ throughout the year its change is relatively small and is assumed to be constant for most calculations. Although $G_s = 1353 \text{ W/m}^2$ at the edge of the earth's atmosphere, the following figure shows how it is dispersed as it approaches the surface of the earth.



Appendix A I

Direct and Diffuse Radiation

$$\text{Global Radiation} = \text{Direct} + \text{Diffuse Radiation}$$

AM1.5 Global AM1.5G irradiance for equator facing 37° tilted surface on earth (app.A I)

Integral over all wavelengths is 970 W/m² (or 1000 W/m² for normalized spectrum)
is a standard to rate PV Close to maximum power received at the earths surface.

Table A.1. Standard AM0, global AM1.5, and direct and circumsolar AM1.5 spectra. (Extracted, with permission, from G173-03 Standard Tables for Reference Solar Spectral Irradiances: Direct Normal and Hemispherical on 37° Tilted Surface, copyright ASTM International, 100 Barr Harbor Drive, West Conshohocken, PA 19428.)

wave-length	AM0	global AM1.5	direct and circumsolar AM1.5	wave-length	AM0	global AM1.5	direct and circumsolar AM1.5
(nm)	(W/m ² /nm)	(W/m ² /nm)	(W/m ² /nm)	(nm)	(W/m ² /nm)	(W/m ² /nm)	(W/m ² /nm)
280	8.2000E-02	4.7309E-23	2.5361E-26	660	1.5580E+00	1.3992E+00	1.2668E+00
290	5.6300E-01	6.0168E-09	5.1454E-10	670	1.5340E+00	1.4196E+00	1.2853E+00
300	4.5794E-01	1.0205E-03	4.5631E-04	680	1.4940E+00	1.3969E+00	1.2650E+00
310	5.3300E-01	5.0939E-02	2.7826E-02	690	1.4790E+00	1.1821E+00	1.0746E+00
320	7.7500E-01	2.0527E-01	1.1277E-01	700	1.4220E+00	1.2823E+00	1.1636E+00
330	1.1098E+00	4.7139E-01	2.6192E-01	710	1.4040E+00	1.3175E+00	1.1954E+00

Standard Spectrum is compared to Actual Spectrum for a site Solar Insolation Levels

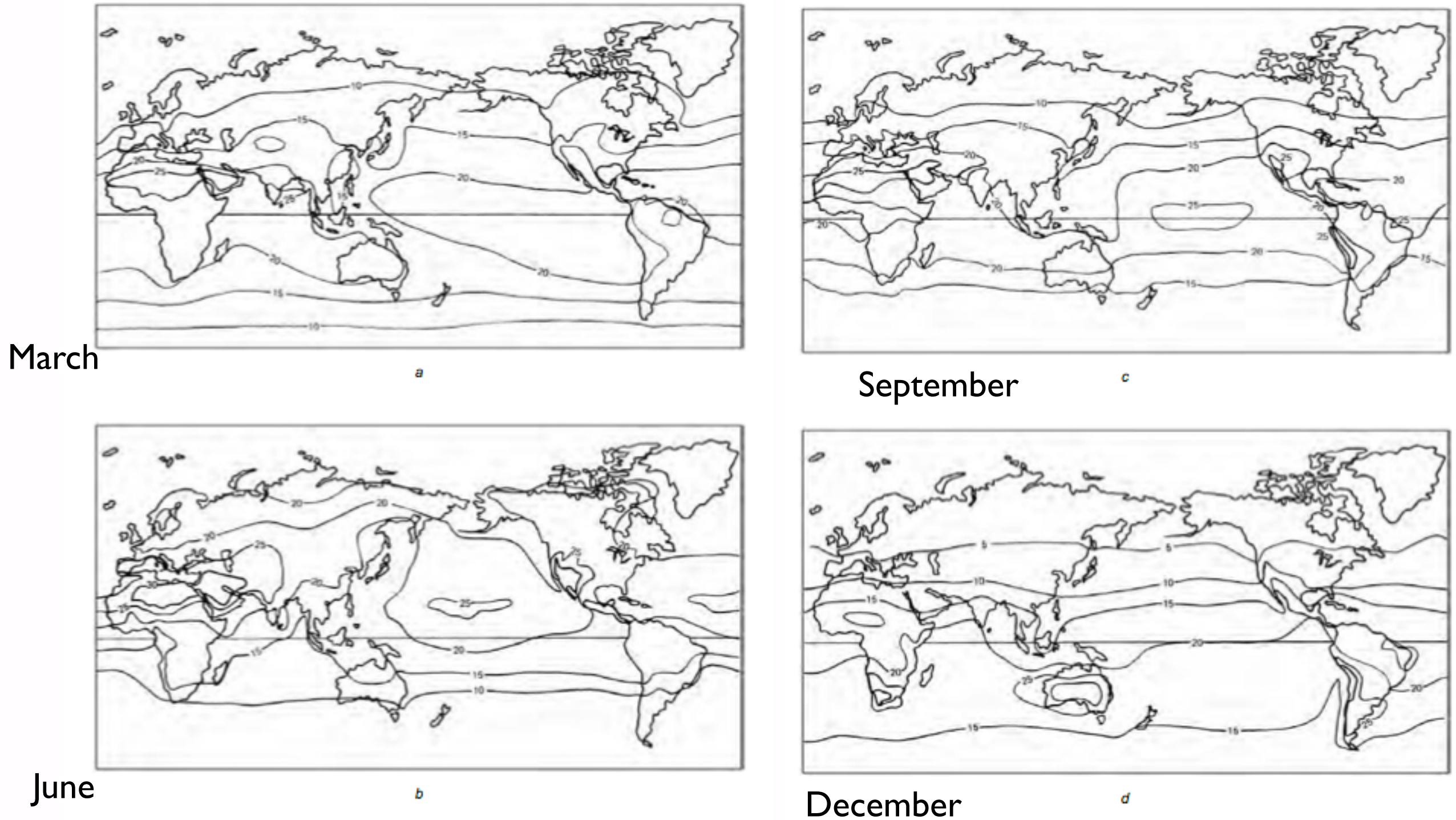


Figure 1.12. Average quarterly global isoflux contours of total insolation per day in MJ/m^2 falling on a horizontal surface ($1 \text{ MJ}/\text{m}^2 = 0.278 \text{ kWh}/\text{m}^2$). (a) March quarter, (b) June quarter (Used with permission of the authors, Meinel & Meinel, 1976).

Figure 1.12 (continued). Average quarterly global isoflux contours of total insolation per day in MJ/m^2 falling on a horizontal surface ($1 \text{ MJ}/\text{m}^2 = 0.278 \text{ kWh}/\text{m}^2$). (c) September quarter, (d) December quarter (Used with permission of the authors, Meinel & Meinel, 1976).

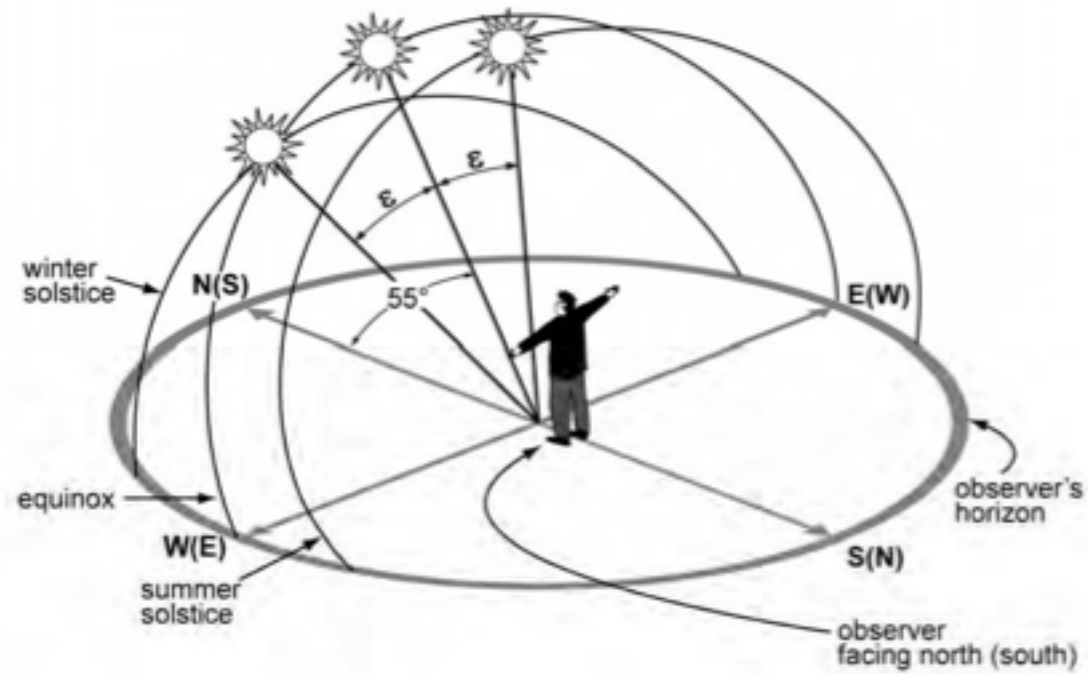


Figure 1.10. Apparent motion of the sun for an observer at 35°S (or N), where ϵ is the inclination of the earth's axis of rotation relative to its plane of revolution about the sun ($= 23^{\circ}27' = 23.45^{\circ}$).

Cape Town/Melbourne/Chattanooga
Gibraltar/Beirut/Shanghai

Appendix B

EQUATIONS FOR CALCULATING SUN POSITION

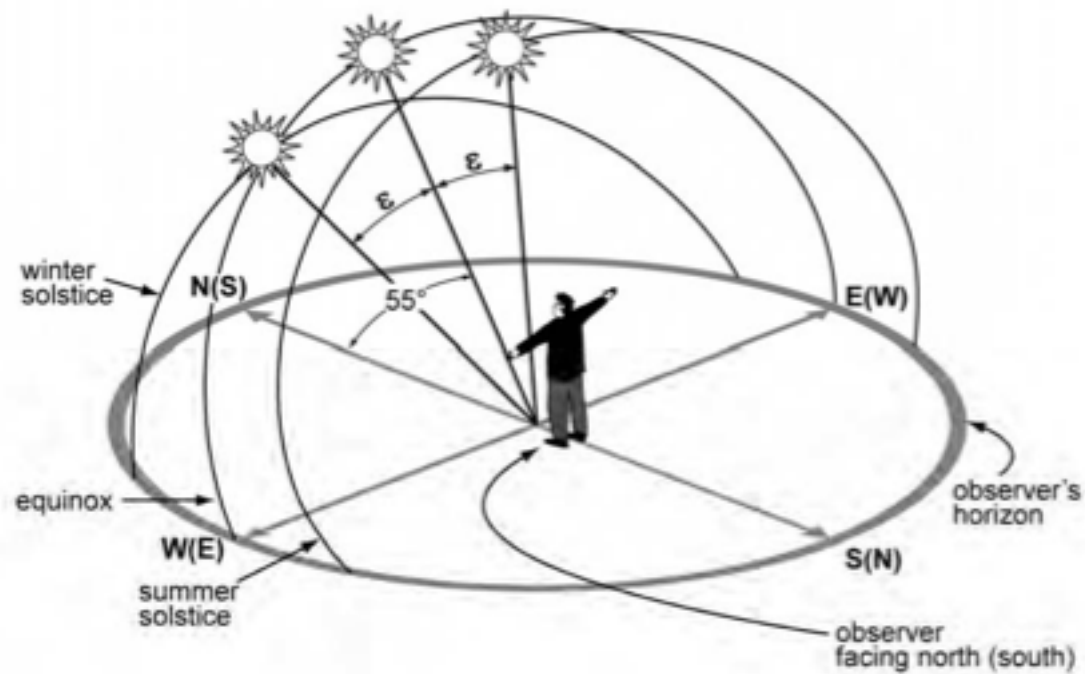


Figure 1.10. Apparent motion of the sun for an observer at 35°S (or N), where ϵ is the inclination of the earth's axis of rotation relative to its plane of revolution about the sun ($= 23^{\circ}27' = 23.45^{\circ}$).

AZI = solar azimuth (0–360°)
 ALT = solar altitude (elevation), relative to horizontal (zenith = 90°)
 ZEN = zenith angle, relative to vertical = $90^\circ - ALT$
 ORI = orientation of surface normal relative to azimuth
 HSA = horizontal shadow angle
 VSA = vertical shadow angle on perpendicular normal plane
 INC = angle of incidence relative to surface normal
 LAT = geographical latitude of site (negative for South)
 DEC = declination (between sun-earth line and equatorial plane)
 HRA = hour angle from solar noon (15° per hour)
 SRA = sunrise azimuth (i.e. azimuth at sunrise)
 SRT = sunrise time
 NDY = number of day of year
 N = day angle
 TIL = tilt angle of surface relative to horizontal

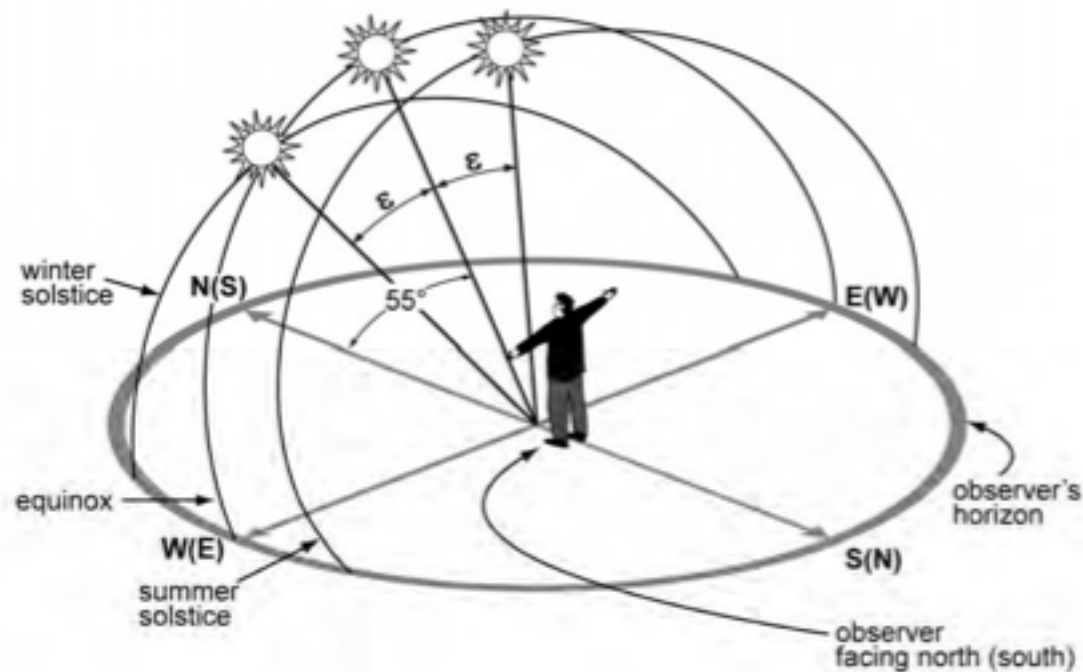


Figure 1.10. Apparent motion of the sun for an observer at 35°S (or N), where ϵ is the inclination of the earth's axis of rotation relative to its plane of revolution about the sun ($= 23^\circ 27' = 23.45^\circ$).

$$DEC = 23.45^\circ \sin \left[\frac{2\pi}{365} (284 + NDY) \right]$$

or more accurately

$$DEC = 0.33281 - 22.984 \cos N + 3.7372 \sin N - 0.3499 \cos(2N) + 0.03205 \sin(2N) - 0.1398 \cos(3N) + 0.07187 \sin(3N)$$

$$N = \frac{360^\circ}{365} NDY$$

$$HRA = 15^\circ (\text{hour} - 12)$$

$$ALT = \text{asin}[\sin DEC \sin LAT + \cos DEC \cos LAT \cos HRA]$$

$$AZI' = \text{acos} \left[\frac{\cos LAT \sin DEC - \cos DEC \sin LAT \cos HRA}{\cos ALT} \right]$$

$$AZI = \begin{cases} AZI', & \text{for } HRA < 0 \text{ (i.e. AM)} \\ 360^\circ - AZI', & \text{for } HRA > 0 \text{ (i.e. PM)} \end{cases}$$

$$HSA = AZI - ORI$$

$$VSA = \text{atan} \left[\frac{\tan ALT}{\cos HRA} \right]$$

$$INC = \text{acos}[\sin ALT \cos TIL + \cos ALT \sin TIL \cos HSA]$$

$$= \begin{cases} \text{acos}[\cos ALT \cos HSA], & \text{for vertical surfaces} \\ ZEN = 90^\circ - ALT, & \text{for horizontal surfaces} \end{cases}$$

$$SRA = \text{acos}[\cos LAT \sin DEC + \tan LAT \tan DEC \sin LAT \cos DEC]$$

$$SRT = 12 - \frac{\text{acos}(-\tan LAT \tan DEC)}{15^\circ}$$

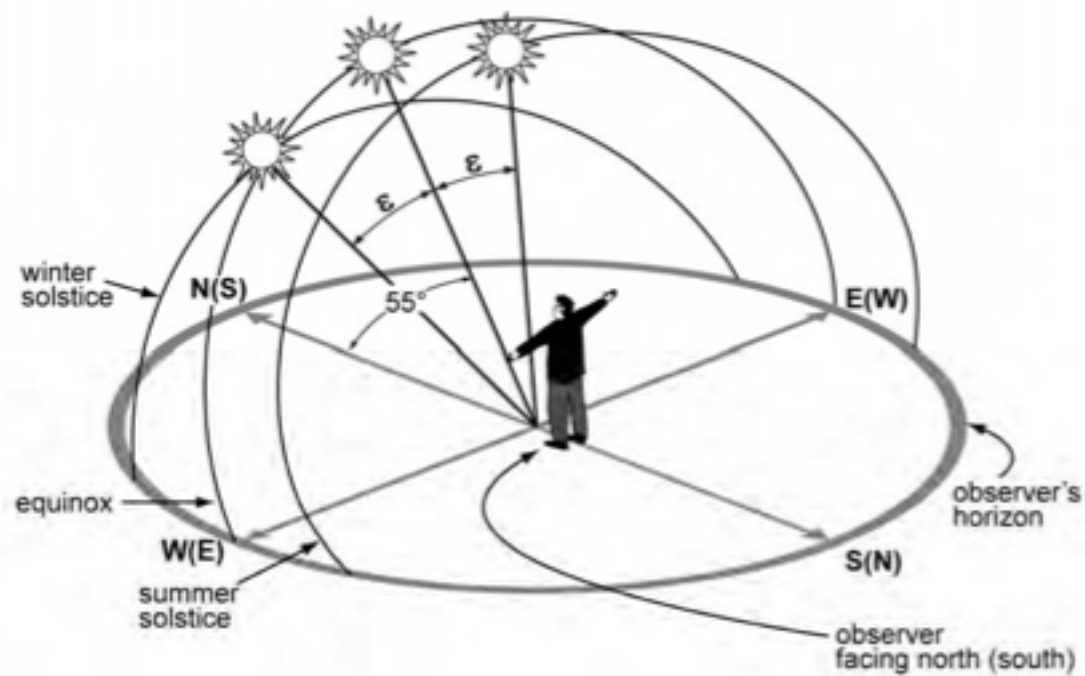


Figure 1.10. Apparent motion of the sun for an observer at 35°S (or N), where ϵ is the inclination of the earth's axis of rotation relative to its plane of revolution about the sun ($= 23^{\circ}27' = 23.45^{\circ}$).

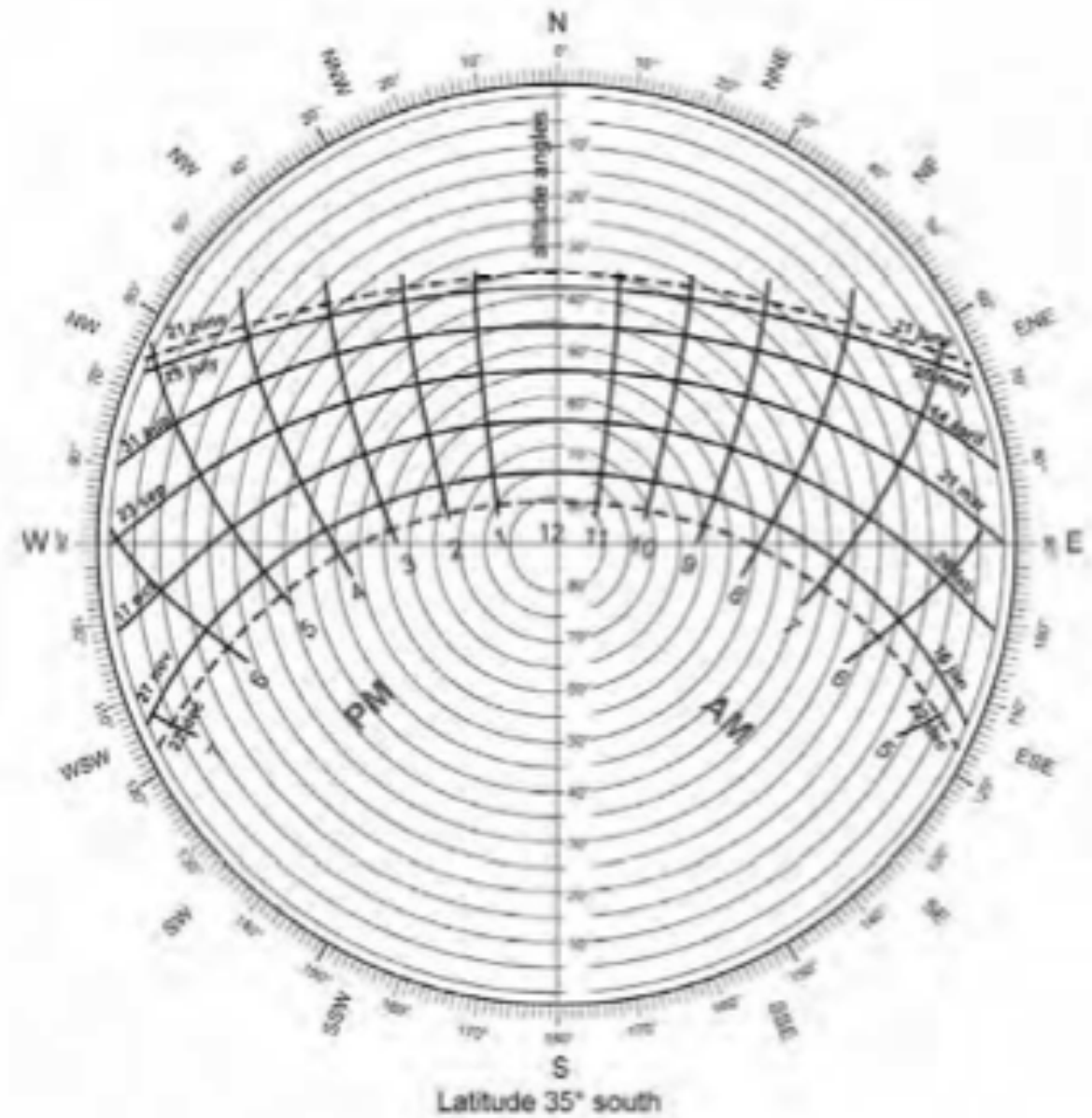


Figure 1.11. Polar chart showing the apparent motion of the sun for an observer at 35°S. ("Copyright © CSIRO 1992, Reproduced by permission of CSIRO PUBLISHING, Melbourne Australia from Sunshine and Shade in Australasia 6th edition (R.O. Phillips) <http://www.publish.csiro.au/pid/147.htm>)

Need:

- Global radiation on a horizontal surface
- Horizontal direct and diffuse components of global value
- Estimate for tilted plane value

Equations given in Chapter on Sunlight

Peak sun hours reduces a days variation to a fixed number of peak hours for calculations

SSH = Sunshine Hours

Total number of hours above 210 W/m^2 for a month

Equations in Chapter I to convert SSH to a useful form.

Estimates of Diffuse Component

Clearness Index $K_T = \text{diffuse}/\text{total}$

This is calculated following the algorithm given in the chapter

Use number of sunny and cloudy days to calculate diffuse and direct insolation
Described in the book

Tilted Surfaces

PV is mounted at a fixed tilt angle

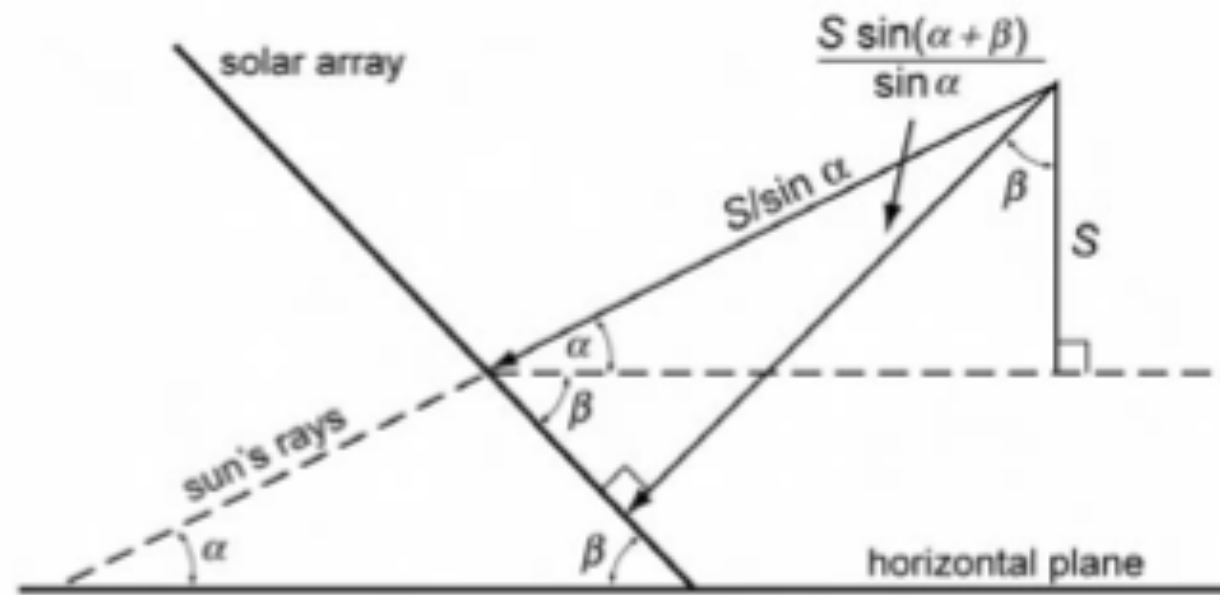


Figure 1.15. Light incident on a surface tilted to the horizontal (after Mack, 1979).

Sunny versus Cloudy

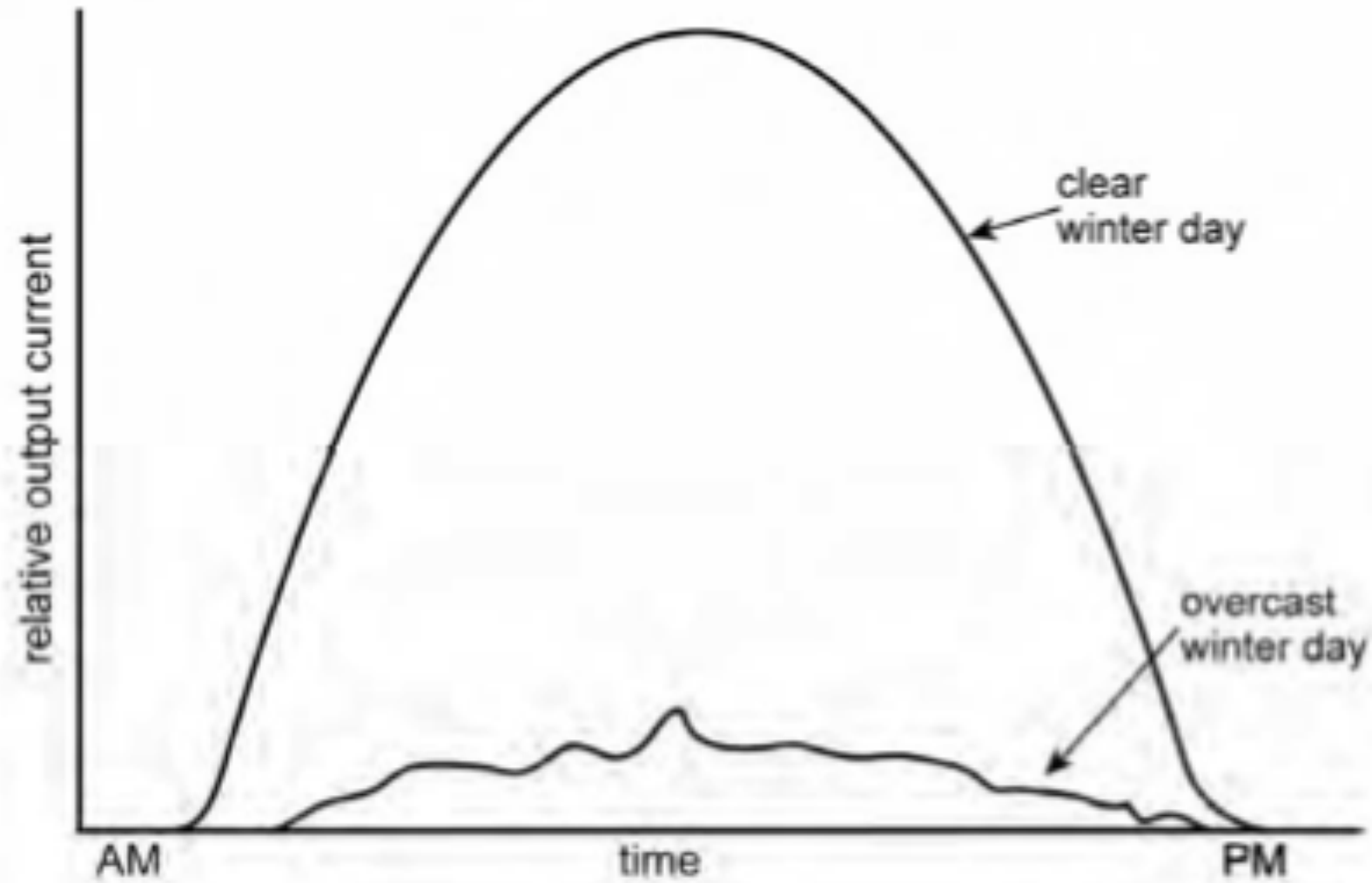


Figure 1.16. Relative output current from a photovoltaic array on a sunny and a cloudy winter's day in Melbourne (38°S) with an array tilt angle of 60° (after Mack, 1979).

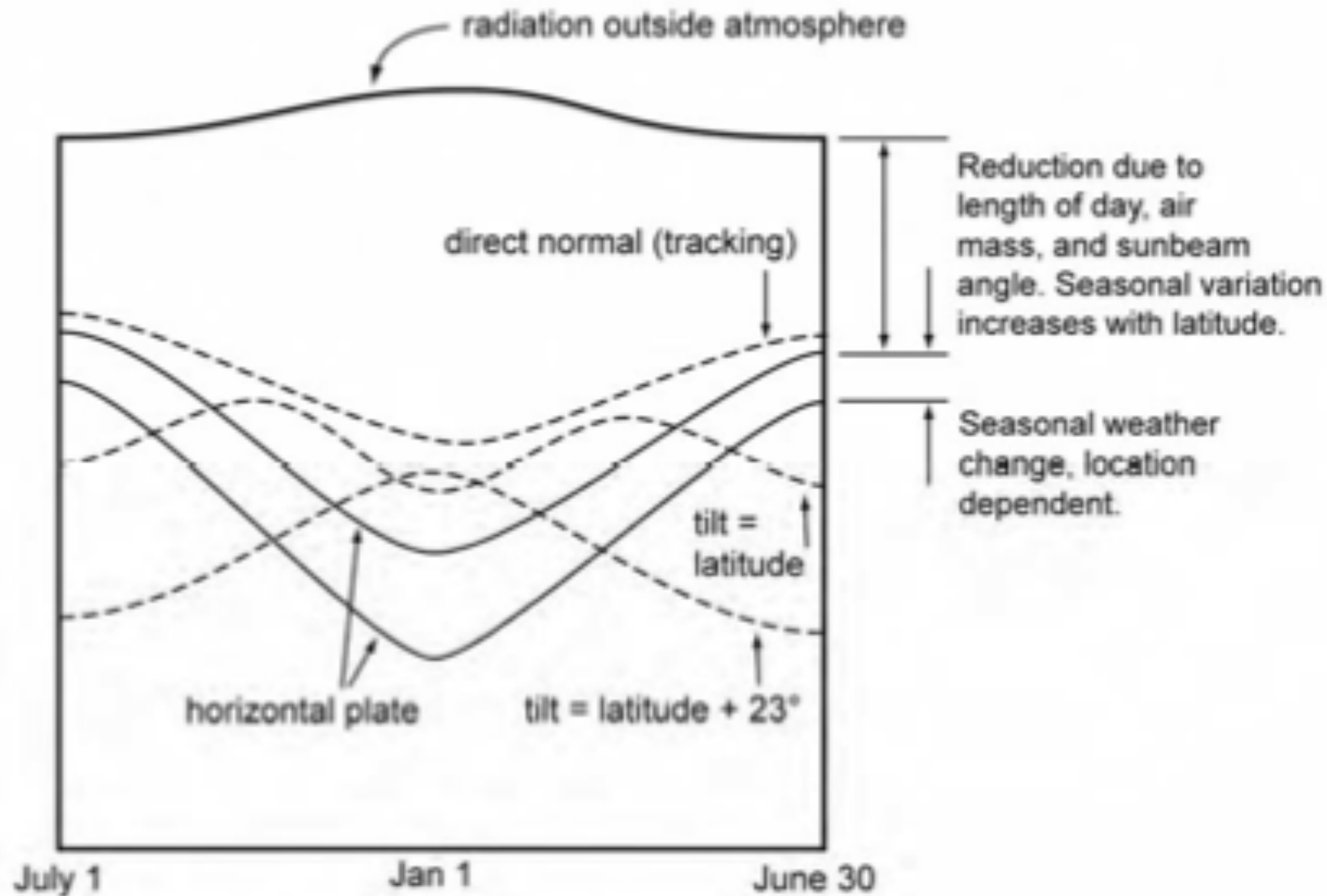
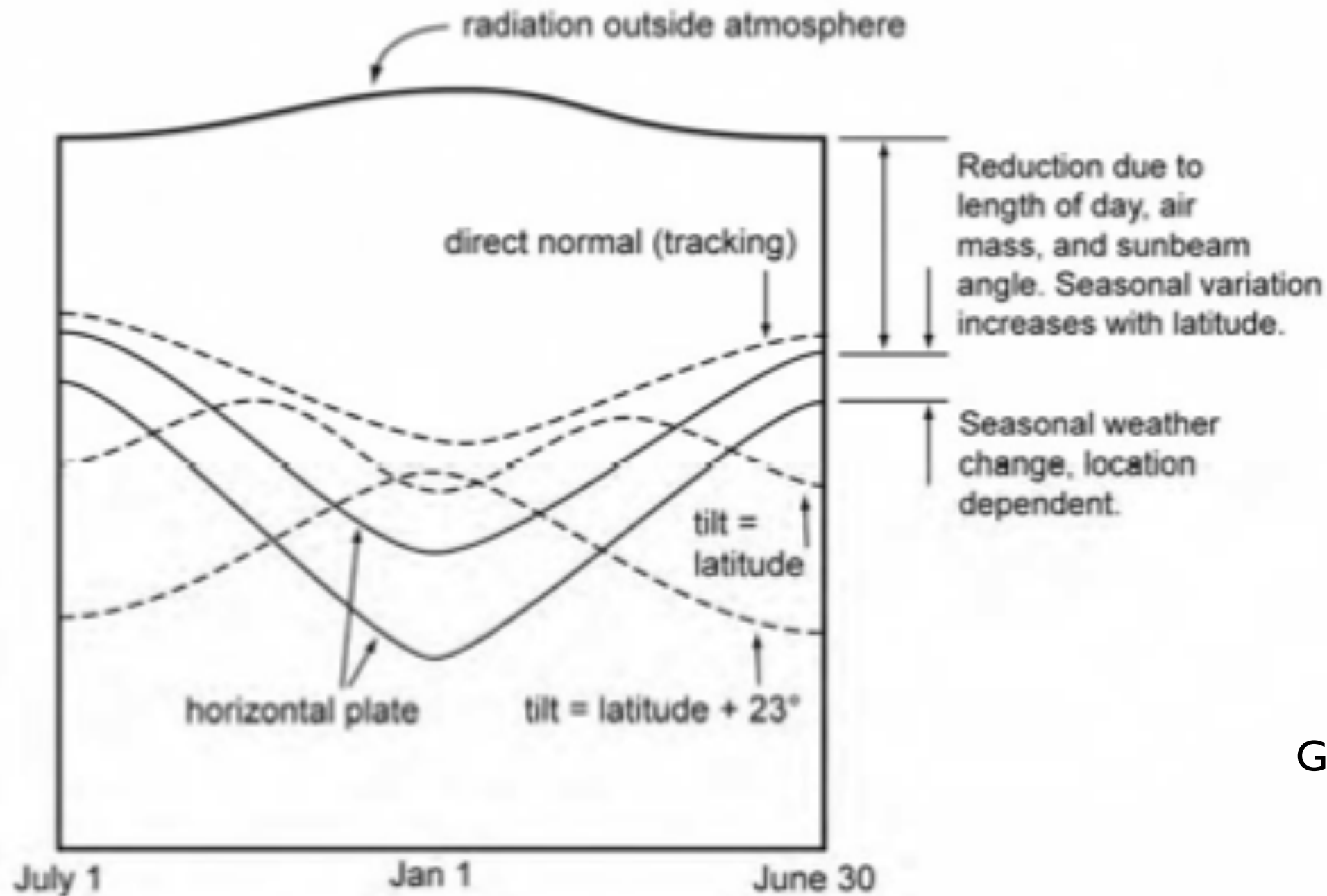


Figure 1.17. The effect of array tilting on the total insolation received each day for a location at latitude 23.4°N (Used with permission of McGraw-Hill Companies, Hu, C. & White, R.M. (1983), *Solar Cells: From Basic to Advanced Systems*, McGraw-Hill, New York.).



Calculation for
Optimal Tilt Angle
Given in the Chapter

Figure 1.17. The effect of array tilting on the total insolation received each day for a location at latitude 23.4°N (Used with permission of McGraw-Hill Companies, Hu, C. & White, R.M. (1983), *Solar Cells: From Basic to Advanced Systems*, McGraw-Hill, New York.).

EXERCISES

- 1.1 The sun is at an altitude of 30° to the horizontal. What is the corresponding air mass?
- 1.2 What is the length of the shadow cast by a vertical post with a height of 1 m under AM1.5 illumination?
- 1.3 Calculate the sun's altitude at solar noon on 21 June in Sydney (latitude 34°S) and in San Francisco (latitude 38°N).
- 1.4 The direct radiation falling on a surface normal to the sun's direction is 90 mW/cm^2 at solar noon on one summer solstice in Albuquerque, New Mexico (latitude 35°N). Calculate the direct radiation falling on a surface facing south at an angle of 40° to the horizontal.
- 1.5 To design appropriate photovoltaic systems, good data on the insolation (i.e. amount of sunshine) is essential for each particular location. List the sources and nature of insolation data available for your region (state or country).

$$\frac{1}{\cos\theta}$$

$$AM = \sqrt{1 + (s/h)^2}$$

P-N Junctions and Commercial Photovoltaic Devices

Chapter 2

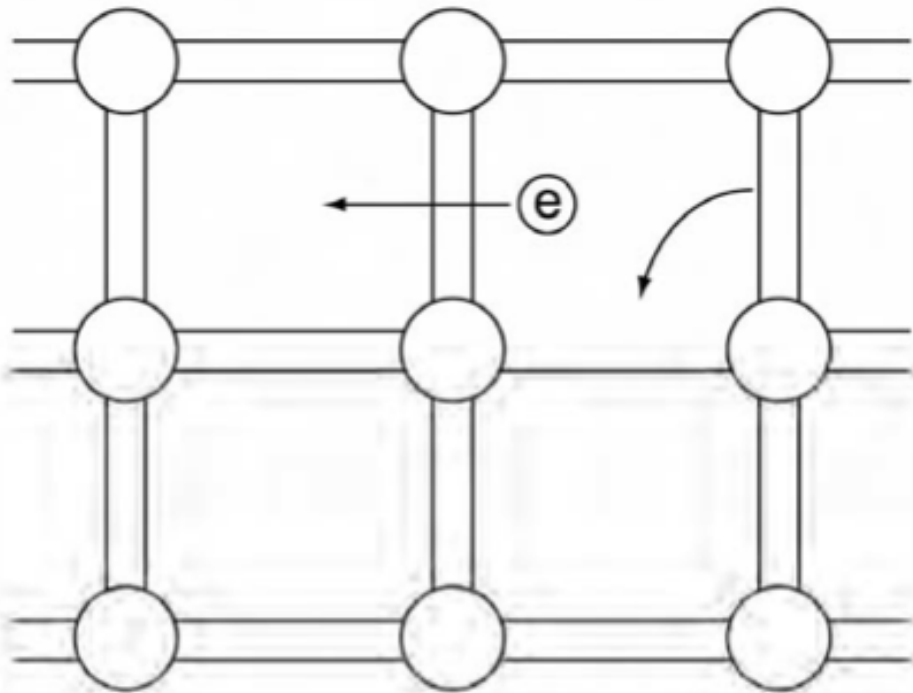


Figure 2.1. Schematic representation of covalent bonds in a silicon crystal lattice.

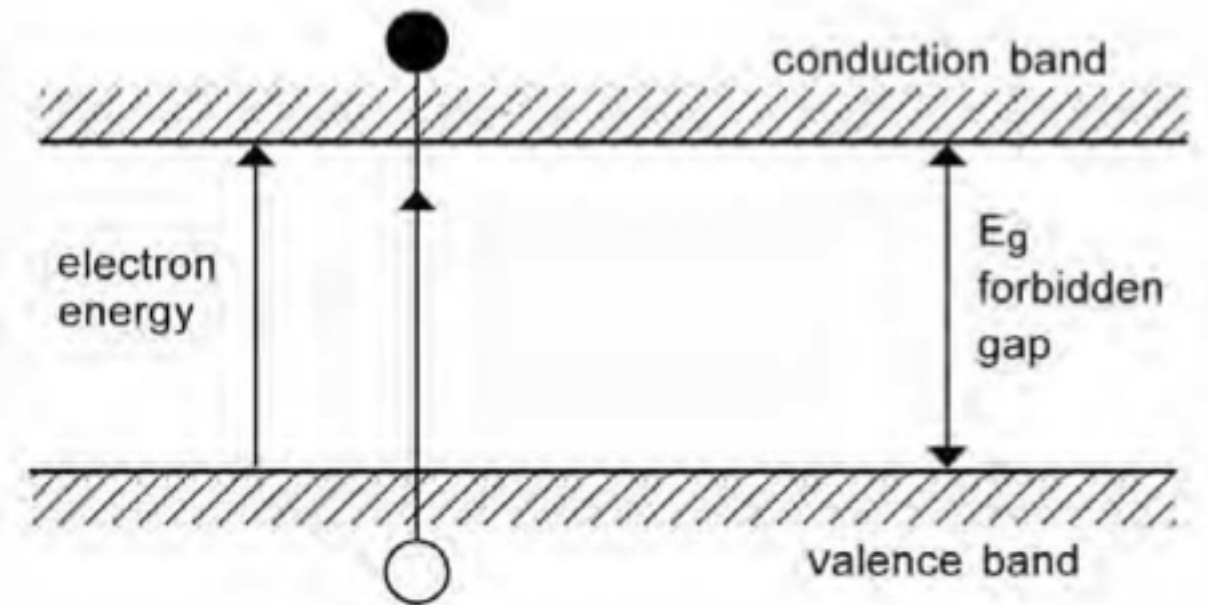


Figure 2.2. Schematic of the energy bands for electrons in a solid.

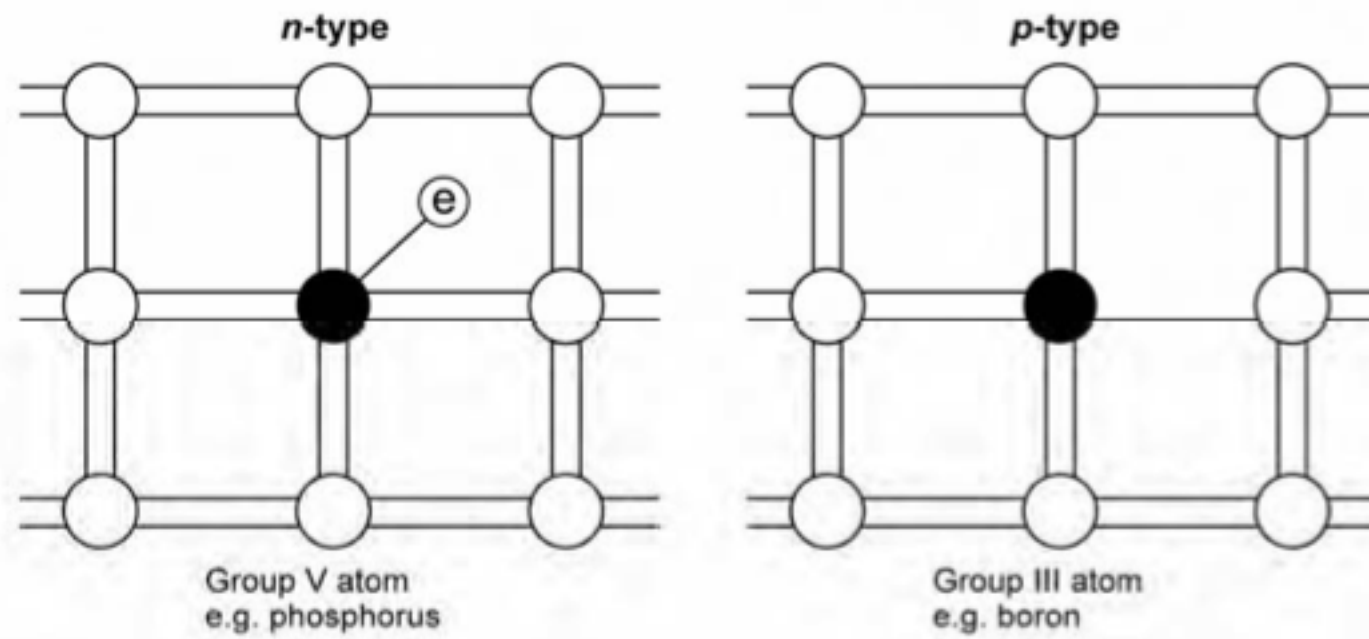
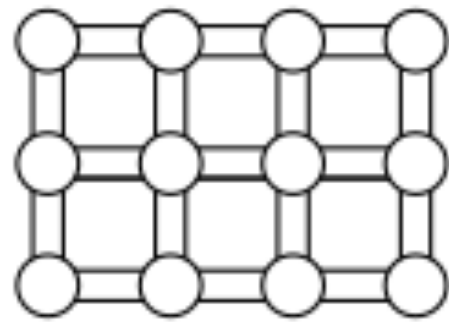
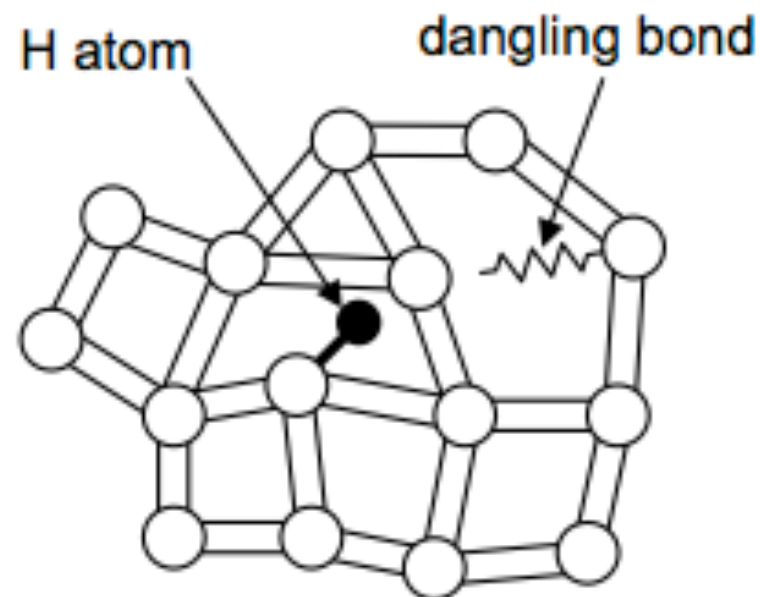
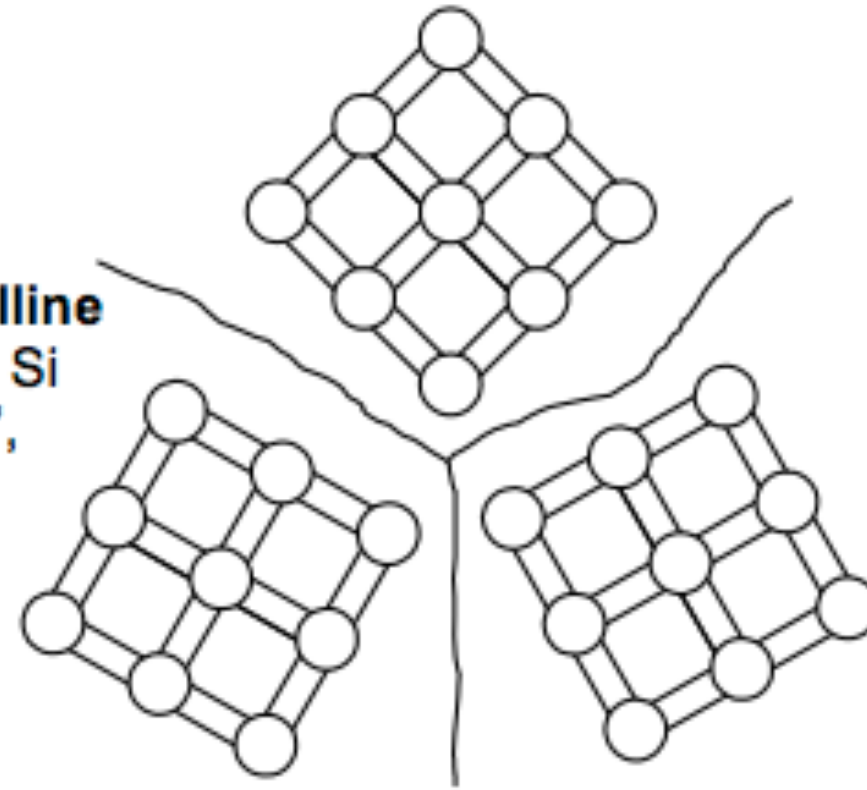


Figure 2.3. Schematic of a silicon crystal lattice doped with impurities to produce *n*-type and *p*-type semiconductor material.



crystalline (c-Si)—atoms arranged in a regular pattern.

multicrystalline or polycrystalline (poly Si)—regions of crystalline Si separated by 'grain boundaries', where bonding is irregular.

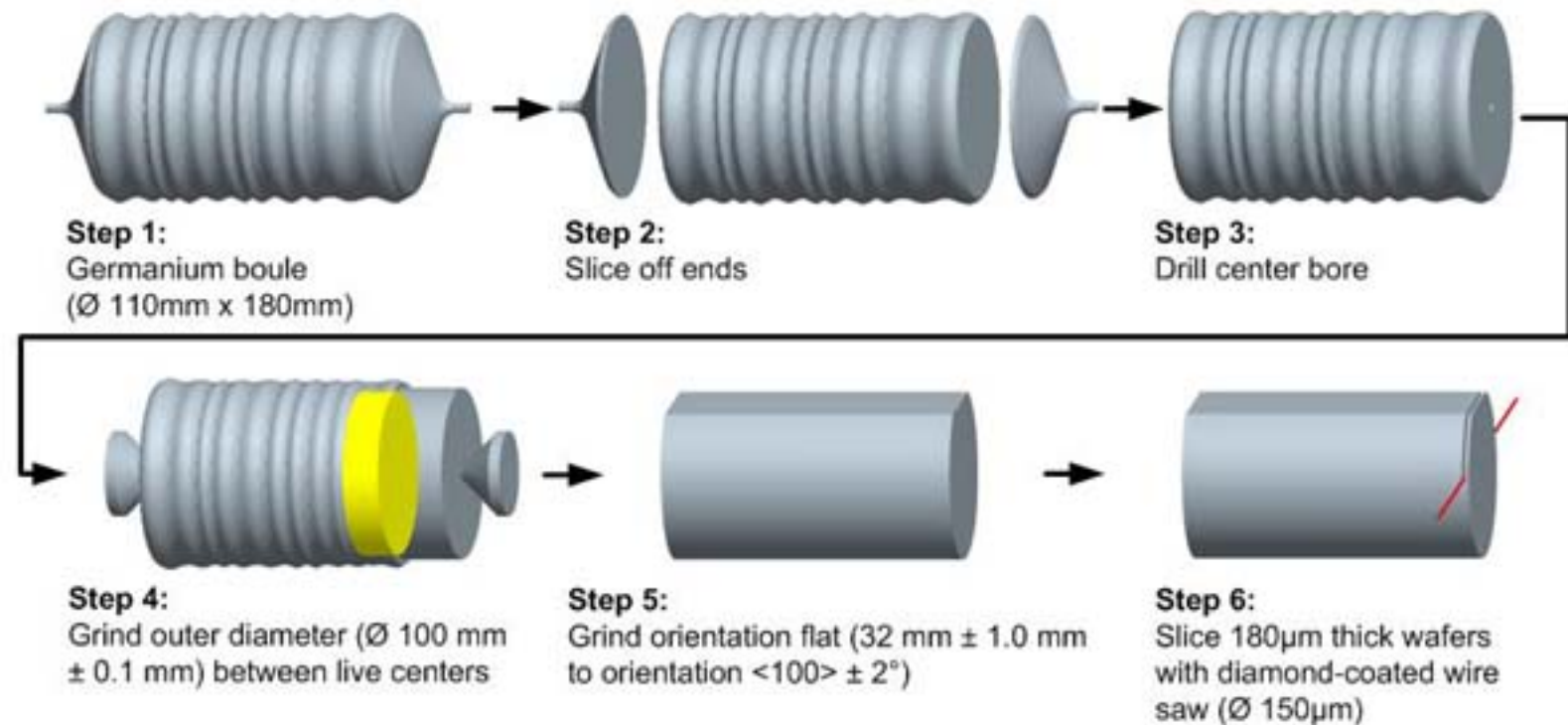
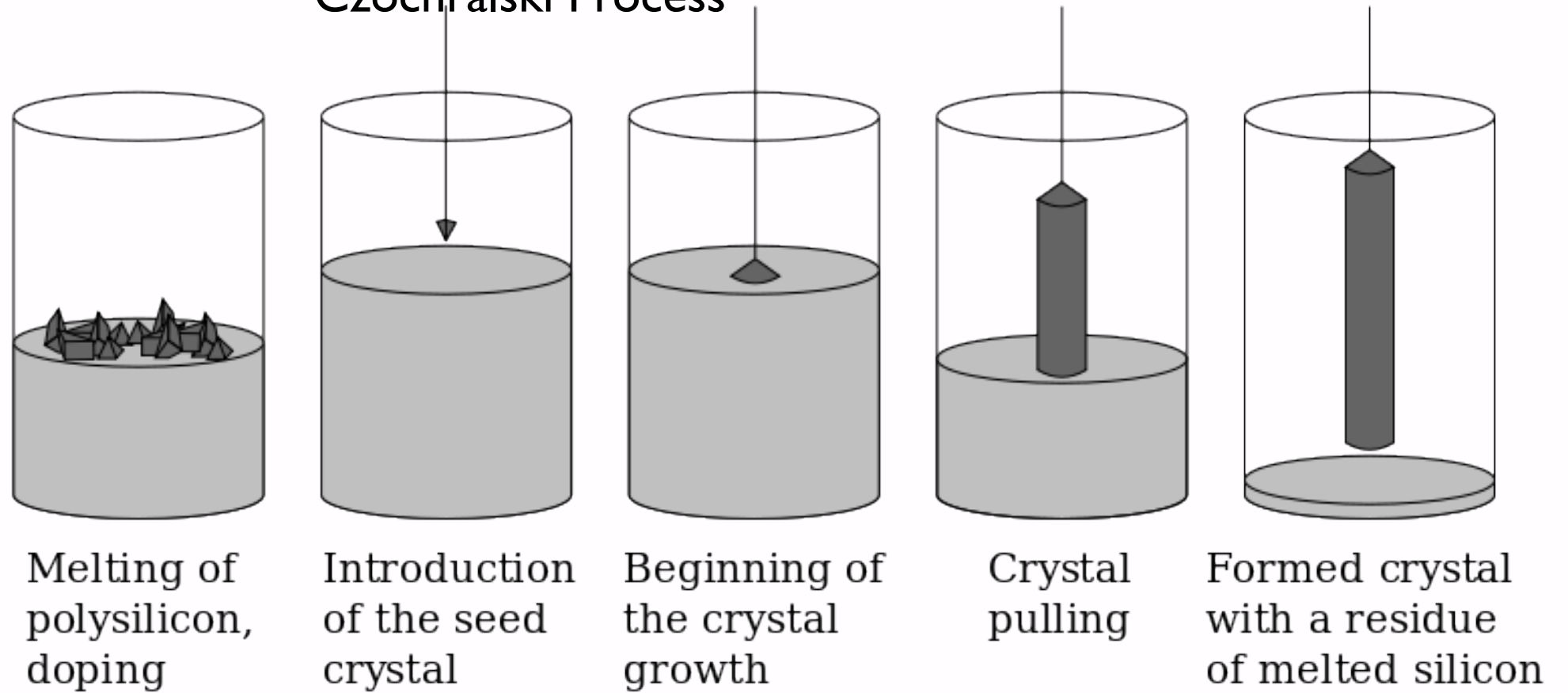


amorphous (a-Si:H)—less regular arrangement of atoms, leading to 'dangling bonds', which can be passivated by hydrogen.

Figure 2.4. The structure of crystalline, multicrystalline and amorphous silicon.

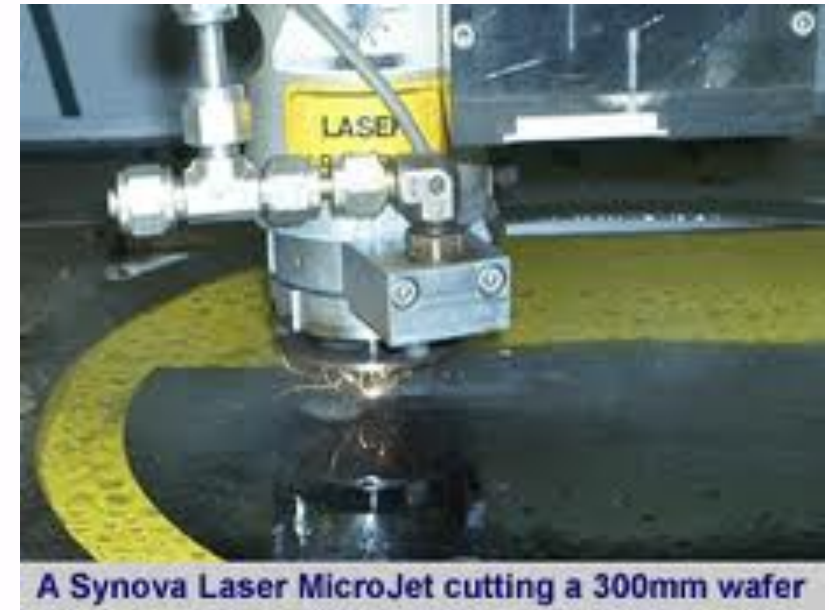
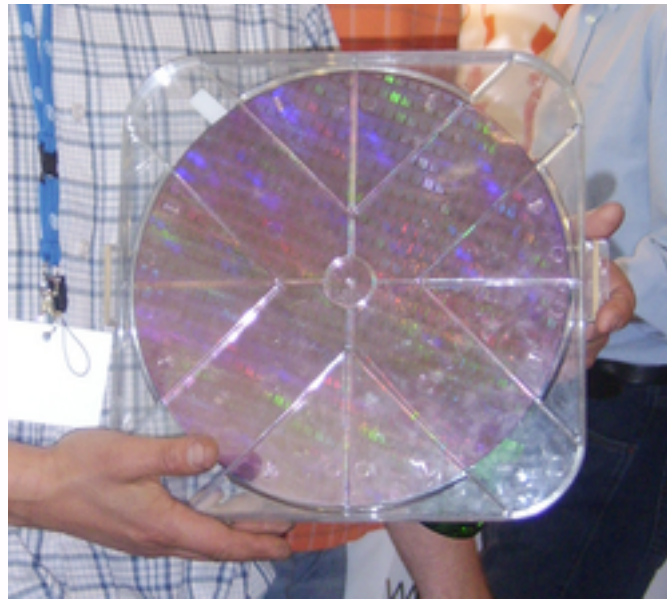


Czochralski Process



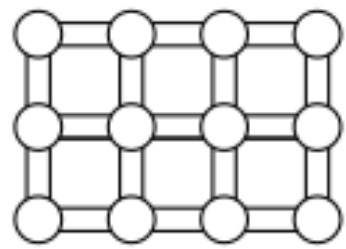


A section of 300mm ingot is loaded into a wire saw



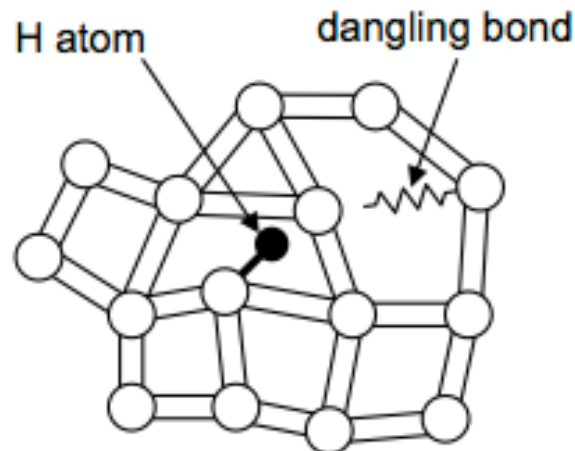
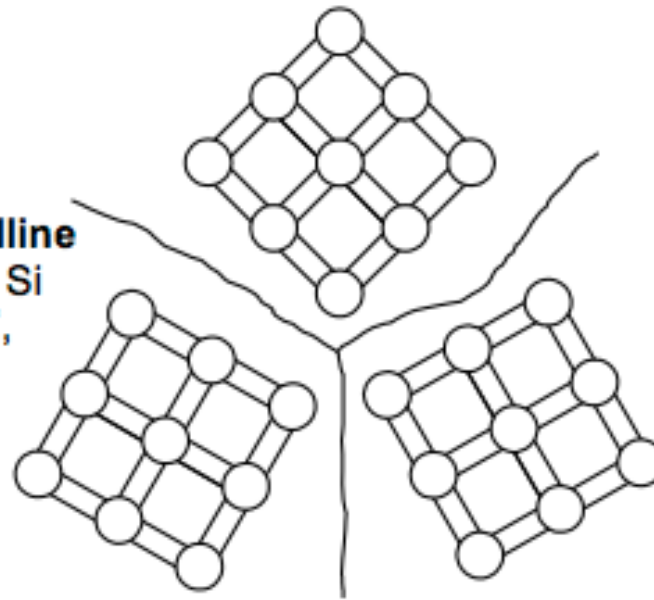
A Synova Laser MicroJet cutting a 300mm wafer

Silicon and other semiconductor materials used for solar cells can be crystalline, multicrystalline, polycrystalline, microcrystalline or amorphous. Although usages of these terms vary, we follow the definitions by planar grain size according to Basore (1994). Microcrystalline material has grains smaller than $1\ \mu\text{m}$, polycrystalline smaller than $1\ \text{mm}$ and multicrystalline smaller than $10\ \text{cm}$. The structure of the different material types is illustrated in Fig. 2.4.



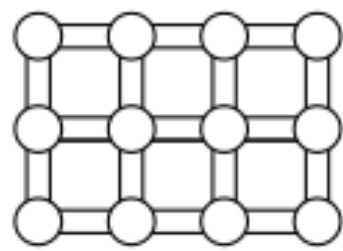
crystalline (c-Si)—atoms arranged in a regular pattern.

multicrystalline or polycrystalline (poly Si)—regions of crystalline Si separated by 'grain boundaries', where bonding is irregular.



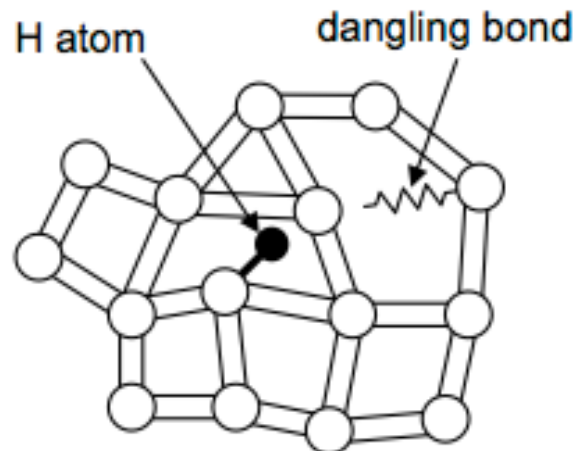
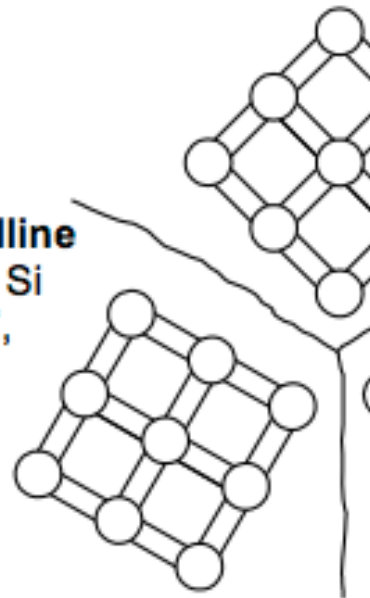
amorphous (a-Si:H)—less regular arrangement of atoms, leading to 'dangling bonds', which can be passivated by hydrogen.

Figure 2.4. The structure of crystalline, multicrystalline and amorphous silicon.



crystalline (c-Si)—atoms arranged in a regular pattern.

multicrystalline or polycrystalline (poly Si)—regions of crystalline Si separated by 'grain boundaries', where bonding is irregular.



amorphous (a-Si:H)—less regular arrangement of atoms, leading to 'dangling bonds', which can be passivated by hydrogen.

Amorphous silicon can be produced, in principle, even more cheaply than polysilicon. With amorphous silicon, there is no long-range order in the structural arrangement of the atoms, resulting in areas within the material containing unsatisfied, or 'dangling' bonds. These in turn result in extra energy levels within the forbidden gap, making it impossible to dope the semiconductor when pure, or to obtain reasonable current flows in a solar cell configuration.

It has been found that the incorporation of atomic hydrogen in amorphous silicon, to a level of 5–10%, saturates the dangling bonds and improves the quality of the material. It also increases the bandgap (E_g) from 1.1 eV in crystalline silicon to 1.7 eV, making the material much more strongly absorbing for photons of energy above the latter threshold. The thickness of material required to form a functioning solar cell is therefore much smaller.

The minority carrier diffusion lengths in such silicon-hydrogen alloys, (a-Si:H), are much less than 1 μm . The depletion region therefore forms most of the active carrier-collecting volume of the cell. Different design approaches to those discussed above for crystalline silicon are therefore used. In particular, as large a 'depletion region' as possible is created. Fig. 2.5 illustrates the general design of an a-Si:H solar cell.

Figure 2.4. The structure of crystalline, multicrystalline and amorphous silicon.

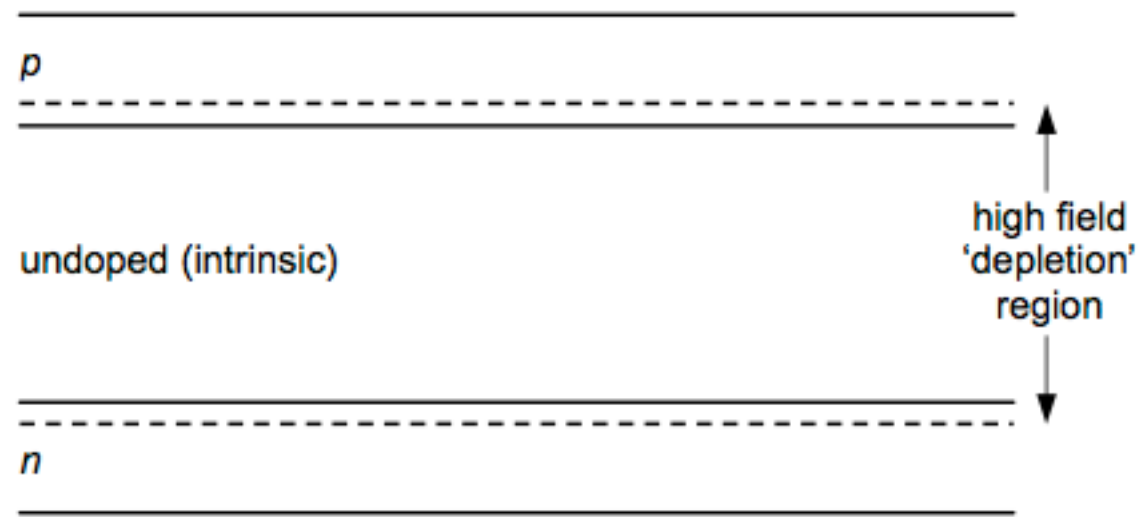
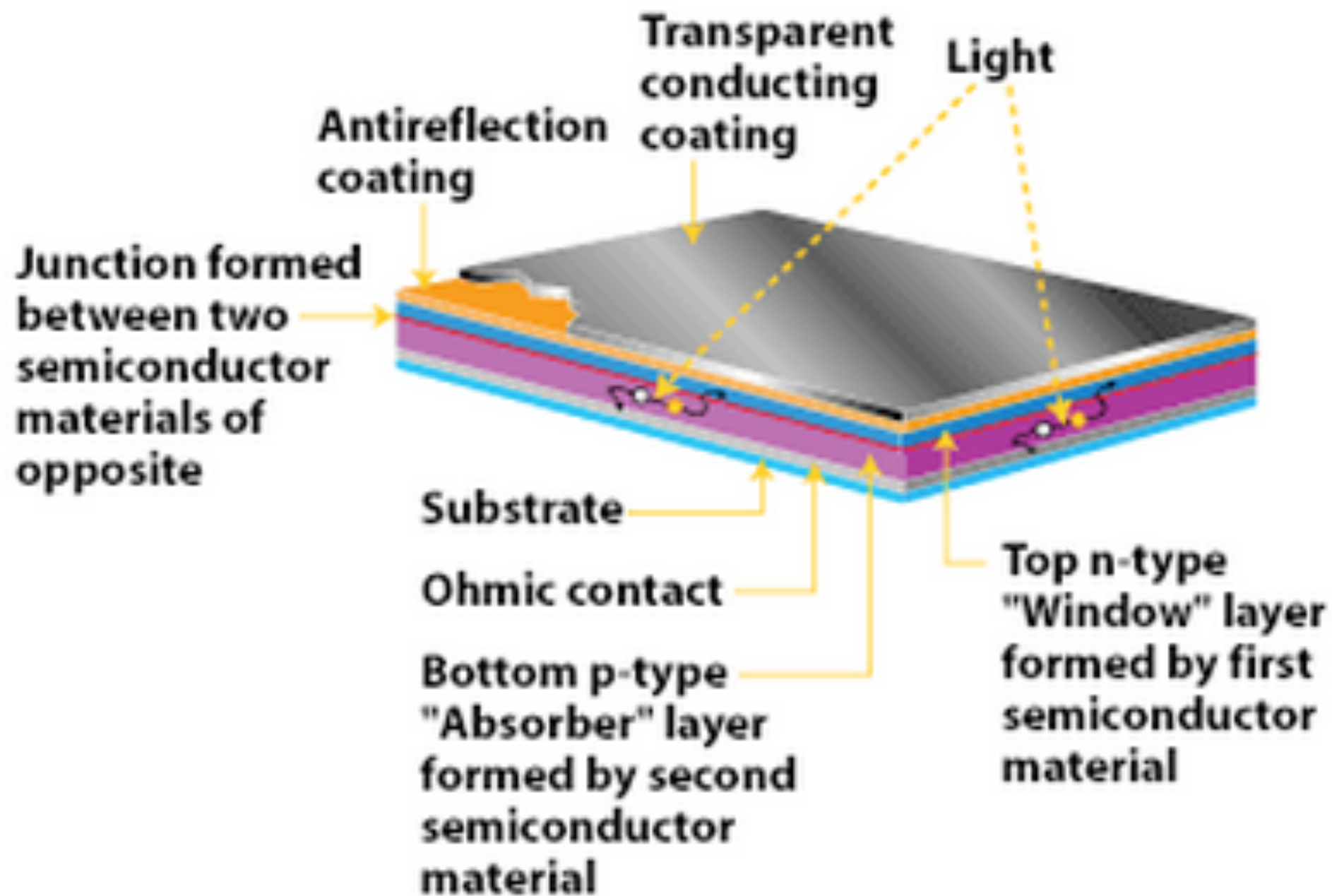


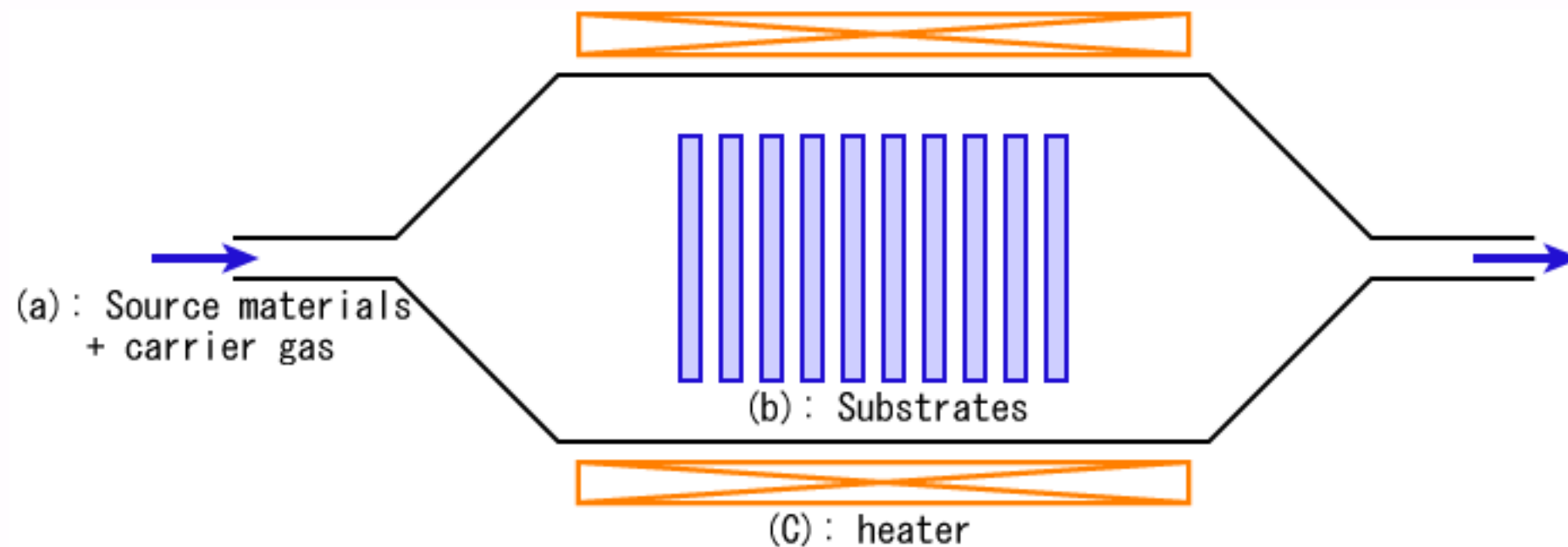
Figure 2.5. Schematic of an a-Si:H solar cell.

Amorphous silicon and other 'thin film' technologies for solar cell manufacture, where films of very thin semiconductor material are deposited onto glass or other substrates, are used in many small consumer products, such as calculators and watches, 'non-critical' outdoor applications and, increasingly also for large scale applications. In principle, thin films provide a very low cost means of cell production, although at present their efficiencies and lifetimes are lower than for crystalline products. Research into thin film and other potentially low cost solar cell materials may see these technologies dominate the solar cell market over coming decades.



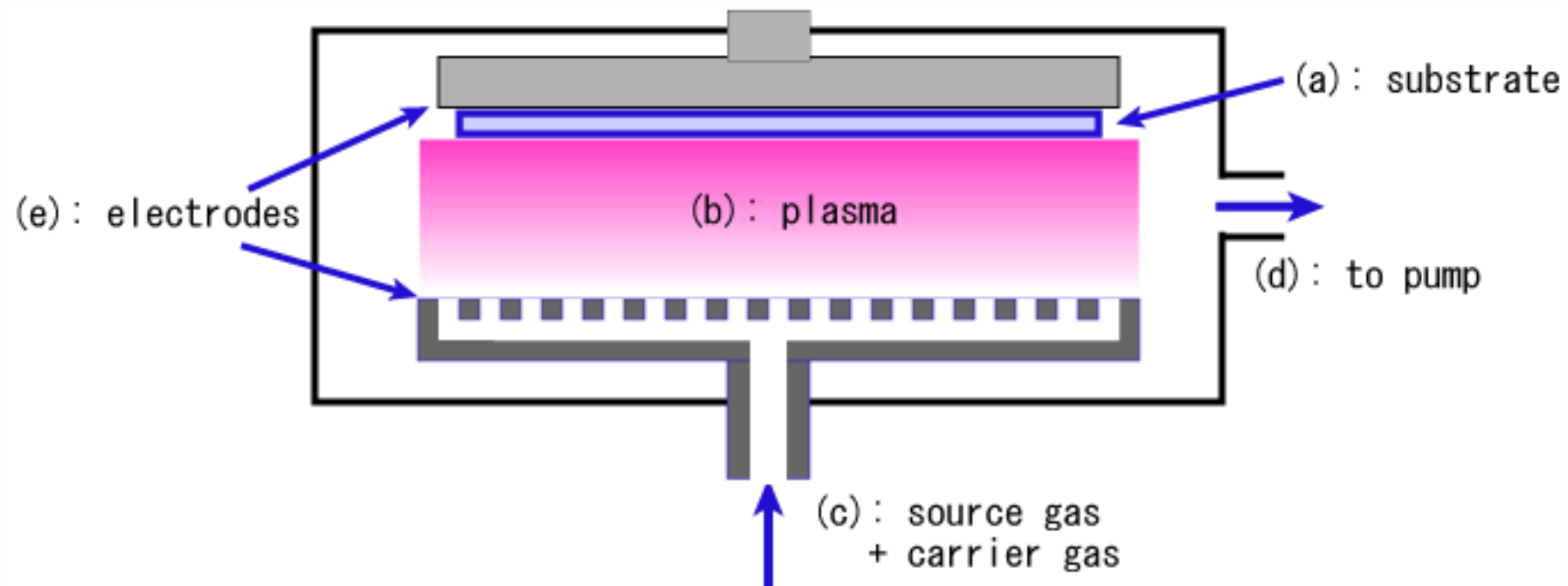
Amorphous silicon and other 'thin film' technologies for solar cell manufacture, where films of very thin semiconductor material are deposited onto glass or other substrates, are used in many small consumer products, such as calculators and watches, 'non-critical' outdoor applications and, increasingly also for large scale applications. In principle, thin films provide a very low cost means of cell production, although at present their efficiencies and lifetimes are lower than for crystalline products. Research into thin film and other potentially low cost solar cell materials may see these technologies dominate the solar cell market over coming decades.

Hot Wall CVD



Amorphous silicon and other 'thin film' technologies for solar cell manufacture, where films of very thin semiconductor material are deposited onto glass or other substrates, are used in many small consumer products, such as calculators and watches, 'non-critical' outdoor applications and, increasingly also for large scale applications. In principle, thin films provide a very low cost means of cell production, although at present their efficiencies and lifetimes are lower than for crystalline products. Research into thin film and other potentially low cost solar cell materials may see these technologies dominate the solar cell market over coming decades.

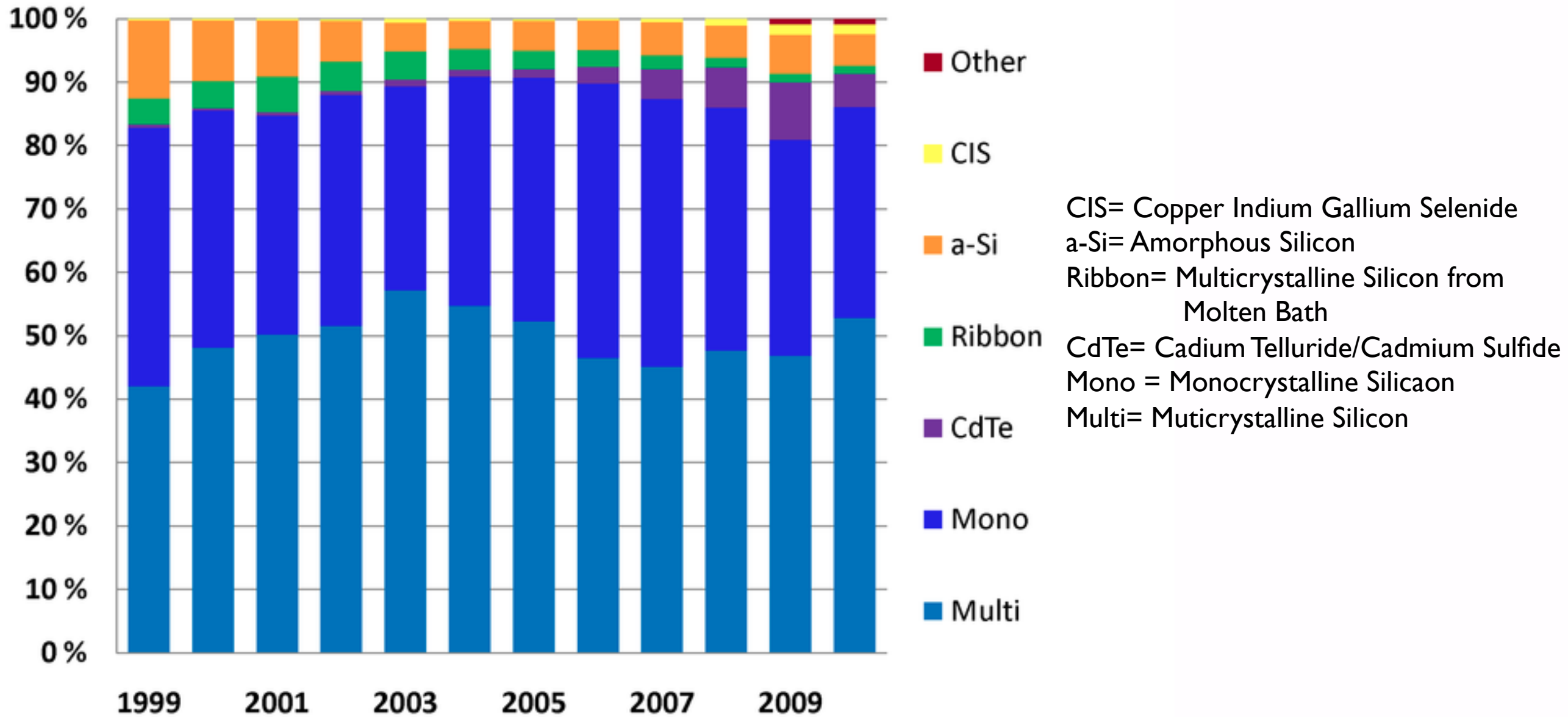
Plasma CVD



Amorphous silicon and other 'thin film' technologies for solar cell manufacture, where films of very thin semiconductor material are deposited onto glass or other substrates, are used in many small consumer products, such as calculators and watches, 'non-critical' outdoor applications and, increasingly also for large scale applications. In principle, thin films provide a very low cost means of cell production, although at present their efficiencies and lifetimes are lower than for crystalline products. Research into thin film and other potentially low cost solar cell materials may see these technologies dominate the solar cell market over coming decades.



Market Share



Formation of a *P-n* junction

P-n junctions are formed by joining *n*-type and *p*-type semiconductor materials, as shown below. Since the *n*-type region has a high electron concentration and the *p*-type a high hole concentration, electrons diffuse from the *n*-type side to the *p*-type side. Similarly, holes flow by diffusion from the *p*-type side to the *n*-type side. If the electrons and holes were not charged, this diffusion process would continue until the concentration of electrons and holes on the two sides were the same, as happens if two gasses come into contact with each other. However, in a *p-n* junction, when the electrons and holes move to the other side of the junction, they leave behind exposed charges on dopant atom sites, which are fixed in the crystal lattice and are unable to move. On the *n*-type side, positive ion cores are exposed. On the *p*-type side, negative ion cores are exposed. An electric field \hat{E} forms between the positive ion cores in the *n*-type material and negative ion cores in the *p*-type material. This region is called the depletion region since the electric field quickly sweeps free carriers out, hence the region is depleted of free carriers. A "built in" potential V_{bi} due to \hat{E} is formed at the junction.

<http://www.asdn.net/asdn/physics/p-n-junctions.shtml>

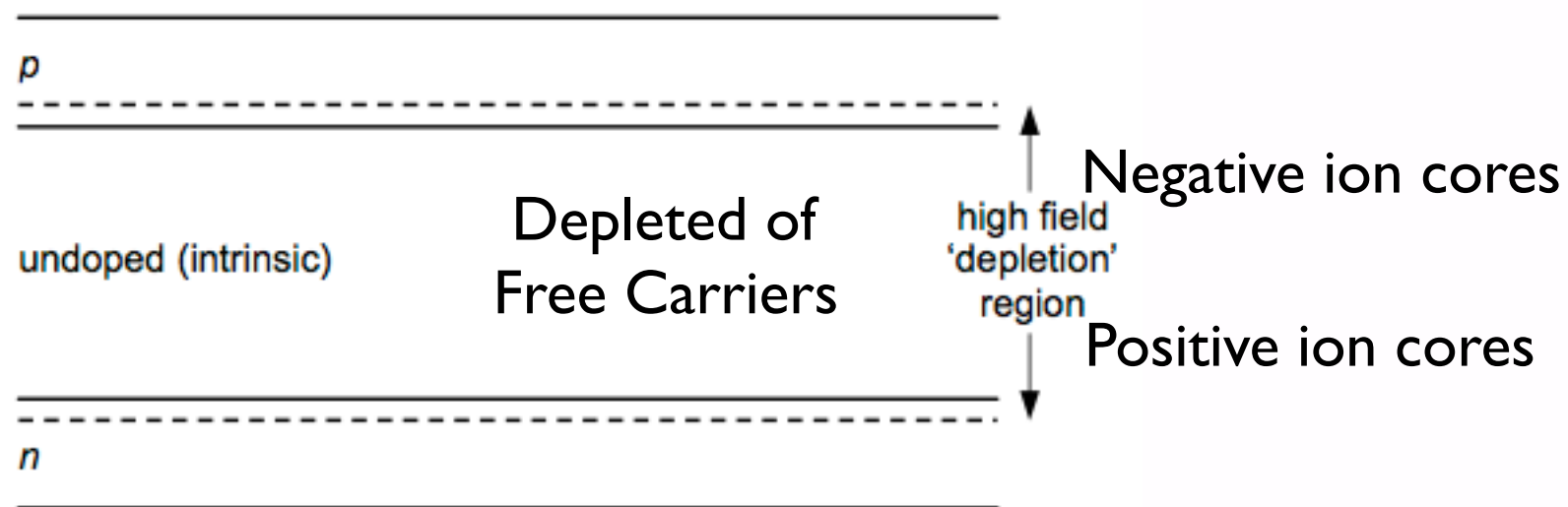


Figure 2.5. Schematic of an a-Si:H solar cell.

Carrier Movement in Equilibrium

A p-n junction with no external inputs represents an equilibrium between carrier generation, recombination, diffusion and drift in the presence of the electric field in the depletion region. Despite the presence of the electric field, which creates an impediment to the diffusion of carriers across the electric field, some carriers still cross the junction by diffusion. In the animation below, most majority carriers which enter the depletion region move back towards the region from which they originated. However, statistically some carriers will have a high velocity and travel in a sufficient net direction such that they cross the junction. Once a majority carrier crosses the junction, it becomes a minority carrier. It will continue to diffuse away from the junction and can travel a distance on average equal to the diffusion length before it recombines. The current caused by the diffusion of carriers across the junction is called a diffusion current. Remember that in an actual p-n junction the number and velocity of the carriers is much greater and that the number of carriers crossing the junction are much larger.

Minority carriers which reach the edge of the diffusion region are swept across it by the electric field in the depletion region. This current is called the drift current. In equilibrium the drift current is limited by the number of minority carriers which are thermally generated within a diffusion length of the junction.

In equilibrium, the net current from the device is zero. The electron drift current and the electron diffusion current exactly balance out (if they did not there would be a net buildup of electrons on either one side or the other of the device). Similarly, the hole drift current and the hole diffusion current also balance each other out.

- Carrier Generation
- Carrier Recombination
- Carrier Diffusion
- Carrier Drift in Depletion Region
due to inherent field

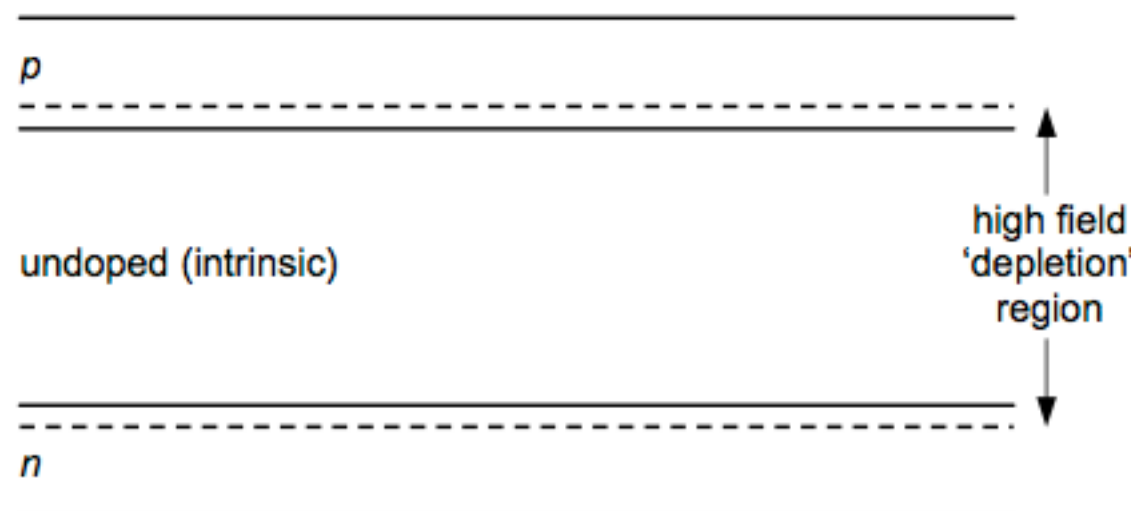


Figure 2.5. Schematic of an a-Si:H solar cell.

On average a minority carrier
Travels the diffusion length
Before recombining
This is the diffusion current

Carriers in the depletion region
Are carried by the electric field
This is the drift current

In equilibrium drift = diffusion
Net current = 0

If an external voltage is placed across the diode with the same polarity as the built-in potential, the depletion zone continues to act as an insulator, preventing any significant electric current flow (unless electron/hole pairs are actively being created in the junction by, for instance, light. see [photodiode](#)). This is the *reverse bias* phenomenon. However, if the polarity of the external voltage opposes the built-in potential, recombination can once again proceed, resulting in substantial electric current through the p–n junction (i.e. substantial numbers of electrons and holes recombine at the junction). For silicon diodes, the built-in potential is approximately 0.7 V (0.3 V for Germanium and 0.2 V for Schottky). Thus, if an external current is passed through the diode, about 0.7 V will be developed across the diode such that the P-doped region is positive with respect to the N-doped region and the diode is said to be "turned on" as it has a *forward bias*.

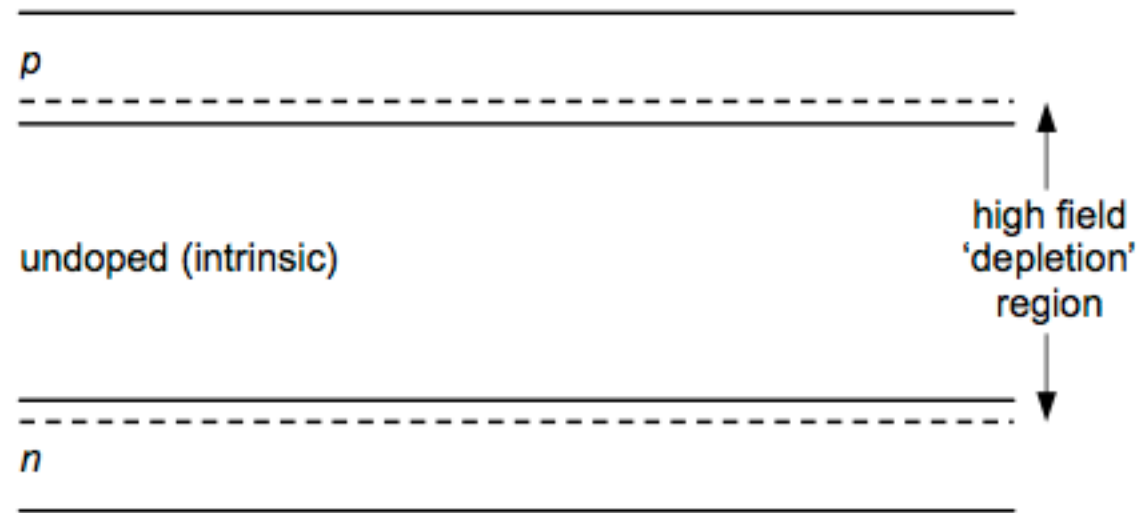
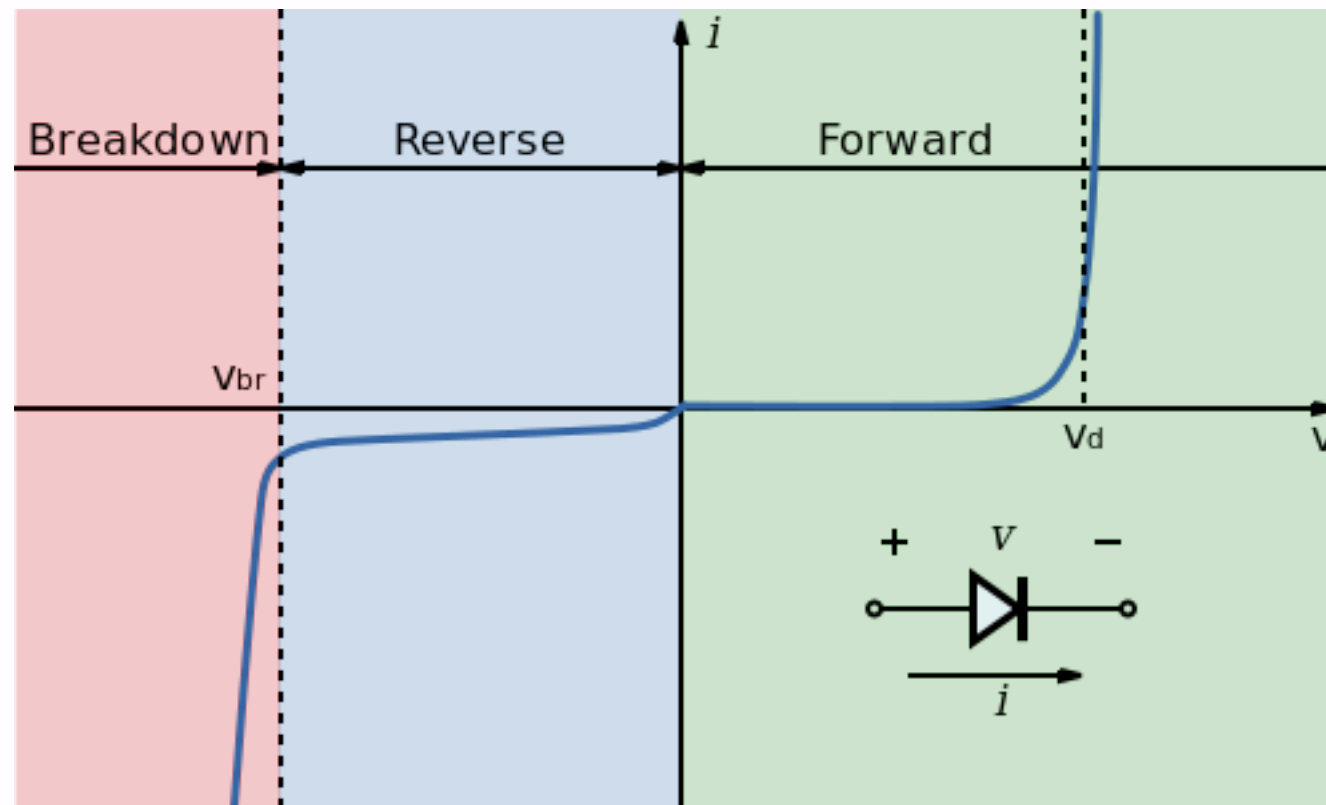


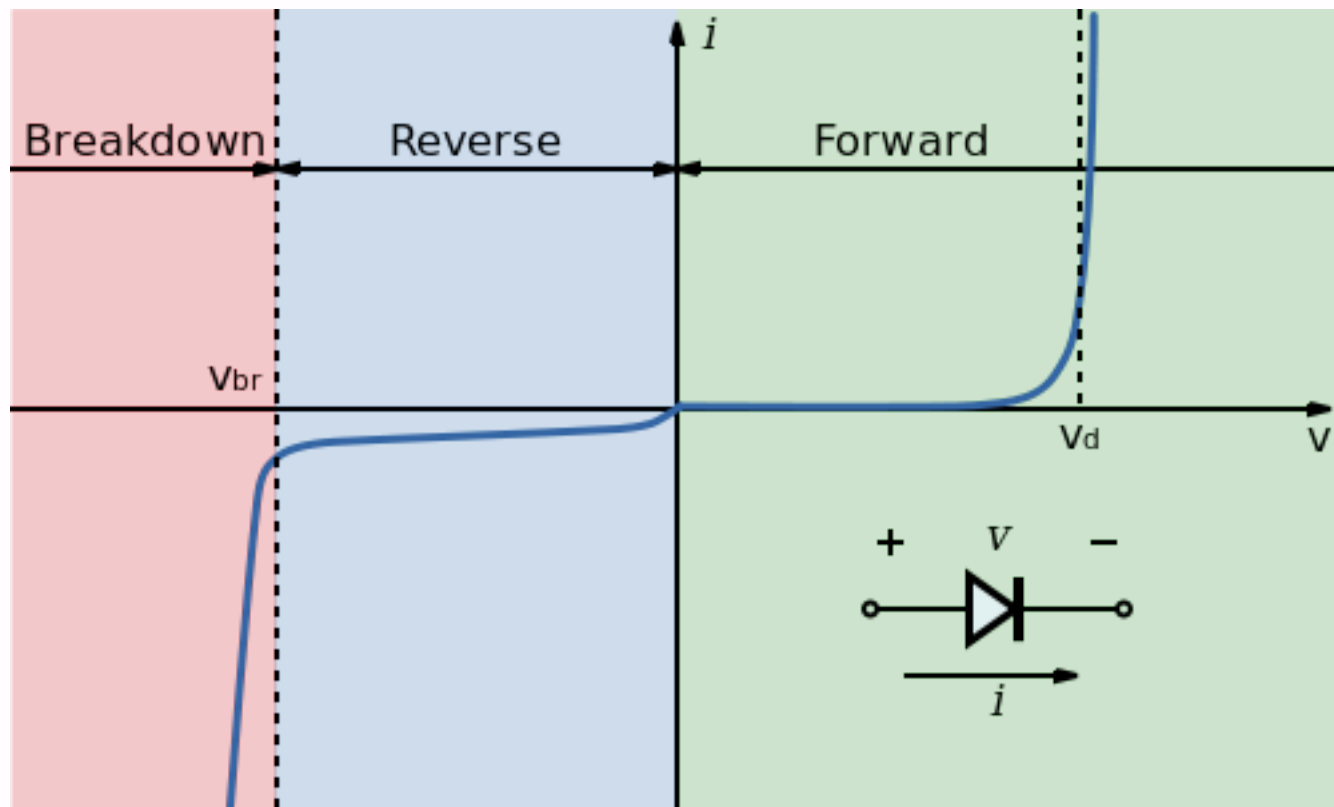
Figure 2.5. Schematic of an a-Si:H solar cell.

If an external voltage is placed across the diode with the same polarity as the built-in potential, the depletion zone continues to act as an insulator, preventing any significant electric current flow (unless electron/hole pairs are actively being created in the junction by, for instance, light. see [photodiode](#)). This is the *reverse bias* phenomenon. However, if the polarity of the external voltage opposes the built-in potential, recombination can once again proceed, resulting in substantial electric current through the p–n junction (i.e. substantial numbers of electrons and holes recombine at the junction). For silicon diodes, the built-in potential is approximately 0.7 V (0.3 V for Germanium and 0.2 V for Schottky). Thus, if an external current is passed through the diode, about 0.7 V will be developed across the diode such that the P-doped region is positive with respect to the N-doped region and the diode is said to be "turned on" as it has a *forward bias*.



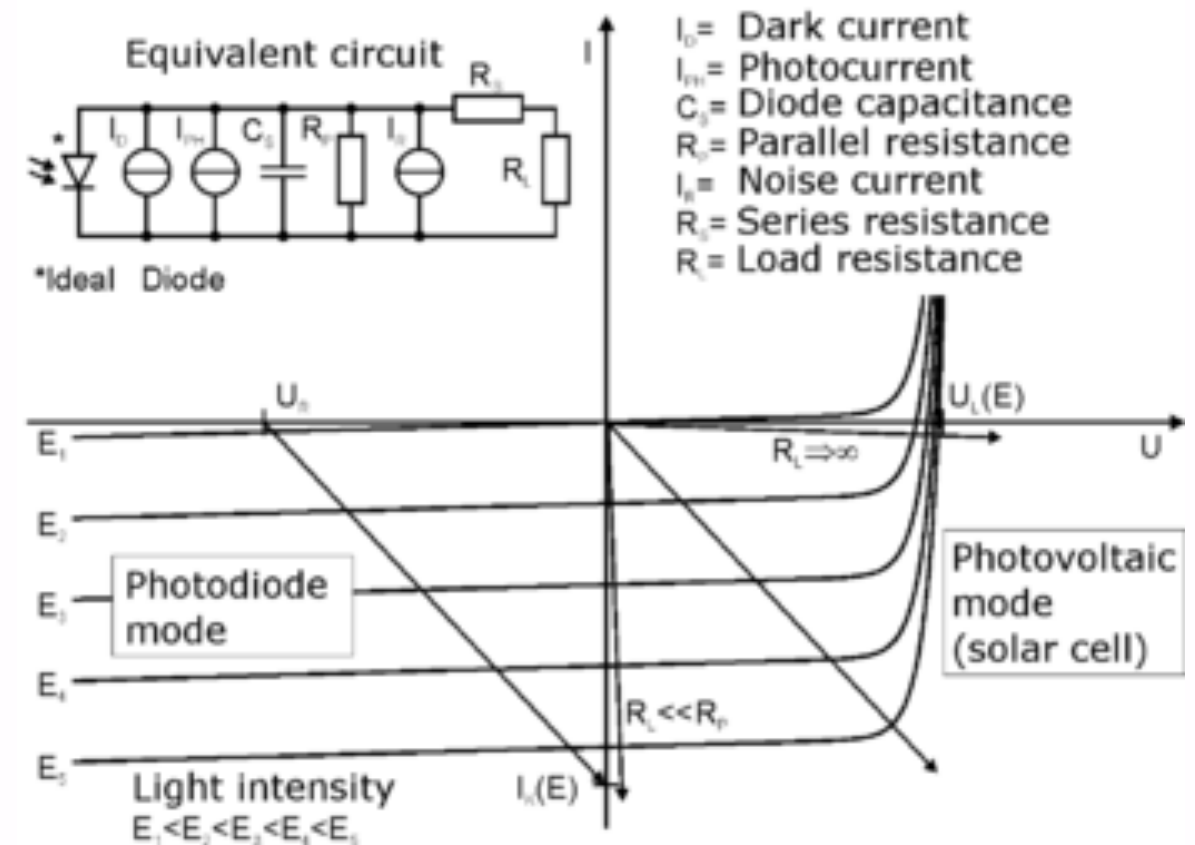
I–V characteristics of a p–n junction diode (not to scale—the current in the reverse region is magnified compared to the forward region, resulting in the apparent slope discontinuity at the origin; the actual I–V curve is smooth across the origin).

<http://en.wikipedia.org/wiki/Diode>



I-V characteristics of a p-n junction diode (not to scale—the current in the reverse region is magnified compared to the forward region, resulting in the apparent slope discontinuity at the origin; the actual I-V curve is smooth across the origin).

<http://en.wikipedia.org/wiki/Diode>



Electron-hole pair

- Generation
- Recombination

Carrier lifetime ($1 \mu\text{s}$)

Carrier diffusion length ($100\text{-}300 \mu\text{m}$)

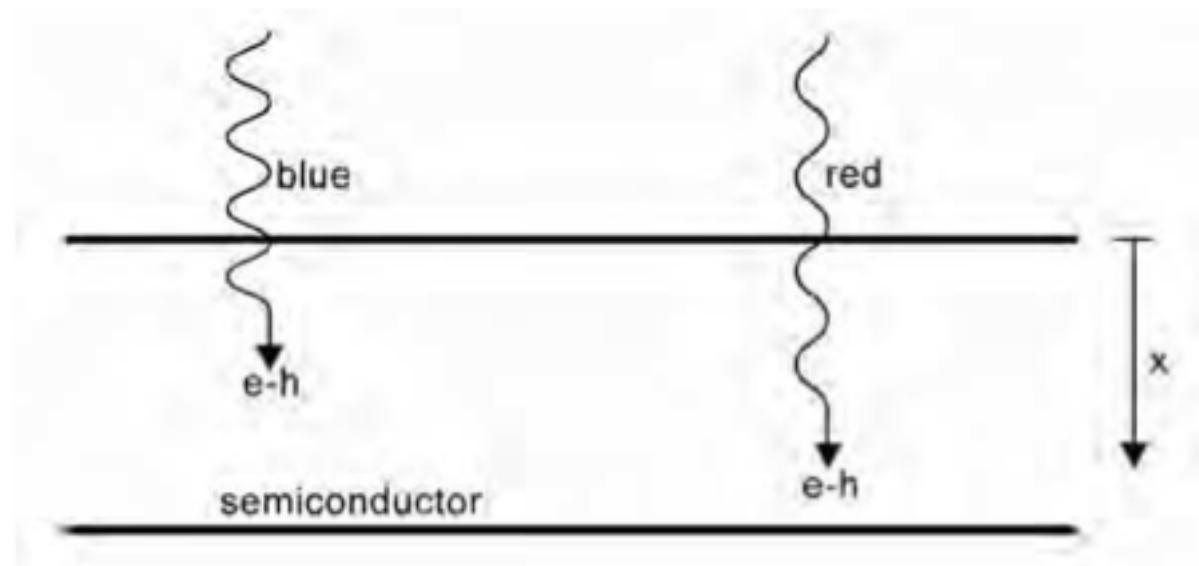


Figure 2.7. The light energy dependency of electron-hole generation.

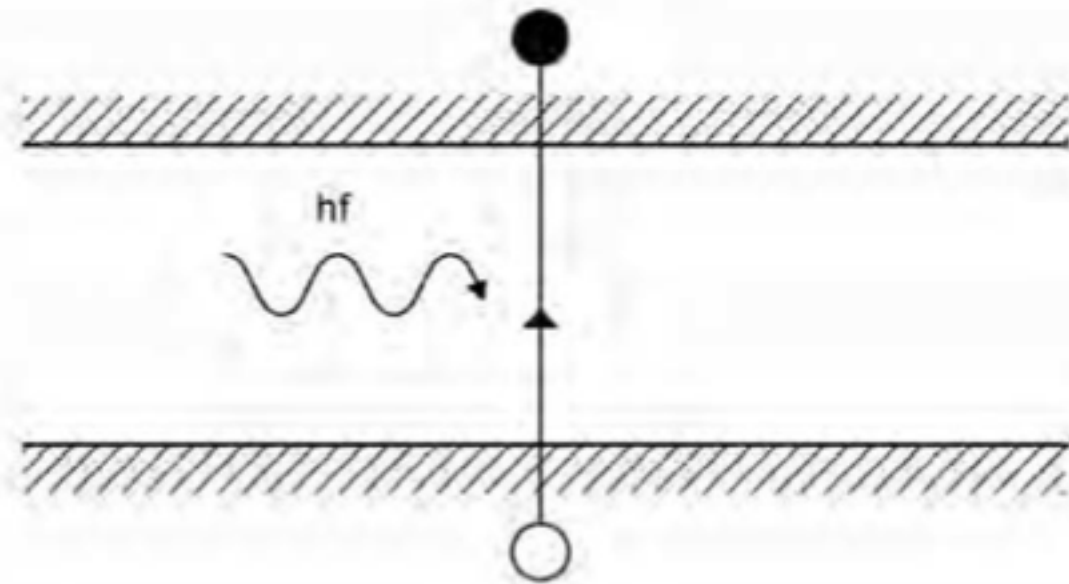


Figure 2.6. The creation of electron-hole pairs when illuminated with light of energy $E_{ph} = hf$, where $E_{ph} > E_g$.

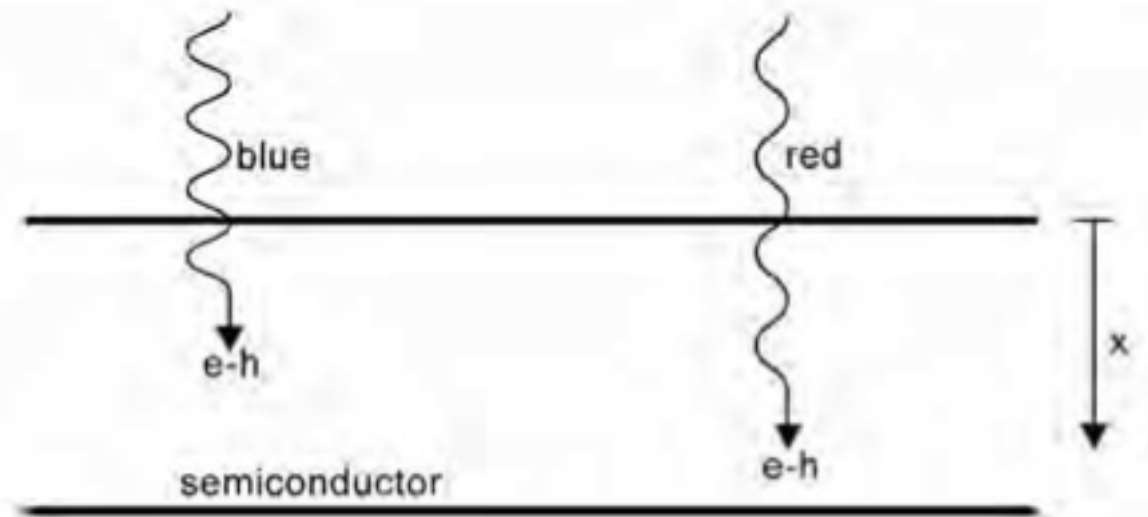


Figure 2.7. The light energy dependency of electron-hole generation.

N=photon flux

α =abs. coef.

x=surface depth

G=generation rate

e-h pairs

$$G = \alpha N e^{-\alpha x}$$

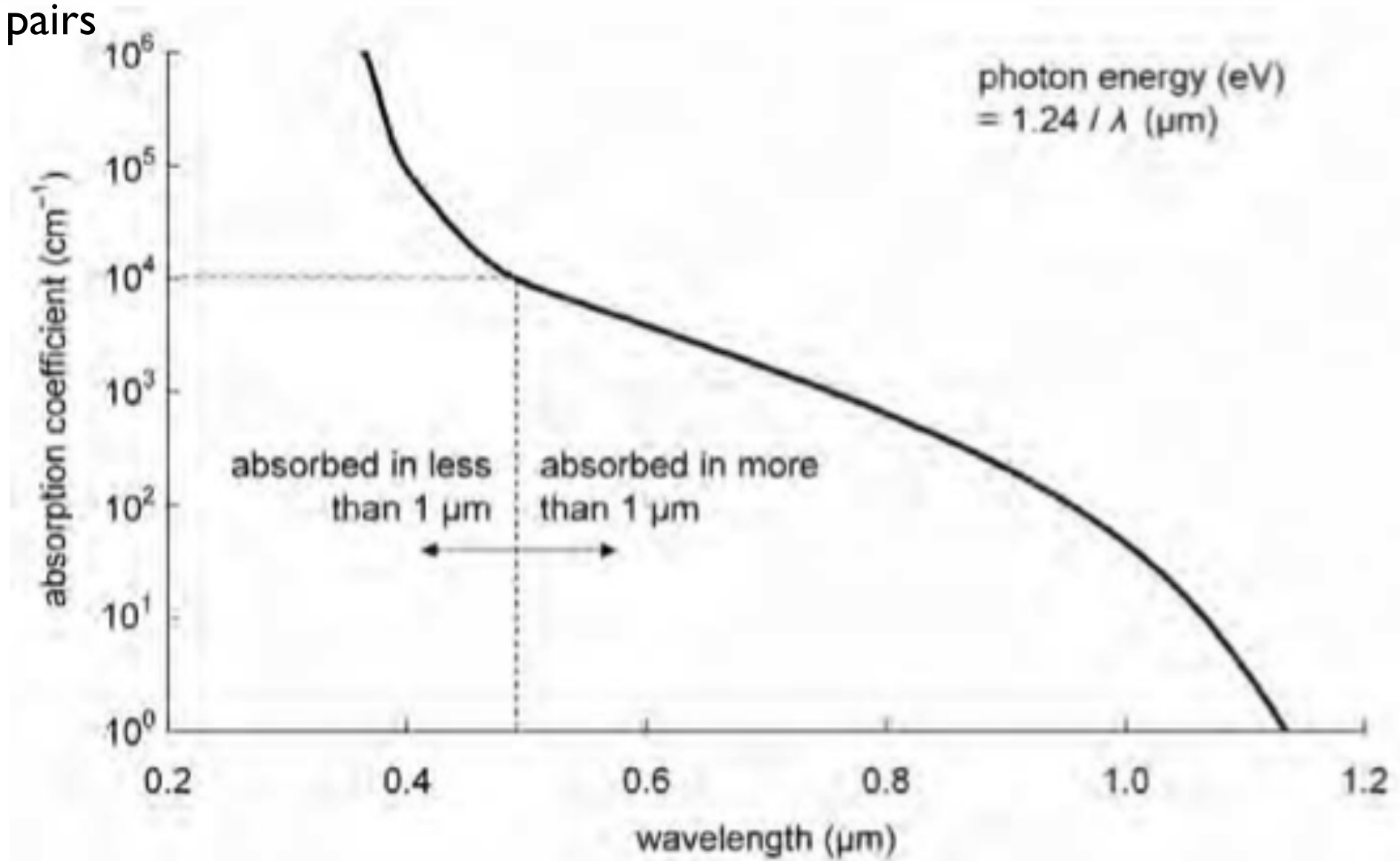


Figure 2.8. The absorption coefficient, α , of silicon at 300 K as a function of the vacuum wavelength of light.

N =photon flux
 α =abs. coef.
 x =surface depth
 G =generation rate
 e-h pairs

$$G = \alpha N e^{-\alpha x}$$

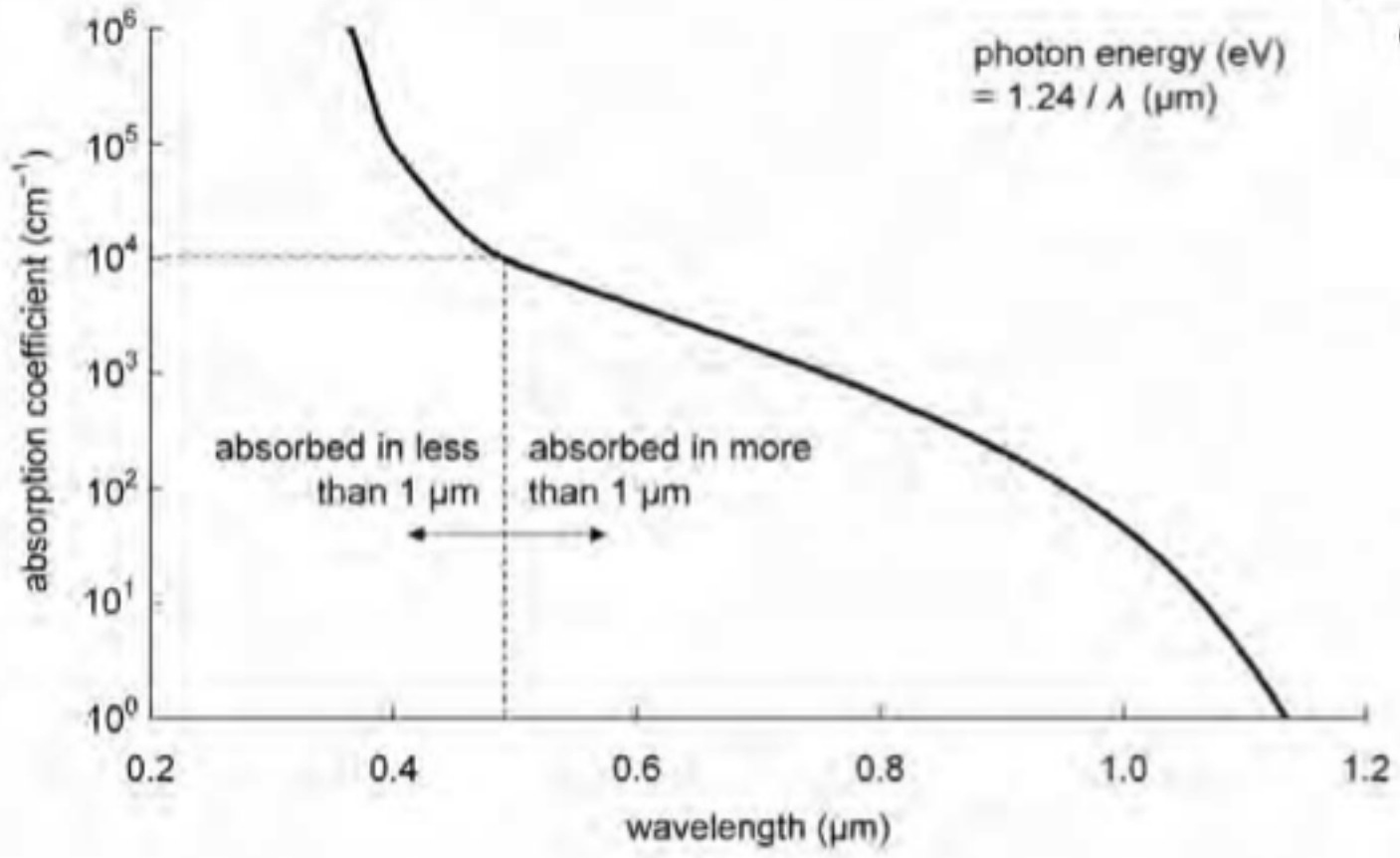


Figure 2.8. The absorption coefficient, α , of silicon at 300 K as a function of the vacuum wavelength of light.

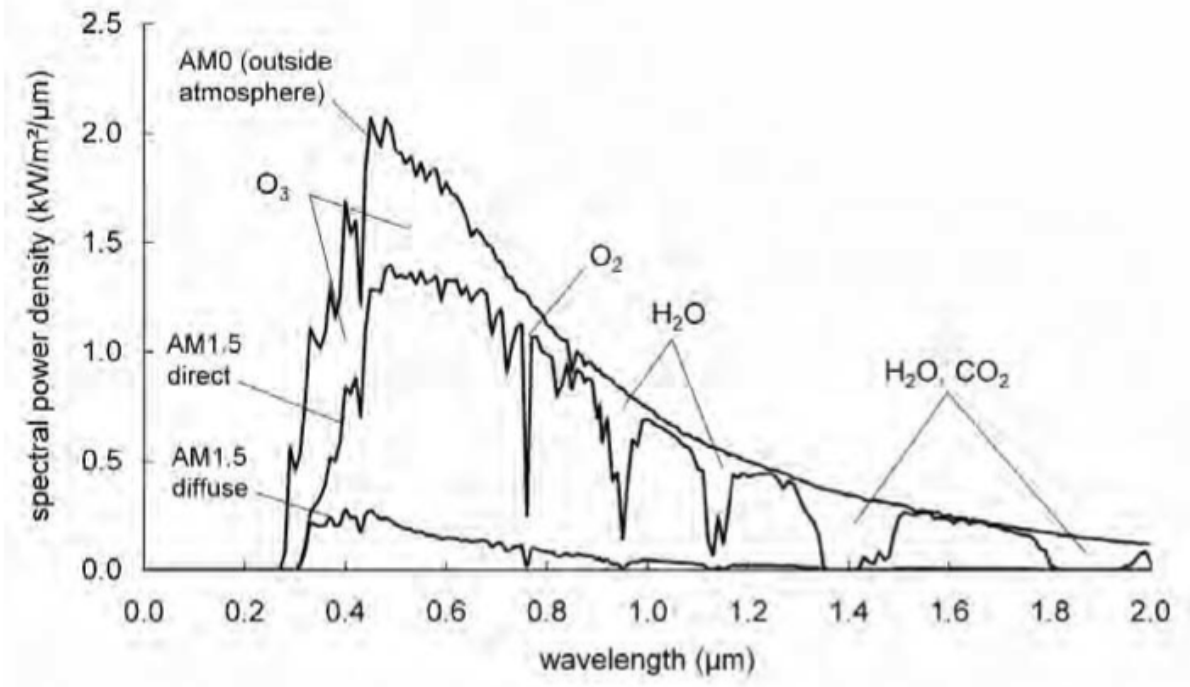


Figure 1.6. The spectral power density of sunlight, outside the atmosphere (AM0) and at the earth's surface (AM1.5), showing absorption from various atmospheric components.

When the light is switched off, the system must return to a state of equilibrium and the electron-hole pairs generated by the light must disappear. With no external source of energy, the electrons and holes wander around until they meet up and *recombine*. Any defects or impurities within or at the surface of the semiconductor promote recombination.

The *carrier lifetime* of a material is defined as the average time for recombination to occur after electron-hole generation. For silicon, this is typically 1 μs . Similarly, the *carrier diffusion length* is the average distance a carrier can move from point of generation until it recombines. For silicon, this is typically 100–300 μm . These two parameters give an indication of material quality and suitability for solar cell use. However, no power can be produced from a semiconductor without a means of giving directionality to the moving electrons. Therefore, functional solar cells are typically produced from semiconductor material by the addition of a rectifying *p-n* junction.

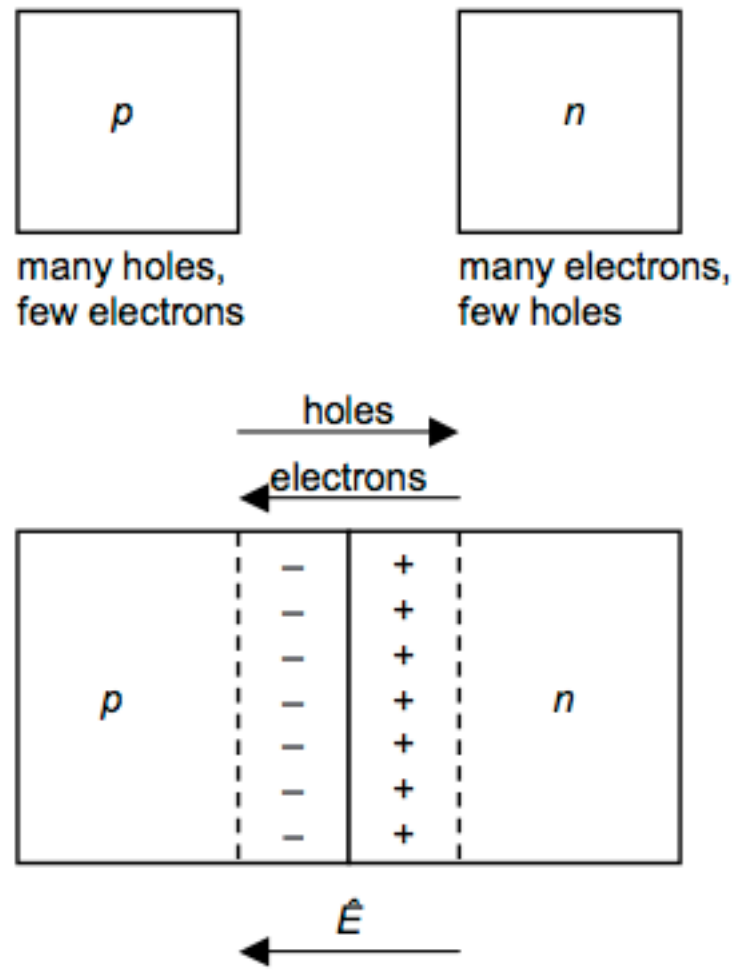


Figure 2.9. Formation of a p - n junction.

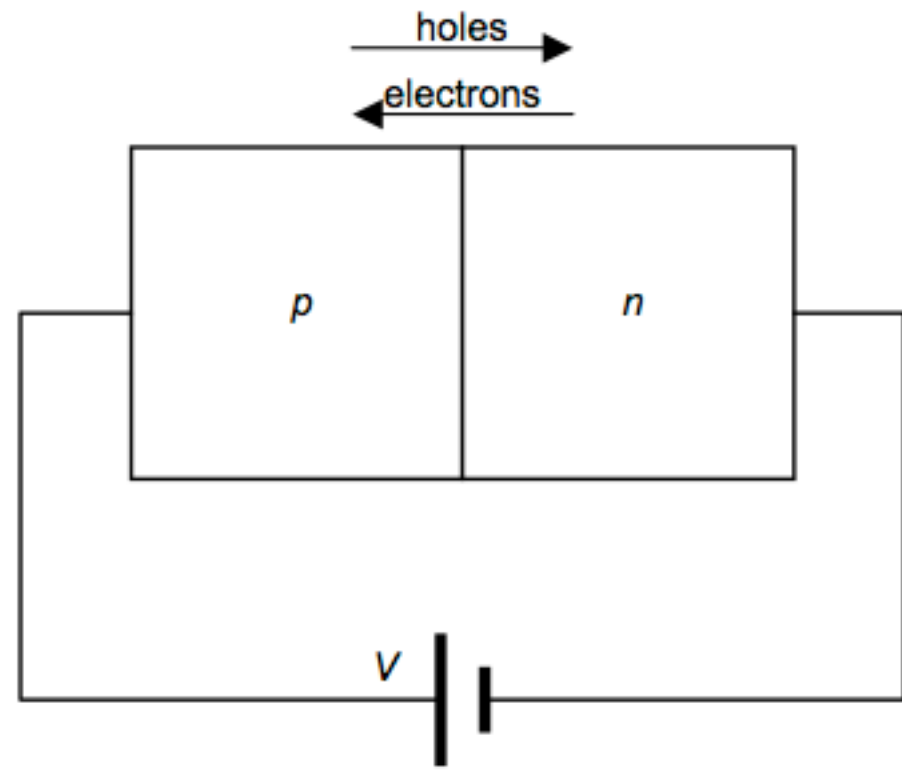


Figure 2.10. Application of a voltage to a p - n junction.

Once \hat{E} is no longer large enough to stop the flow of electrons and holes, a current is produced. The built in potential reduces to $V_{bi} - V$ and the current flow increases exponentially with the applied voltage. This phenomenon results in the *Ideal Diode Law*, expressed as

$$I = I_0 \left[\exp\left(\frac{qV}{kT}\right) - 1 \right] \quad (2.2)$$

where I is the current, I_0 is the dark saturation current (the diode leakage current density in the absence of light), V is the applied voltage, q is the charge on an electron, k is Boltzmann's constant and T is absolute temperature.

Note that

- I_0 increases as T increases
- I_0 decreases as material quality increases
- at 300 K, $kT/q = 25.85$ mV, the *thermal voltage*.

For actual diodes, the Eqn. (2.2) becomes

$$I = I_0 \left[\exp\left(\frac{qV}{nkT}\right) - 1 \right]$$

where n is the ideality factor, a number between 1 and 2 that typically decreases.

I_0 is dark saturation current
 q electron charge
 V applied voltage
 k Boltzmann Constant
 T absolute temperature

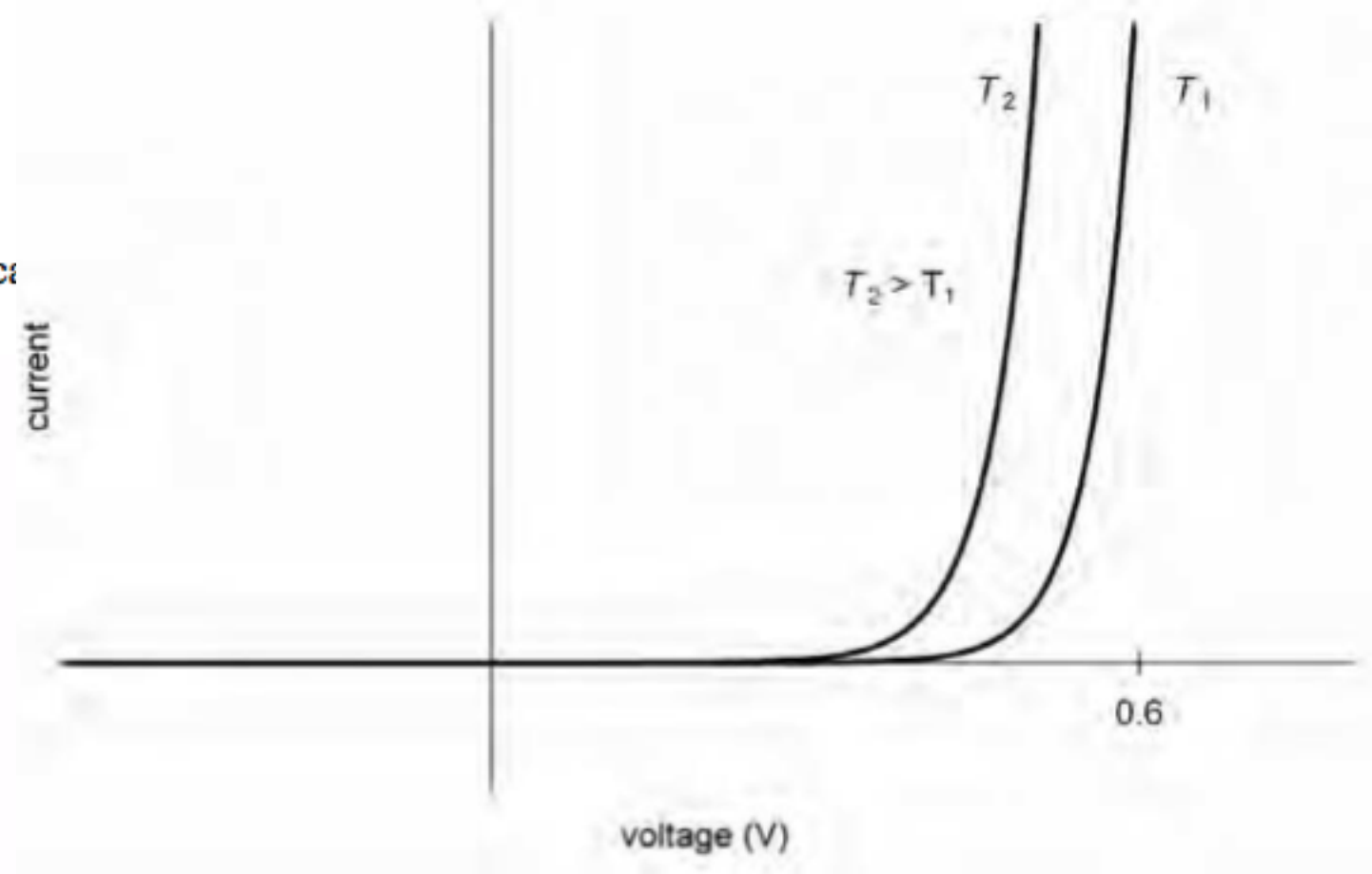


Figure 2.11. The diode law for silicon—current as a function of voltage for temperatures T_1 and T_2 ($T_2 > T_1$). For a given current, the curve shifts by approximately 2 mV/°C.

- 2.1. The absorption coefficient of silicon decreases from $1.65 \times 10^6 \text{ cm}^{-1}$ at $0.3 \text{ }\mu\text{m}$ wavelength, to 4400 cm^{-1} at $0.6 \text{ }\mu\text{m}$ and 3.5 cm^{-1} at $1.1 \text{ }\mu\text{m}$. Assuming zero reflection from both front and rear surfaces at each wavelength, calculate and sketch the generation rate of electron-hole pairs, normalised to the surface generation rate, across a silicon cell of $300 \text{ }\mu\text{m}$ thickness.
- 2.2. In terms of the electronic properties of semiconductors, explain why the absorption coefficient increases with increasing photon energy, for energies near the semiconductor bandgap (see Green, 1992 or similar for further information).

N=photon flux
 α =abs. coef.
 x=surface depth
 G=generation rate
 e-h pairs

$$G = \alpha N e^{-\alpha x}$$

At $x = 0$ $G = \alpha N$
 Function is $G/G_{x=0} = \exp(-\alpha x)$

Electrons absorb the band gap energy

Silicon Solar Cell

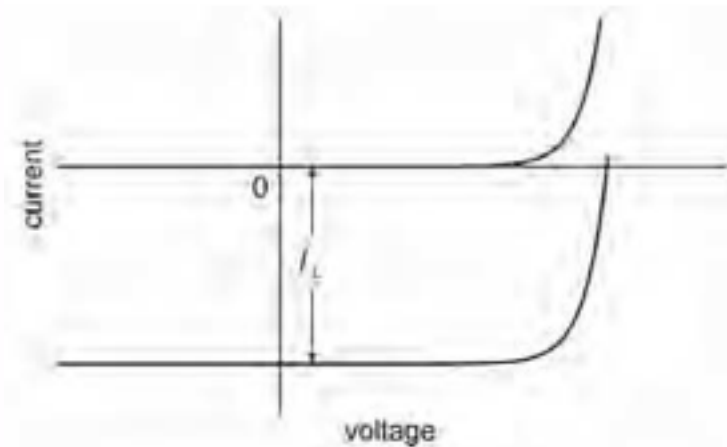
The electric field \hat{E} at the p - n junction sweeps electrons to the n side and holes to the p side. The ideal flow at short circuit is shown in Fig. 3.2. However, some electron-hole (e-h) pairs get lost before collection, as shown in Fig. 3.3.

In general, the closer the point of e-h generation to the p - n junction, the better the chance of 'collection'. 'Collected carriers' are those that generate a finite current when $V = 0$. Chances of collection are particularly good if the e-h pairs are generated within a *diffusion length* of the junction, as discussed in Chapter 2.

$$I = I_0 \left[\exp\left(\frac{qV}{nkT}\right) - 1 \right] - I_L$$

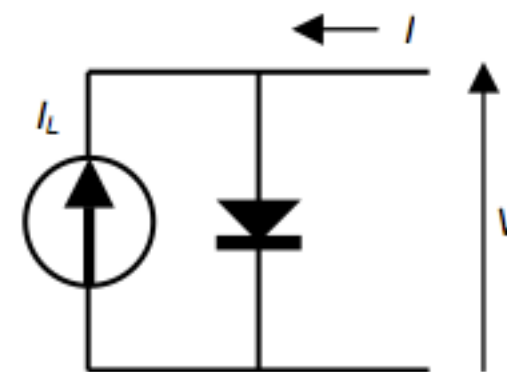
$$I = I_L - I_0 \left[\exp\left(\frac{qV}{nkT}\right) - 1 \right]$$

Diode Equation



(a)

Photovoltaic Equation



(b)

Figure 3.4. The effect of light on the current-voltage characteristics of a p - n junction.

Efficiency of Light Conversion to e-h pair

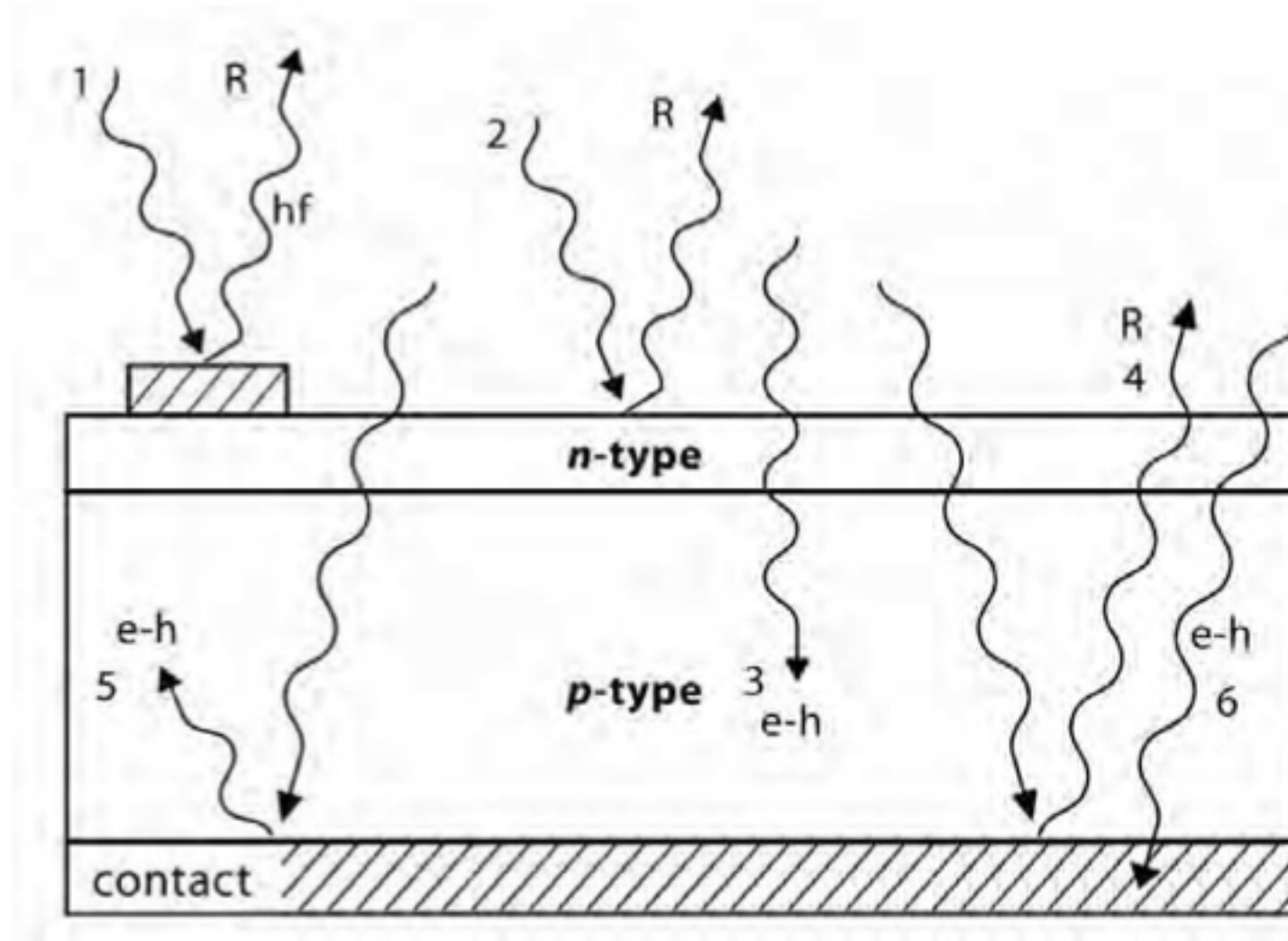


Figure 3.1. Behaviour of light shining on a solar cell. (1) Reflection and absorption at top contact. (2) Reflection at cell surface. (3) Desired absorption. (4) Reflection from rear out of cell—weakly absorbed light only. (5) Absorption after reflection. (6) Absorption in rear contact.

Short Circuit Current, $V = 0$

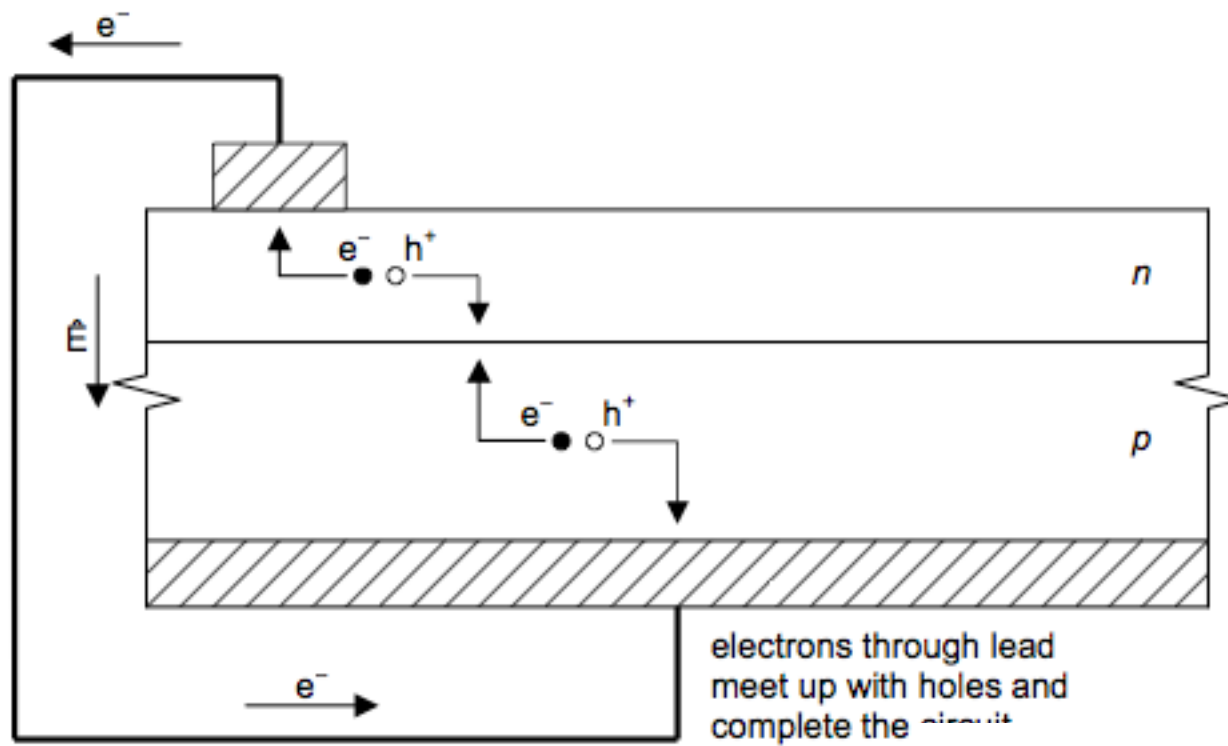


Figure 3.2. The ideal short circuit flow of electrons and holes

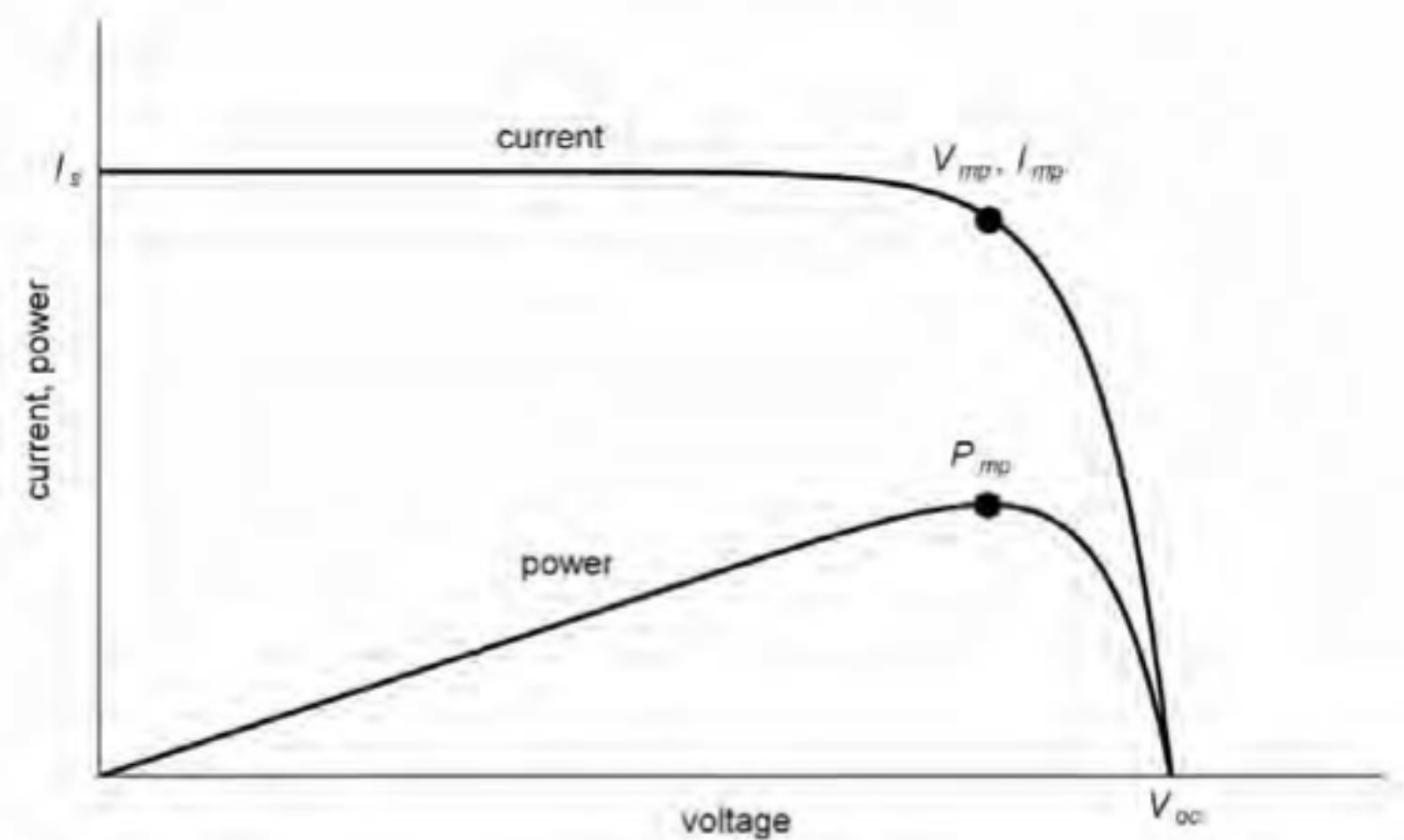


Figure 3.5. Typical representation of an I-V curve, showing short-circuit current (I_{sc}) and open-circuit voltage (V_{oc}) points, as well as the maximum power point (V_{mp}, I_{mp}).

Inefficiency of the e-h pair formation and collection process

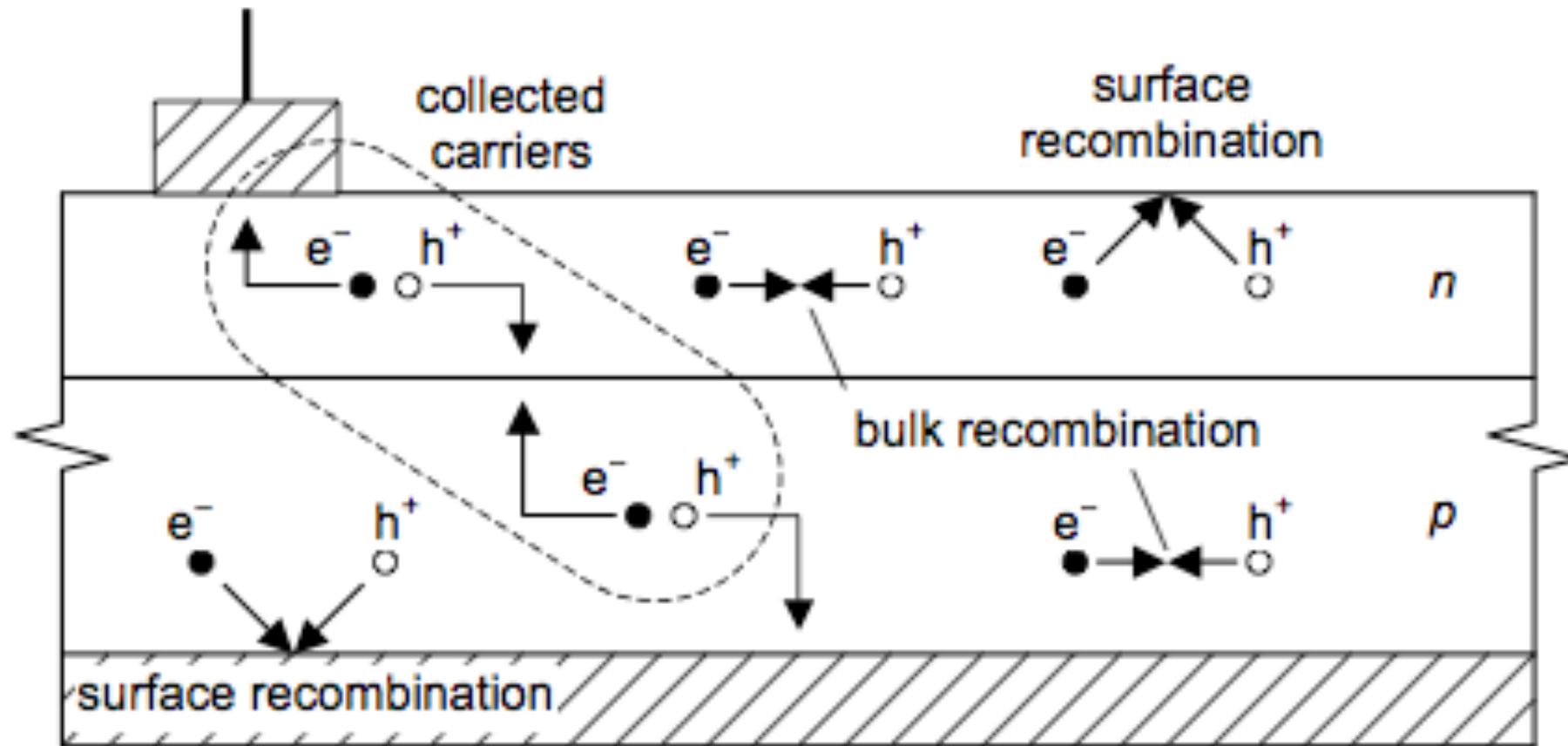
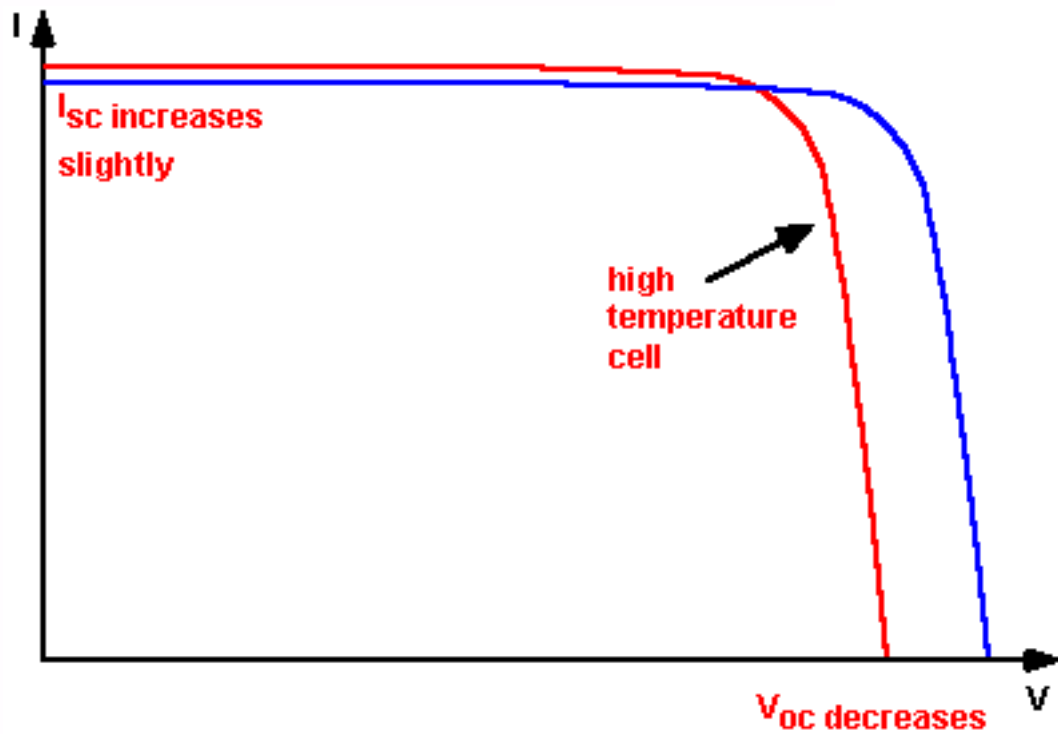
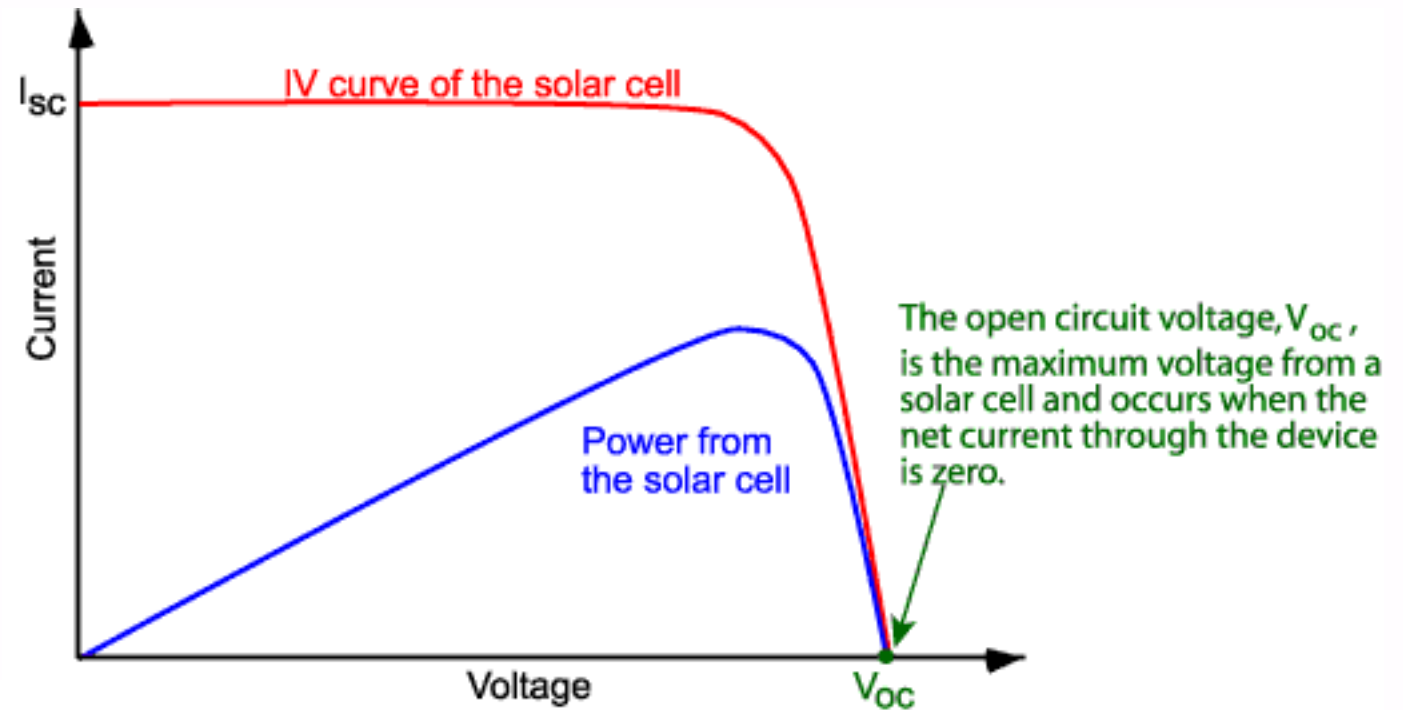


Figure 3.3. Possible modes of recombination of electron-hole pairs, showing 'collection' of carriers that do not recombine.

Open Circuit Voltage



$$V_{OC} = \frac{nkT}{q} \ln \left(\frac{I_L}{I_0} + 1 \right)$$

Voc drops in T because I0 increases

$$I_0 = BT^\gamma \exp \left(\frac{-E_{g0}}{kT} \right)$$

Maximum Power

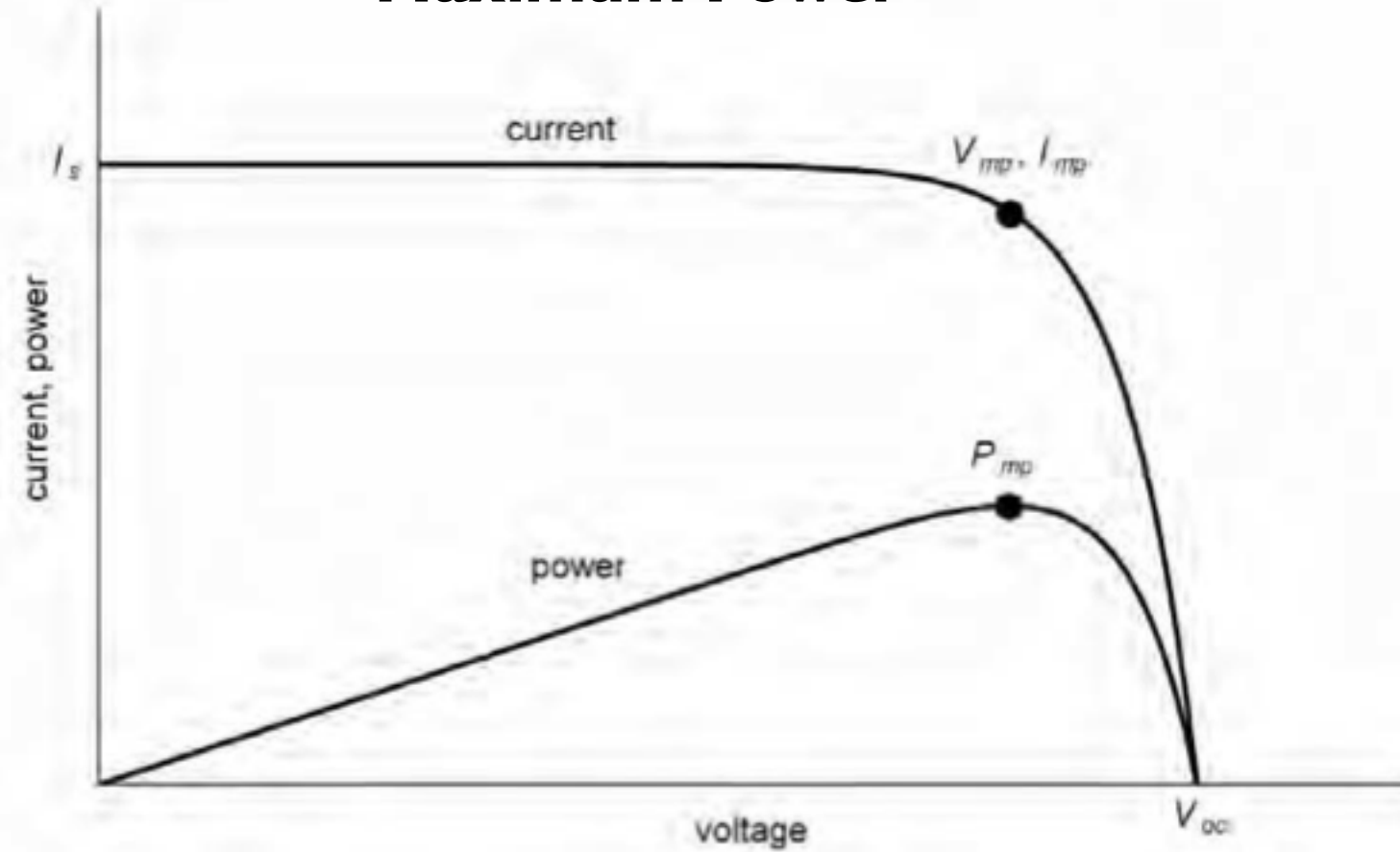


Figure 3.5. Typical representation of an I-V curve, showing short-circuit current (I_{sc} and open-circuit voltage (V_{oc}) points, as well as the maximum power point (V_{mp} , I_{mp}).

$$\frac{d(IV)}{dV} = 0$$

$$V_{mp} = V_{oc} - \frac{nkT}{q} \ln \left(\frac{V_{mp}}{(nkT/q)} + 1 \right)$$

$$I = I_L - I_0 \left[\exp \left(\frac{qV}{nkT} \right) - 1 \right]$$

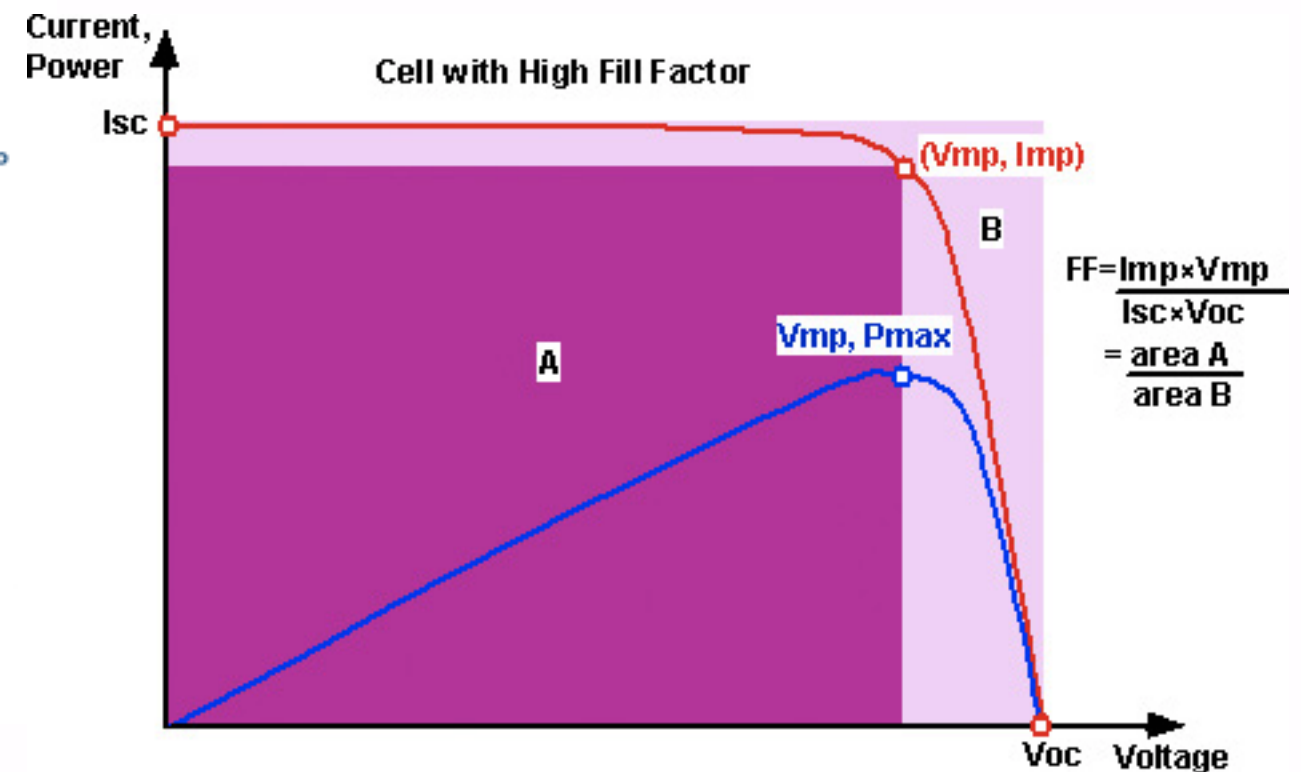
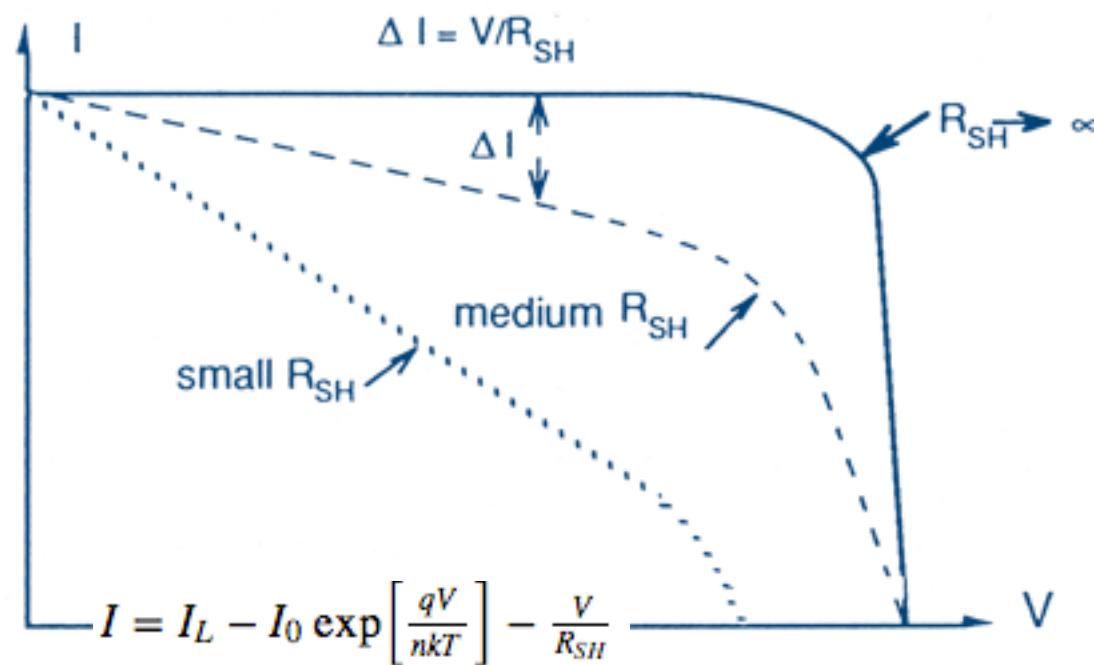
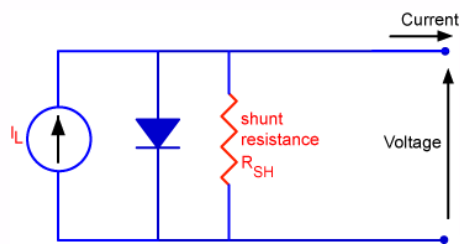
Fill Factor

The *fill factor (FF)*, is a measure of the junction quality and series resistance of a cell. It is defined as

$$FF = \frac{V_{mp} I_{mp}}{V_{oc} I_{sc}} \quad (3.5)$$

Hence

$$P_{mp} = V_{oc} I_{sc} FF \quad (3.6)$$



Effect of Shunt Resistance on fill factor

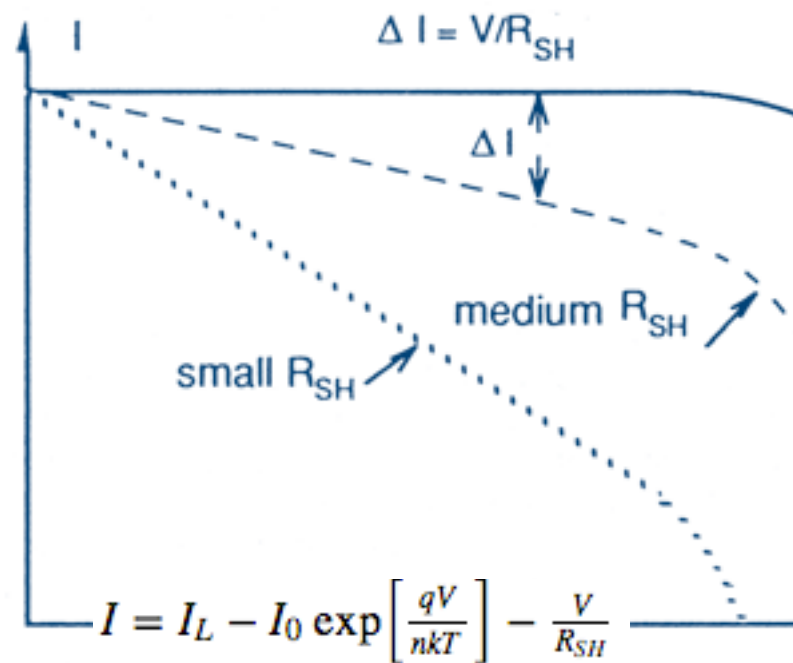
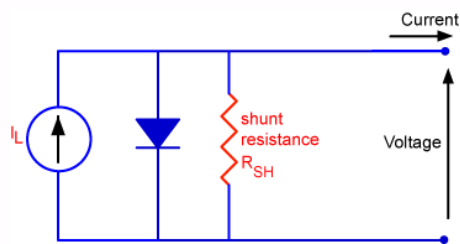
Fill Factor

The *fill factor (FF)*, is a measure of the junction quality and series resistance of a cell. It is defined as

$$FF = \frac{V_{mp} I_{mp}}{V_{oc} I_{sc}} \quad (3.5)$$

Hence

$$P_{mp} = V_{oc} I_{sc} FF \quad (3.6)$$



Effect of Shunt Resistance on fill factor

<http://www.pv.unsw.edu.au/information-for/online-photovoltaics-devices-applications/syllabus>

Solar cells generally have a parasitic series and shunt resistance associated with them, as shown in Fig. 3.10. Both types of parasitic resistance act to reduce the fill-factor.

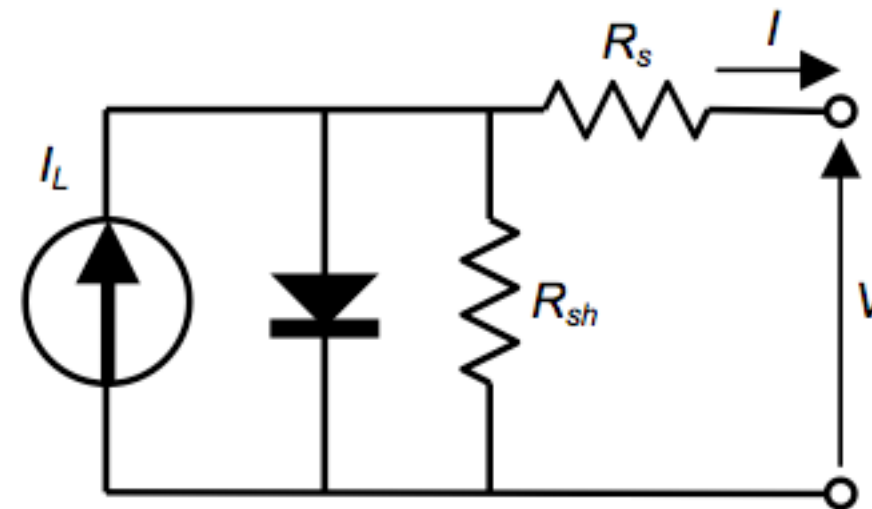


Figure 3.10. Parasitic series and shunt resistances in a solar cell circuit.

The major contributors to the series resistance (R_s) are the bulk resistance of the semiconductor material, the metallic contacts and interconnections, carrier transport through the top diffused layer, and contact resistance between the metallic contacts and the semiconductor. The effect of series resistance is shown in Fig. 3.11.

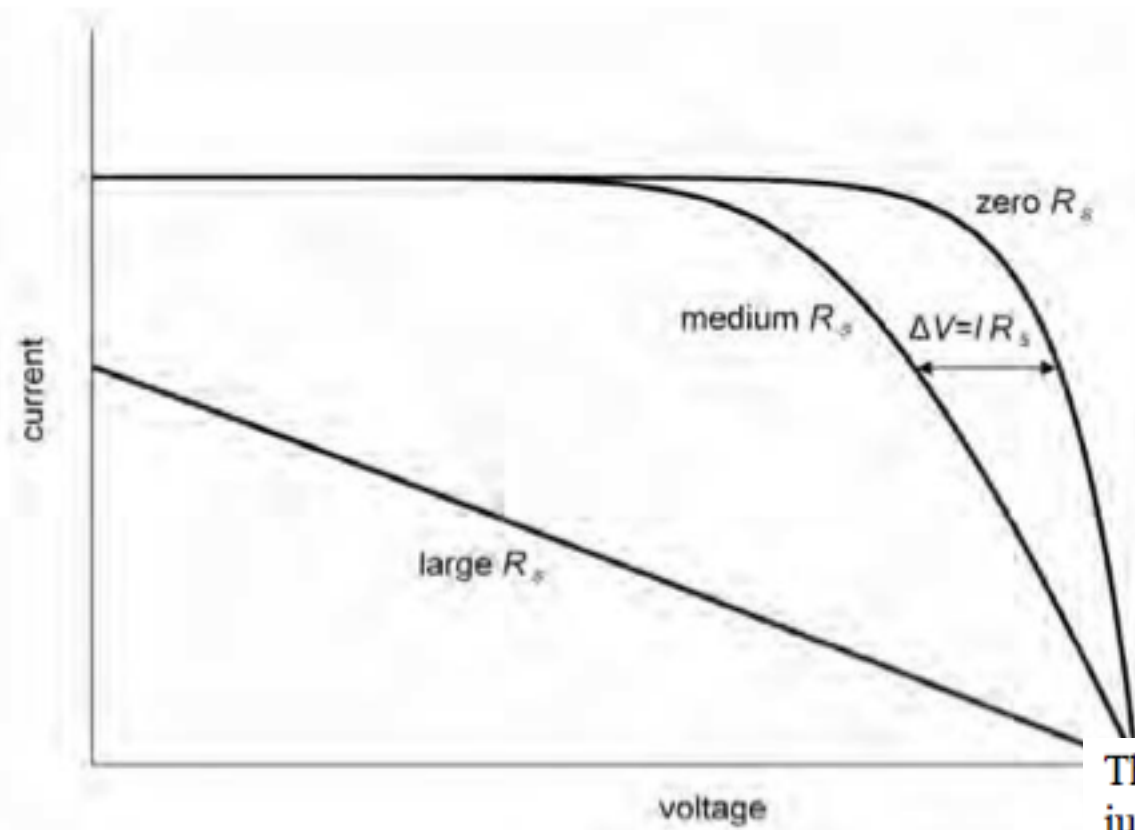


Figure 3.11. The effect of series resistance on fill factor

The shunt resistance (R_{sh}) is due to $p-n$ junction non-idealities and impurities near the junction, which cause partial shorting of the junction, particularly near cell edges. The effect of shunt resistance is shown in Fig. 3.12.

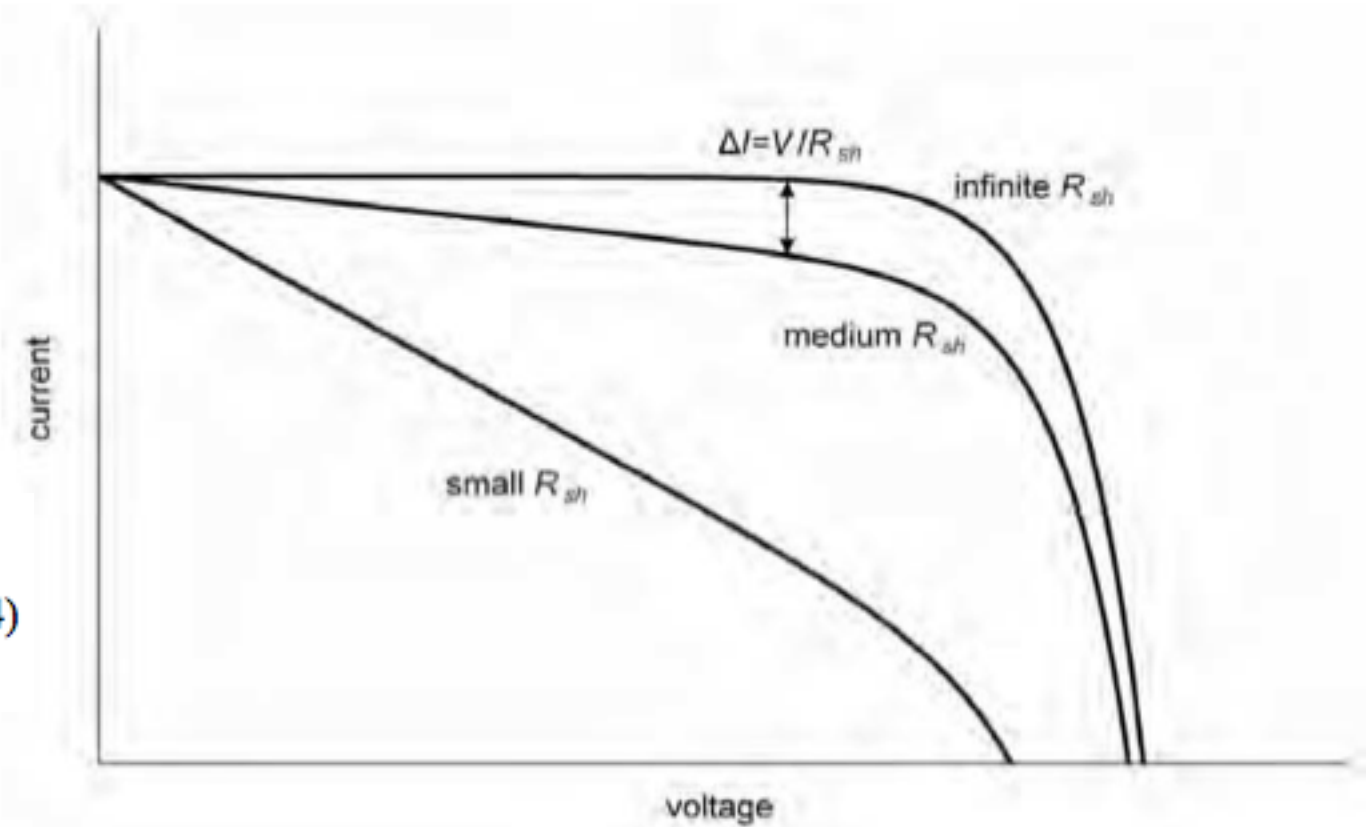


Figure 3.12. The effect of shunt resistance on fill factor in a solar cell.

$$I = I_L - I_0 \left[\exp\left(\frac{V + IR_s}{nkT/q}\right) - 1 \right] - \frac{V + IR_s}{R_{sh}} \quad (3.24)$$

Spectral Response

Solar cells respond to individual photons of incident light by absorbing them to produce an electron-hole pair, provided the photon energy (E_{ph}) is greater than the bandgap energy (E_g). Photon energy in excess of E_g is quickly dissipated as heat, as shown in Fig. 3.6.

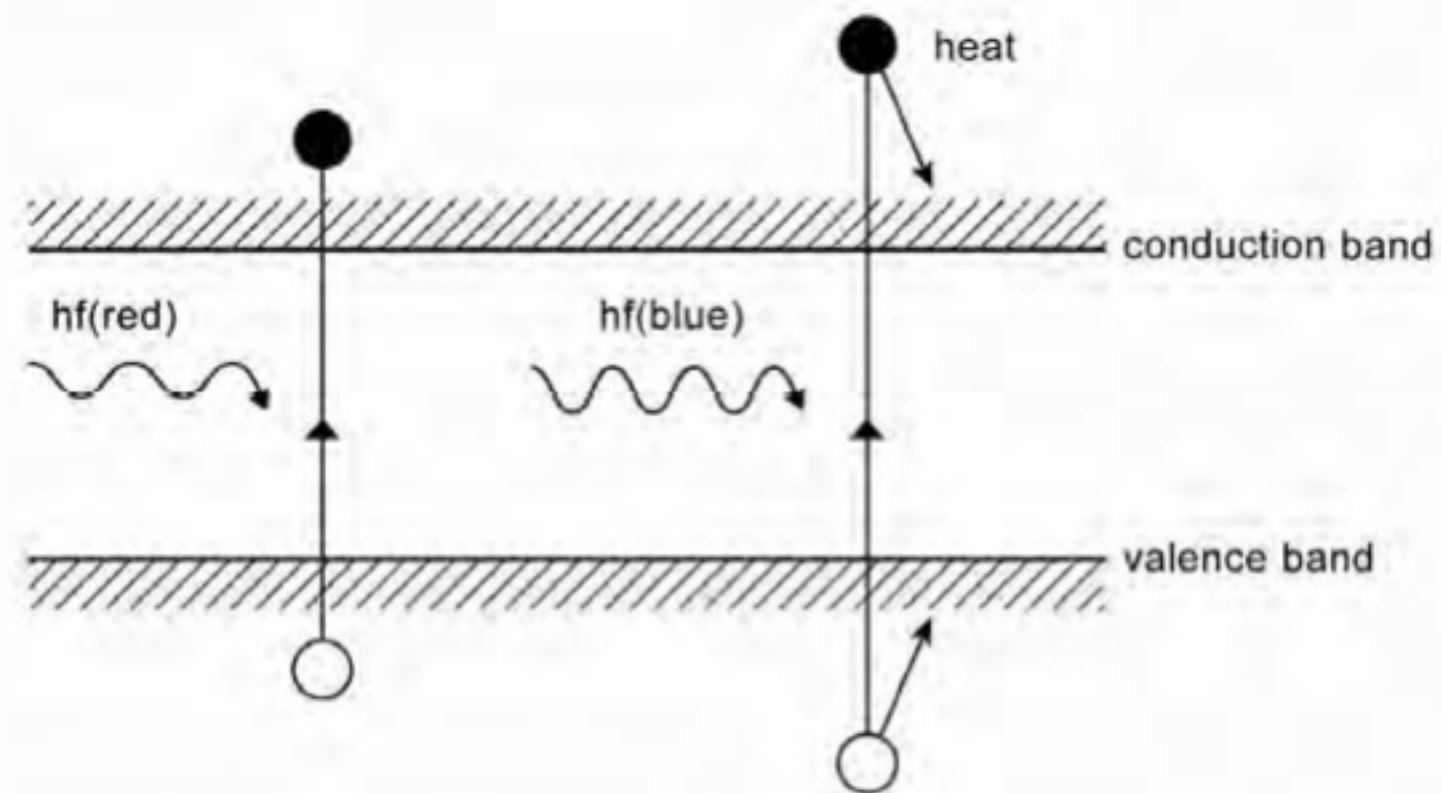


Figure 3.6. The creation of electron-hole pairs and dissipation of energy in excess of E_g .

Quantum Efficiency = number of e-h pairs made per photon

Band gap determines when this is greater than 0

Need band gap between 1.0 and 1.6 eV to match solar spectrum

Si 1.1 eV Cd 1.5 eV

Issues effecting quantum efficiency

Absorption spectrum

Band Gap

Spectral Responsivity = Amps per Watt of Incident Light

Short wavelengths => loss to heat

Long wavelengths => weak absorption/finite diffusion length

Spectral responsivity (SR) can be calculated as follows:

$$SR = \frac{I_{sc}}{P_{in}(\lambda)} = \frac{q \times n_e}{\frac{hc}{\lambda} \times n_{ph}} = \frac{q\lambda}{hc} EQE \quad (3.9)$$

where n_e is the flux of electrons, per unit time, flowing in an external circuit at short circuit conditions and I_{sc} is the short circuit current, n_{ph} is the flux of photons of wavelength λ incident on the cell per unit time, P_{in} is the incident light power and $EQE = (1 - R) \times IQE$ is the external efficiency, which differs from the internal quantum efficiency (IQE) in that the latter excludes the fraction, R , of light reflected from the top surface. $SR \rightarrow 0$ as $\lambda \rightarrow 0$, since there are fewer photons in each watt of incident light.

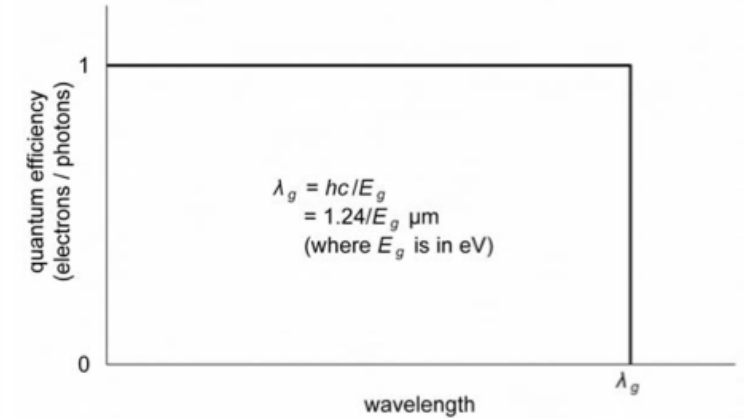


Figure 3.7. Bandgap limitations on the quantum efficiency of silicon solar cells.

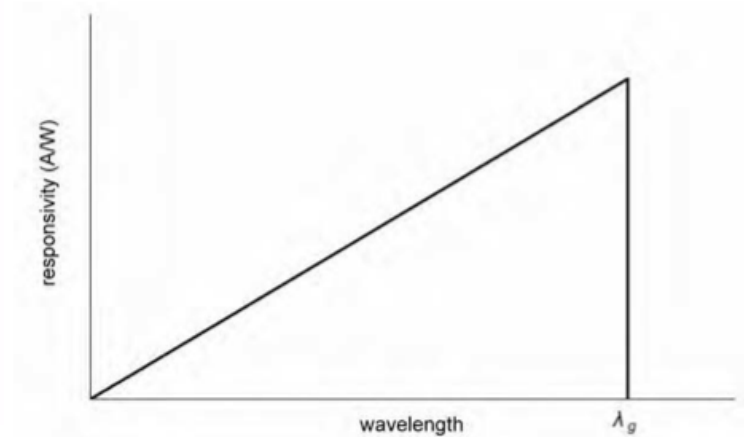


Figure 3.8. The quantum limit of spectral responsivity as a function of wavelength.

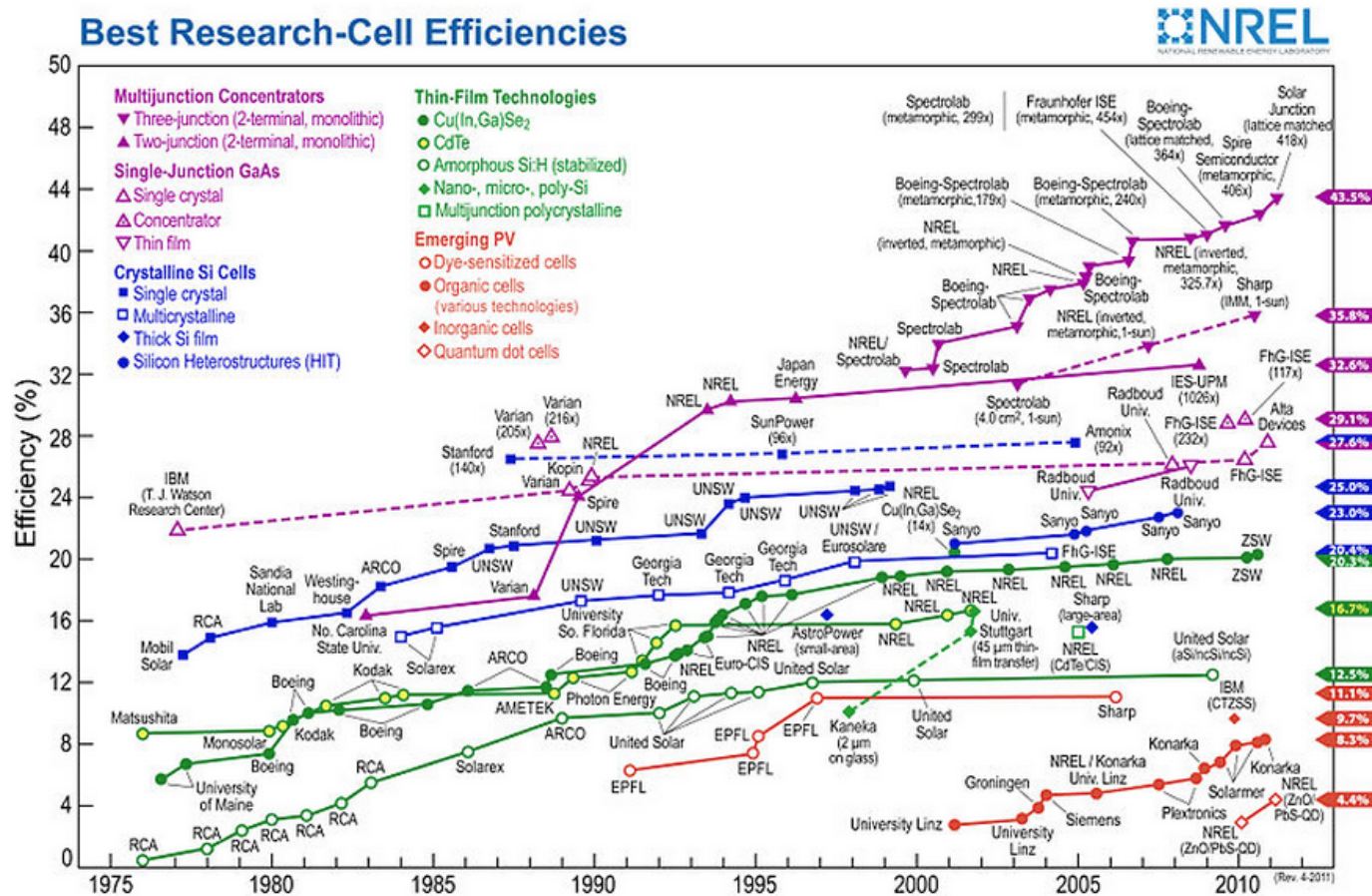
EXERCISES

- 3.1 (a) Taking the silicon bandgap as 1.12 eV, and assuming unity quantum efficiency as in Figs. 3.7 and 3.8, calculate the upper limit on the short circuit current density of a silicon solar cell at 300 K for the standard 'unnormalised' global AM1.5 spectrum supplied in tabulated form in Appendix B.
- (b) Given that, near operating temperatures, the silicon bandgap decreases by 0.273 mV/°C, calculate the normalised temperature coefficient of this current limit at 300 K

$$\frac{1}{I_{sc}} \frac{dI_{sc}}{dT}$$

- 3.2 (a) A silicon solar cell (bandgap 1.12 eV) is uniformly illuminated by monochromatic light of wavelength 800 nm and intensity 20 mW/cm². Given that its quantum efficiency at this wavelength is 0.80, calculate the short circuit current of the cell if its area is 4 cm².
- (b) For the same quantum efficiency, what would be the value of this current if the cell were made from a semiconductor of bandgap (i) 0.7 eV, (ii) 2.0 eV.
- (c) For the silicon cell of part (a), calculate the open circuit voltage, fill factor and energy conversion efficiency, given that its ideality factor is 1.2 and dark saturation current density is 1 pA/cm².
- (d) Estimate the range of values of (i) series resistance and (ii) shunt resistance that would cause a relative reduction in the fill factor and energy conversion efficiency of less than 5%.
- 3.3 (a) When the cell temperature is 300 K, a certain silicon cell of 100 cm² area has an open circuit voltage of 600 mV and a short circuit current of 3.3 A under 1 kW/m² illumination. Assuming that the cell behaves ideally, what is its energy conversion efficiency at the maximum power point?
- (b) What would be its corresponding efficiency if the cell had a series resistance of 0.1 Ω and a shunt resistance of 3 Ω?

Chapter 4 Cell Properties



Lab Efficiency ~ 24%
Commercial Efficiency ~ 14%

Lab processes are not commercially viable

$$C = \frac{\sum_t [(ACC_t + O \& M_t + FUEL_t)(1+r)^{-t}]}{\sum_t [E_t(1+r)^{-t}]} \quad (4.1)$$

C is Cost of Generated Electricity
ACC Capital Cost
O&M is Operating and Maintenance Cost
t is year
E is energy produced in a year
r is discount rate interest rate/(i.r. + 1)

$$C = \frac{\sum_t [(ACC_t + O \& M_t + FUEL_t)(1+r)^{-t}]}{\sum_t [E_t(1+r)^{-t}]} \quad (4.1)$$

C is Cost of Generated Electricity
 ACC Capital Cost
 O&M is Operating and Maintenance Cost
 t is year
 E is energy produced in a year
 r is discount rate interest rate/(i.r. + 1)

Increased Efficiency increases E and lowers C.
 Can also reduce ACC, Installation Costs, Operating Costs
 To improve C

For current single crystal or polycrystalline silicon technology
 Wafer costs account for 1/2 of the module cost.
 1/2 is marketing, shipping, assembly etc.

We can address technically only the efficiency E

Solar Cell Module Efficiency

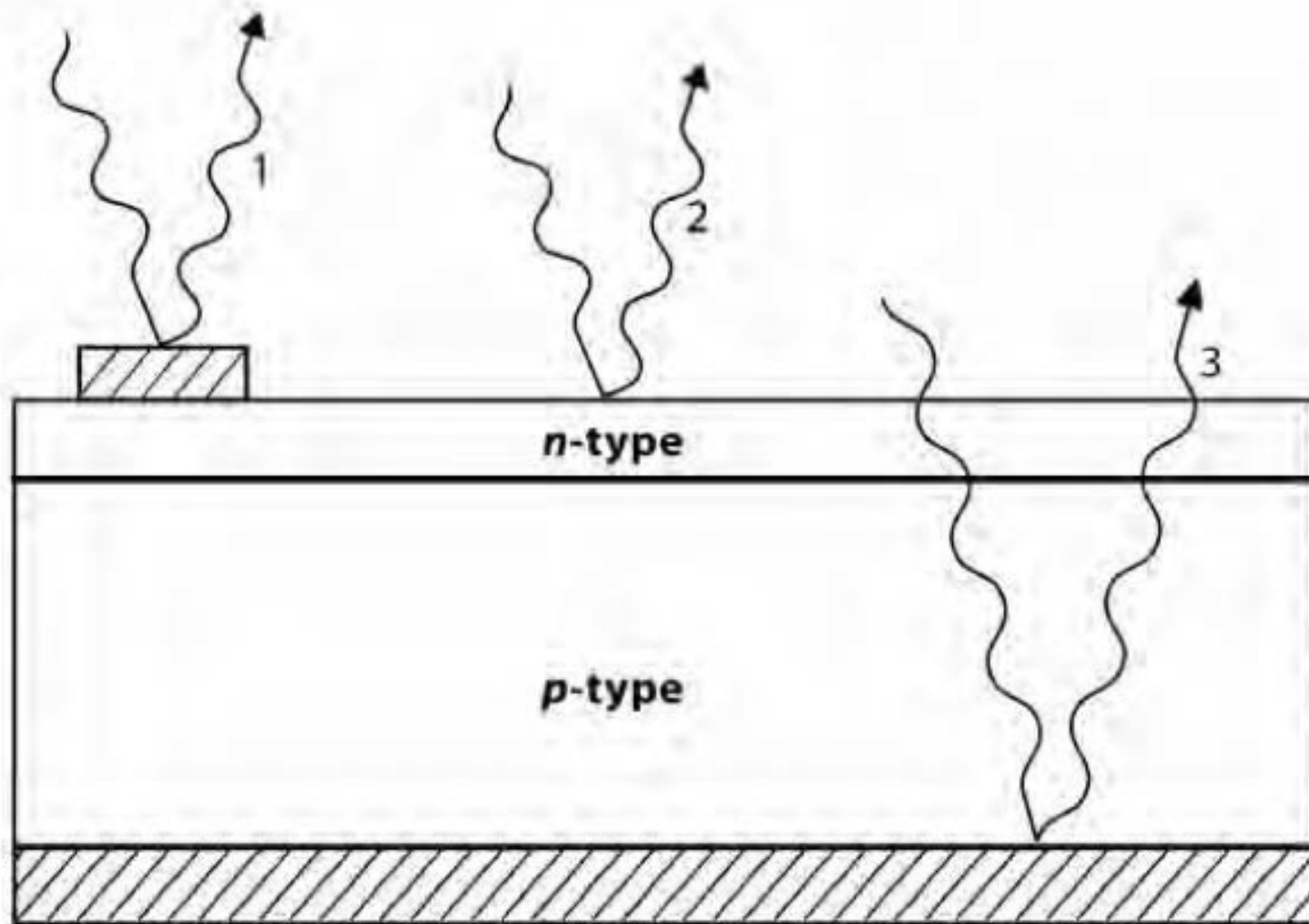


Figure 4.1. Sources of optical loss in a solar cell. (1) Blocking by top contact coverage. (2) Surface reflection. (3) Rear contact reflection.

- 1) Minimize surface contact area
(increases series resistance)
- 2) Antireflection coatings
1/4 wave plate
transparent coating of thickness d
and refractive index n_1
 $d_1 = \lambda_0 / (4n_1)$
 $n_1 = \text{sqrt}(n_0 n_2)$
- 2) Surface Texturing
Encourage light to bounce
back into the cell.
- 3) Absorption in rear cell contact.
Desire reflection but at
Random angle for internal
reflection

Optical Losses Due to Reflection

$$d_1 = \lambda_0 / (4n_1)$$

$$n_1 = \sqrt{n_0 n_2}$$

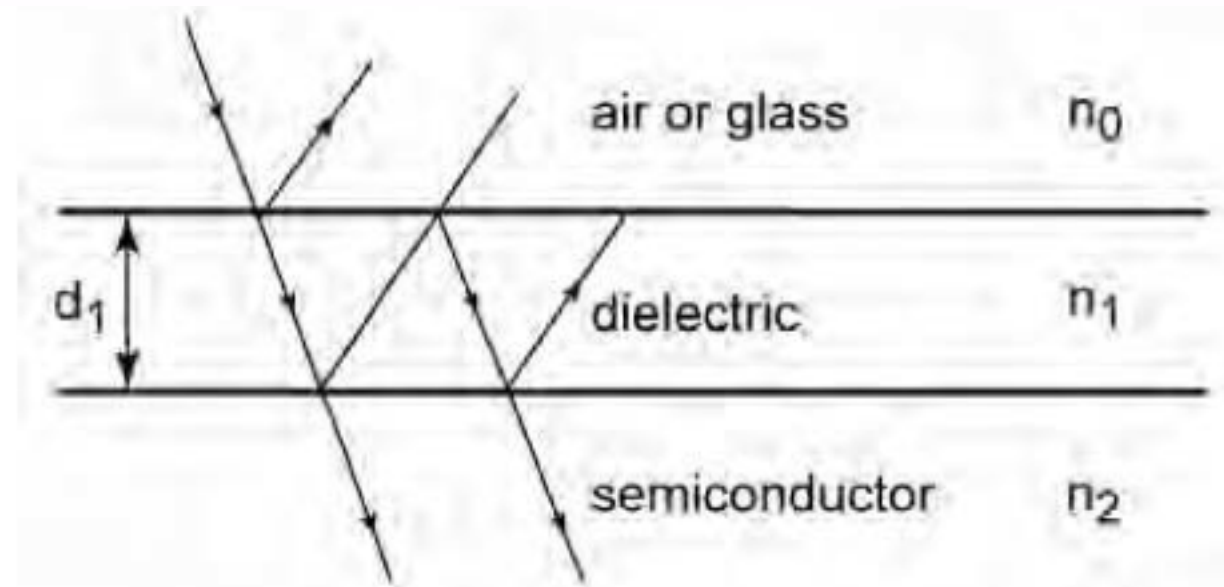


Figure 4.2. Use of a quarter wavelength antireflection coating to counter surface reflection.

An additional benefit of roughened or textured surfaces is that light is obliquely coupled into the silicon in accordance with Snell's law, as given by

$$n_1 \sin \theta_1 = n_2 \sin \theta_2 \quad (4.4)$$

where θ_1 and θ_2 are the angles for the light incident on the interface relative to the normal plane of the interface within the mediums with refractive indices n_1 and n_2 respectively.

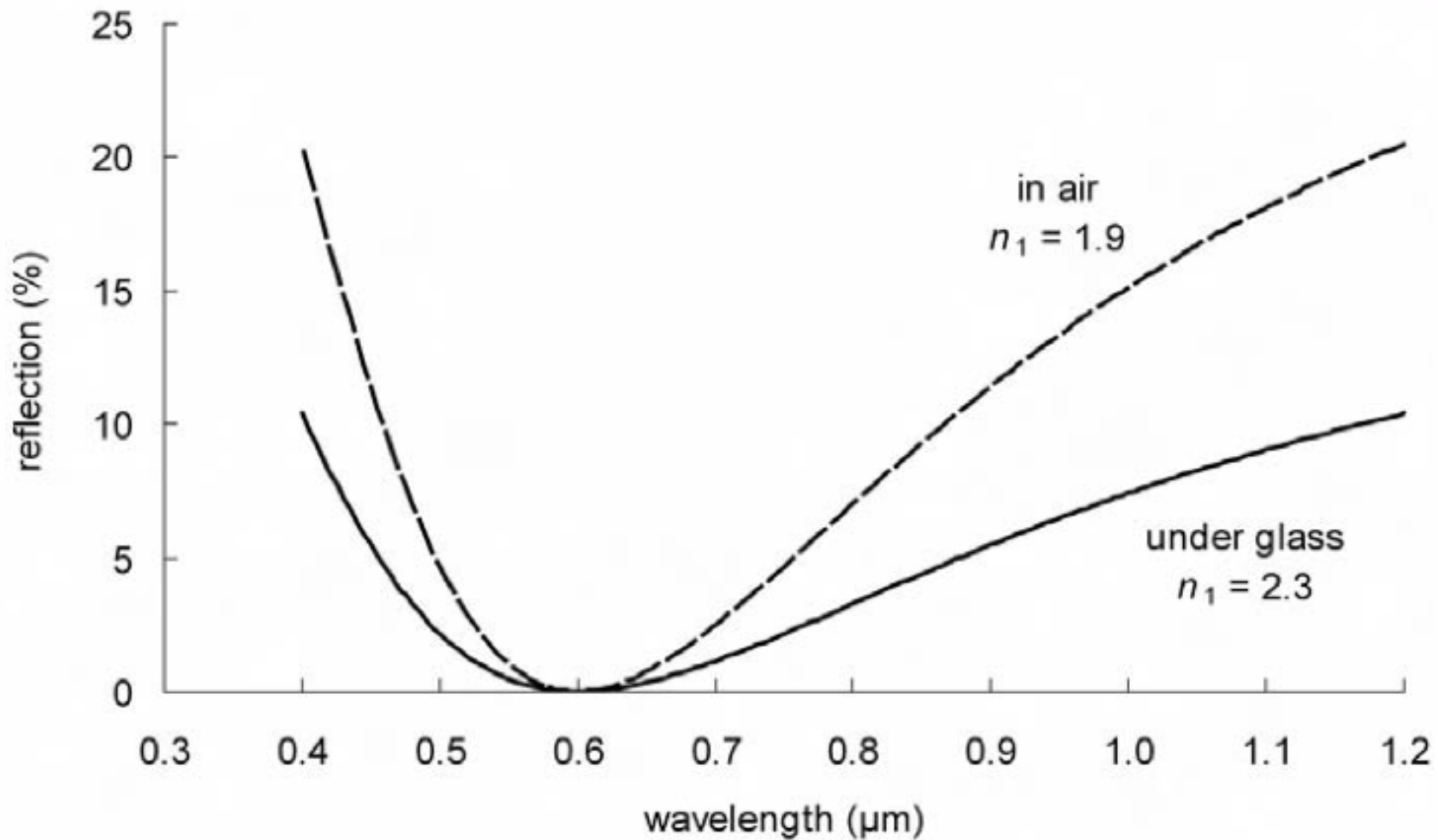


Figure 4.3. Surface reflection from a silicon cell ($n_2 = 3.8$) in air ($n_0 = 1$) and under glass ($n_0 = 1.5$) with an antireflection coating with refractive index and thickness chosen so as to minimise reflection for 0.6 μm wavelength light.

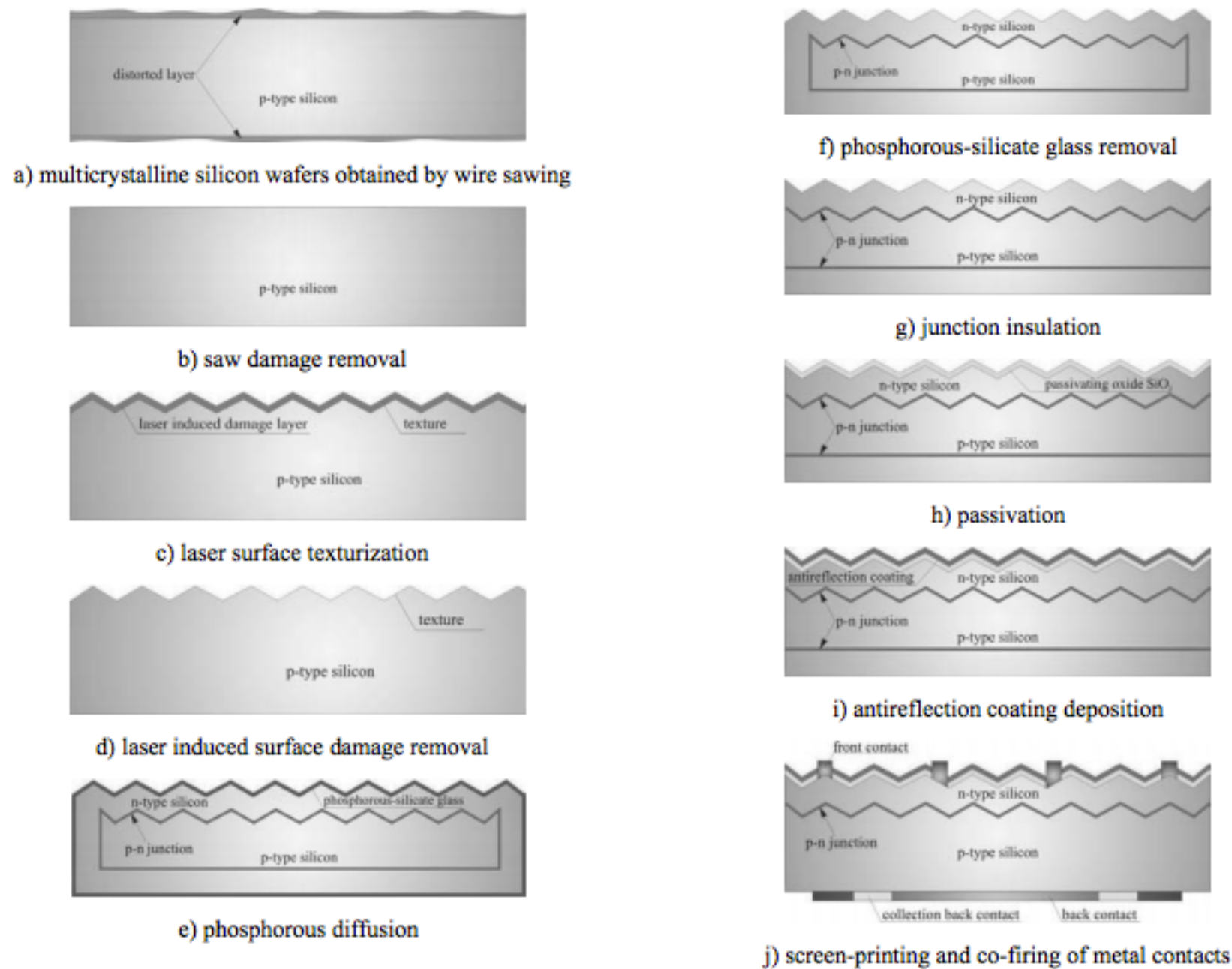


Fig. 1. Applied technology of multicrystalline silicon solar cells

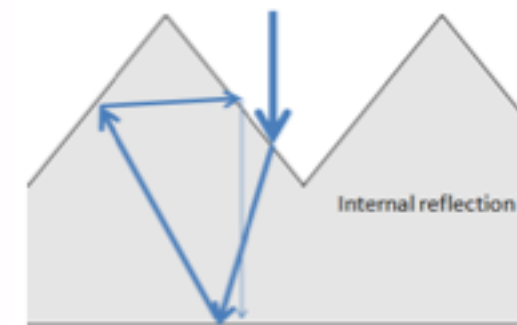


Figure 1: Drawing of a surface textured thin film with incident light entering and internally reflecting due to snell's law.

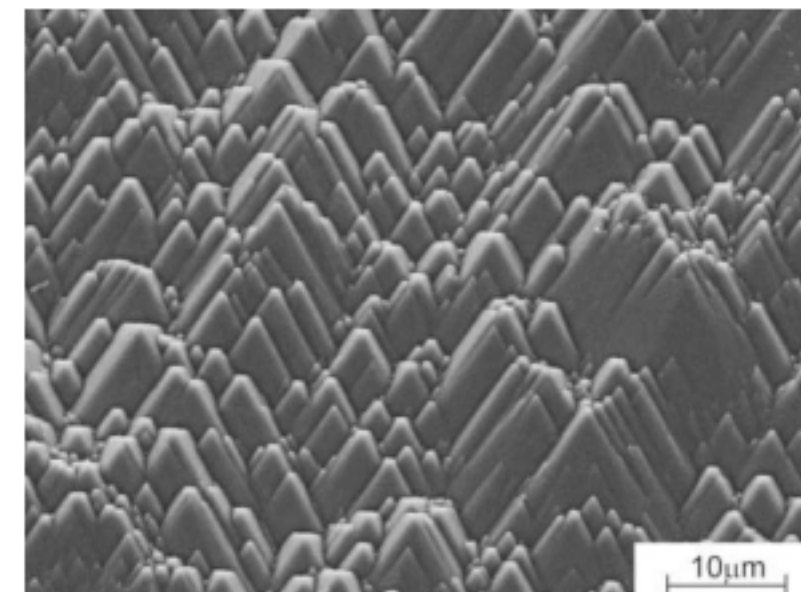


Fig. 2. SEM micrograph of texture formed on (100) silicon surface by etching with 40 % KOH:IPA:DIH₂O and volume ratio 1:3:46 in 15 minutes at temperature 80°C

Dobrzanski, Drygala, *Surface Texturing in Materials and Manufacturing Engineering*, J.Ach. In Mat.And Manuf. Eng. **3** | 77-82 (2008).

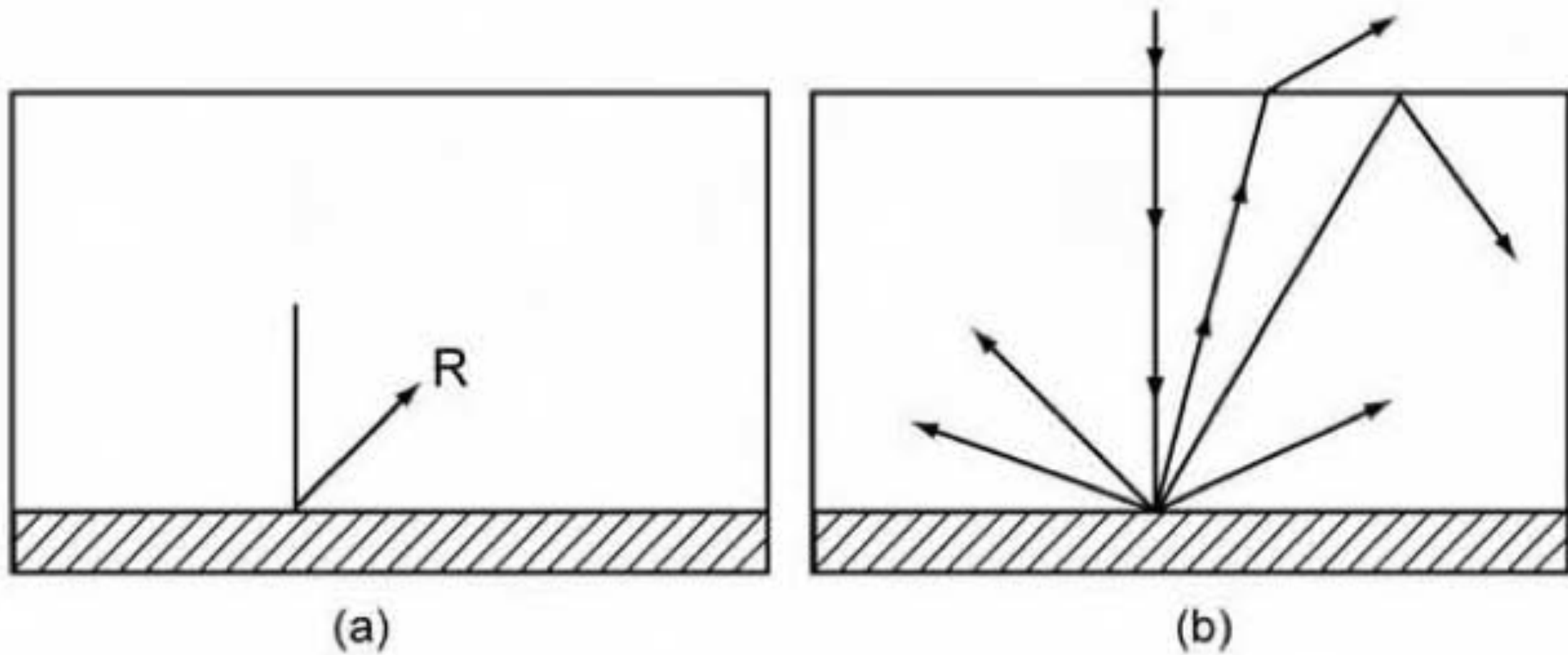


Figure 4.6. (a) Reflection from a rear surface. (b) Randomised reflection resulting in light trapping.

Reduce recombination at contacts by heavily doping near contacts

The efficiency of utilising light of higher wavelengths—the red response—can be improved by adding a *back surface field* (BSF) to the cell, as a means of reducing back surface recombination velocity. This is typically achieved by including a heavily-doped region, such as a screen printed layer of aluminium, at the back of the cell. The interface between this layer and the relatively lightly-doped bulk region of the cell acts as a low recombination velocity surface. A schematic diagram of a BSF is given in Fig. 4.7.

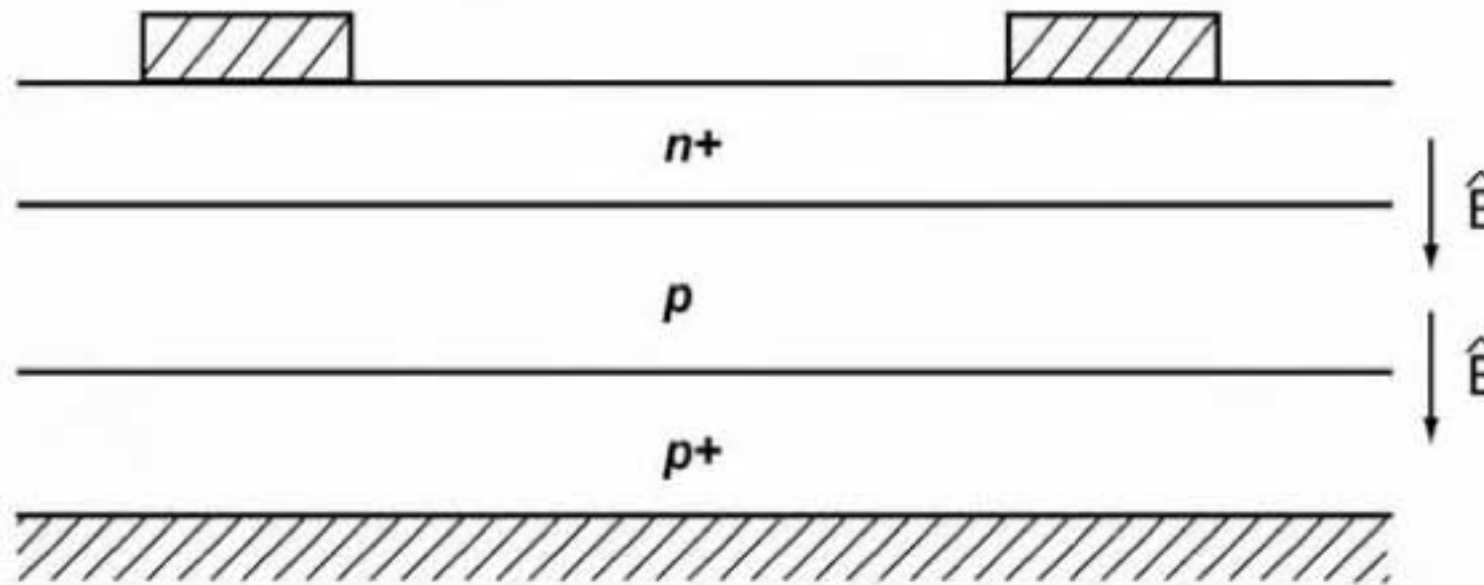


Figure 4.7. Use of a back surface field to reduce rear surface recombination velocities.

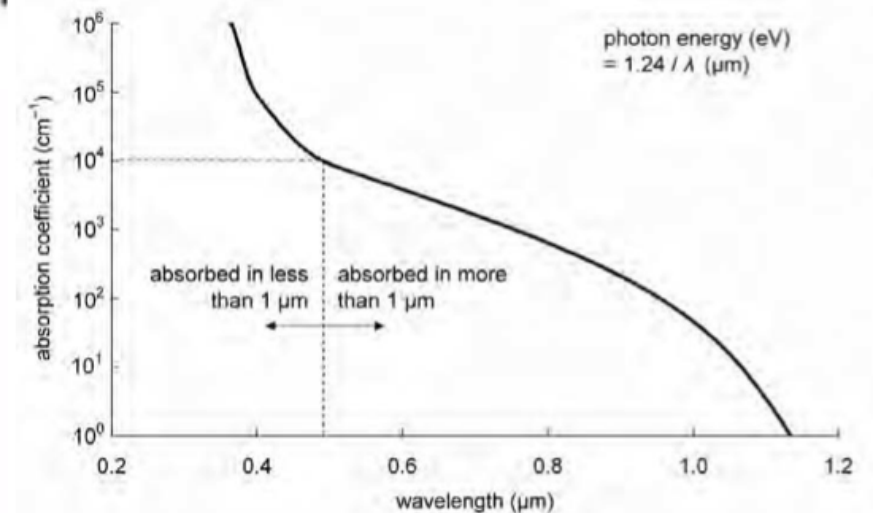


Figure 2.8. The absorption coefficient, α , of silicon at 300 K as a function of the vacuum wavelength of light.

Recombination Losses

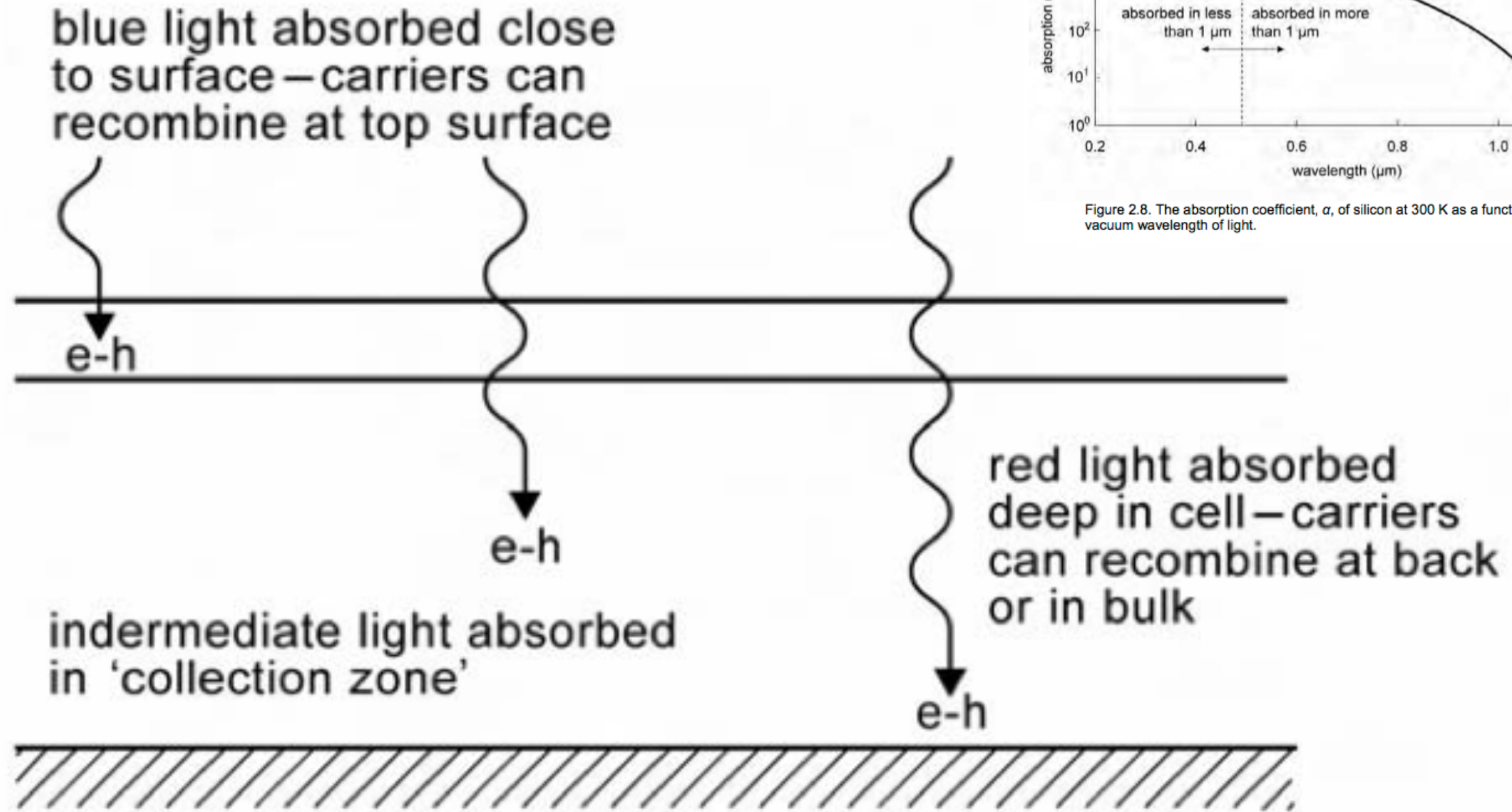


Figure 2.8. The absorption coefficient, α , of silicon at 300 K as a function of the vacuum wavelength of light.

Figure 4.8. Possible sites for recombination of e-h pairs within a PV cell.

Recombination Losses

Recombination can occur via several mechanisms:

1. **Radiative recombination**—the reverse of absorption. Electrons in a high energy state return to a lower energy state, with the release of light energy. This form of recombination is used for semiconductor lasers and light emitting diodes, but is not particularly significant for silicon solar cells.
2. **Auger recombination**—the reverse of ‘impact ionisation’ (Hu & White, 1983). An electron recombining with a hole gives up the excess energy to another electron, which then relaxes back to its original energy state, releasing phonons. Auger recombination is particularly effective in relatively highly-doped material, becoming the dominant recombination process when impurity levels exceed 10^{17} cm^{-3} .
3. **Recombination through traps**—This can occur when impurities in the semiconductor or interface traps at the surfaces give rise to allowed energy levels in the otherwise forbidden energy gap. Electrons can thus recombine with holes in a two-stage process, first relaxing to the defect energy level, then to the valence band.

Recombination Losses

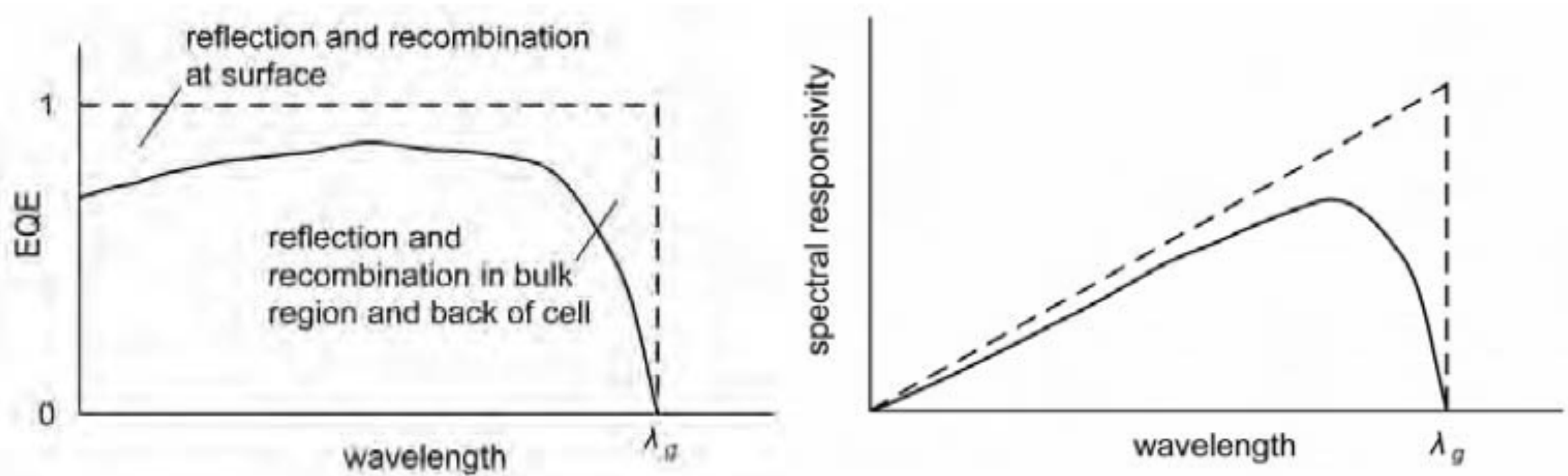


Figure 4.9. Typical external quantum efficiency and responsivity in actual solar cells, illustrating the impact of optical and recombination losses.

To convert from responsivity (R_λ , in A/W) to QE_λ ^[5] (on a scale 0 to 1):

$$QE_\lambda = \frac{R_\lambda}{\lambda} \times \frac{hc}{e} \approx \frac{R_\lambda}{\lambda} \times (1240 \text{ W} \cdot \text{nm/A})$$

where λ is in nm, h is the Planck constant, c is the speed of light in a vacuum, and e is the elementary charge.

4.4 TOP CONTACT DESIGN

Metallic top contacts are necessary to collect the current generated by a solar cell. *Busbars* are connected directly to the external leads, while *fingers* are finer areas of metallisation that collect current for delivery to the busbars. A simple top contact design is shown in Fig. 4.10. Top contact design aims to optimise current collection against losses owing to internal resistances and cell shadowing.

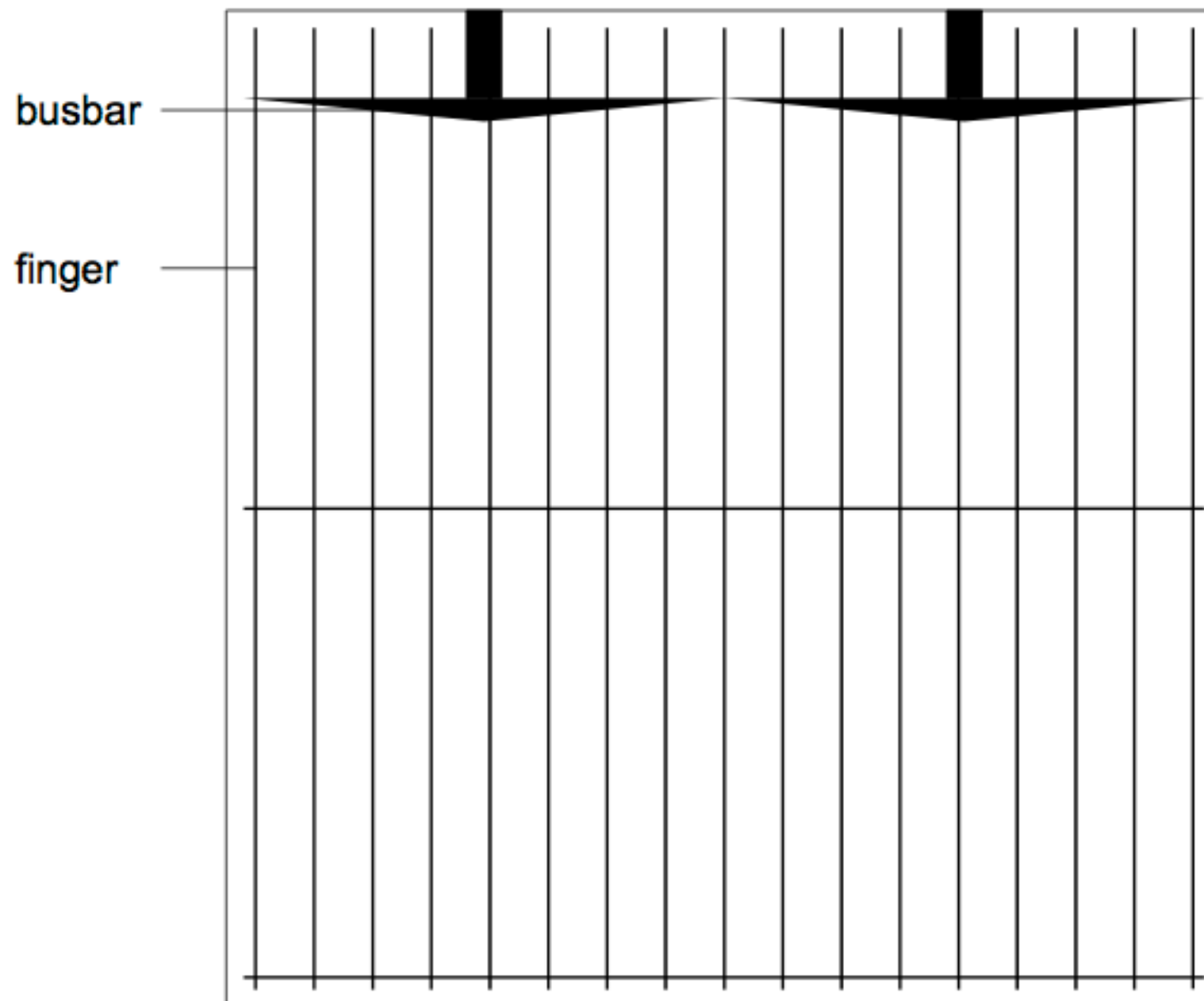
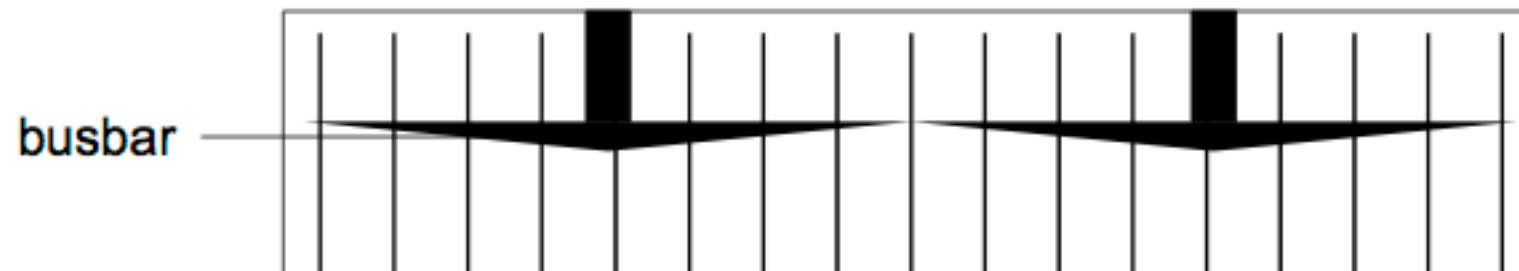


Figure 4.10. Top contact design of a solar cell.

4.4 TOP CONTACT DESIGN

Metallic top contacts are necessary to collect the current generated by a solar cell. *Busbars* are connected directly to the external leads, while *fingers* are finer areas of metallisation that collect current for delivery to the busbars. A simple top contact design is shown in Fig. 4.10. Top contact design aims to optimise current collection against losses owing to internal resistances and cell shadowing.



In brief, it can be shown (Serreze, 1978) that:

1. The optimum width of the busbar (W_b) occurs when the resistive loss in the busbar equals its shadowing loss.
2. A tapered busbar has lower losses than a busbar of constant width.
3. The smaller the unit cell, the finger width (W_f) and the finger spacings (s), the lower the losses.

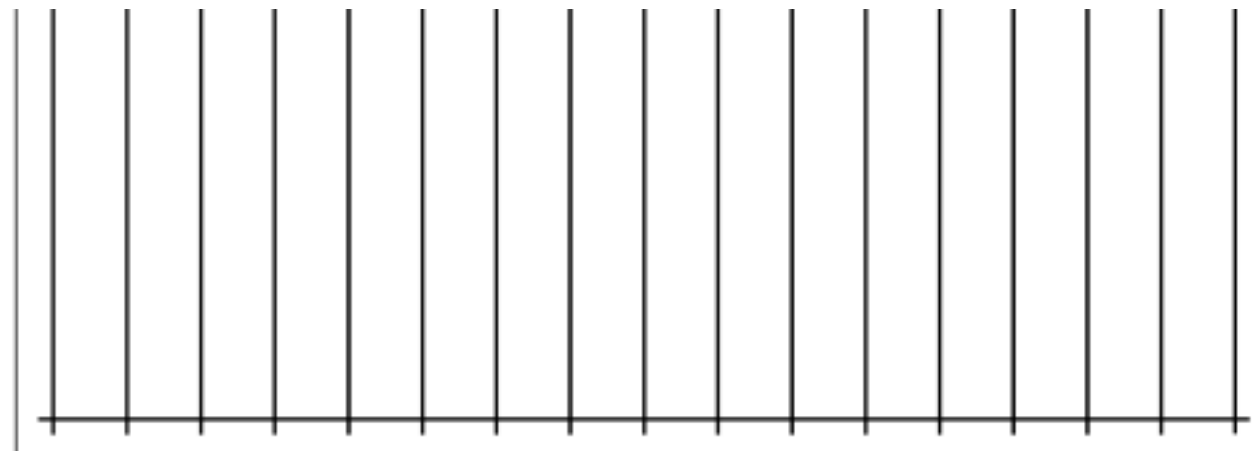


Figure 4.10. Top contact design of a solar cell.

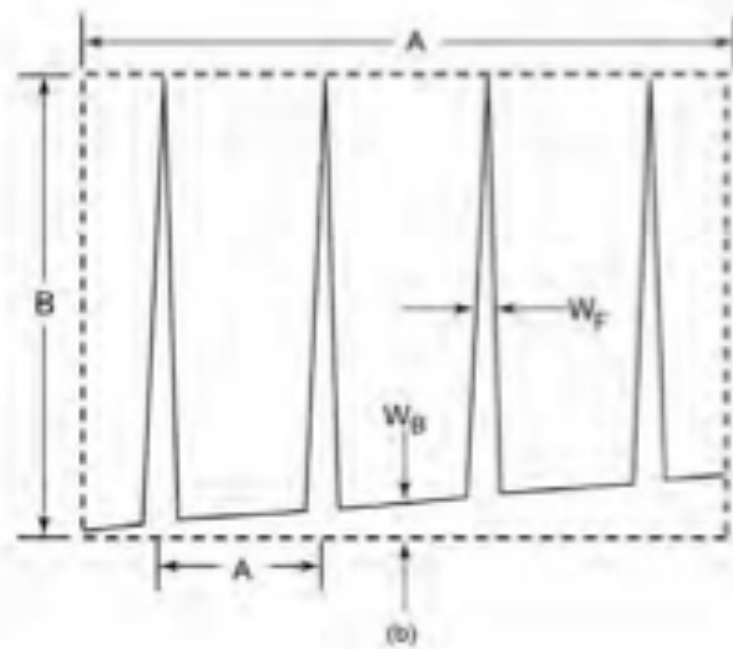
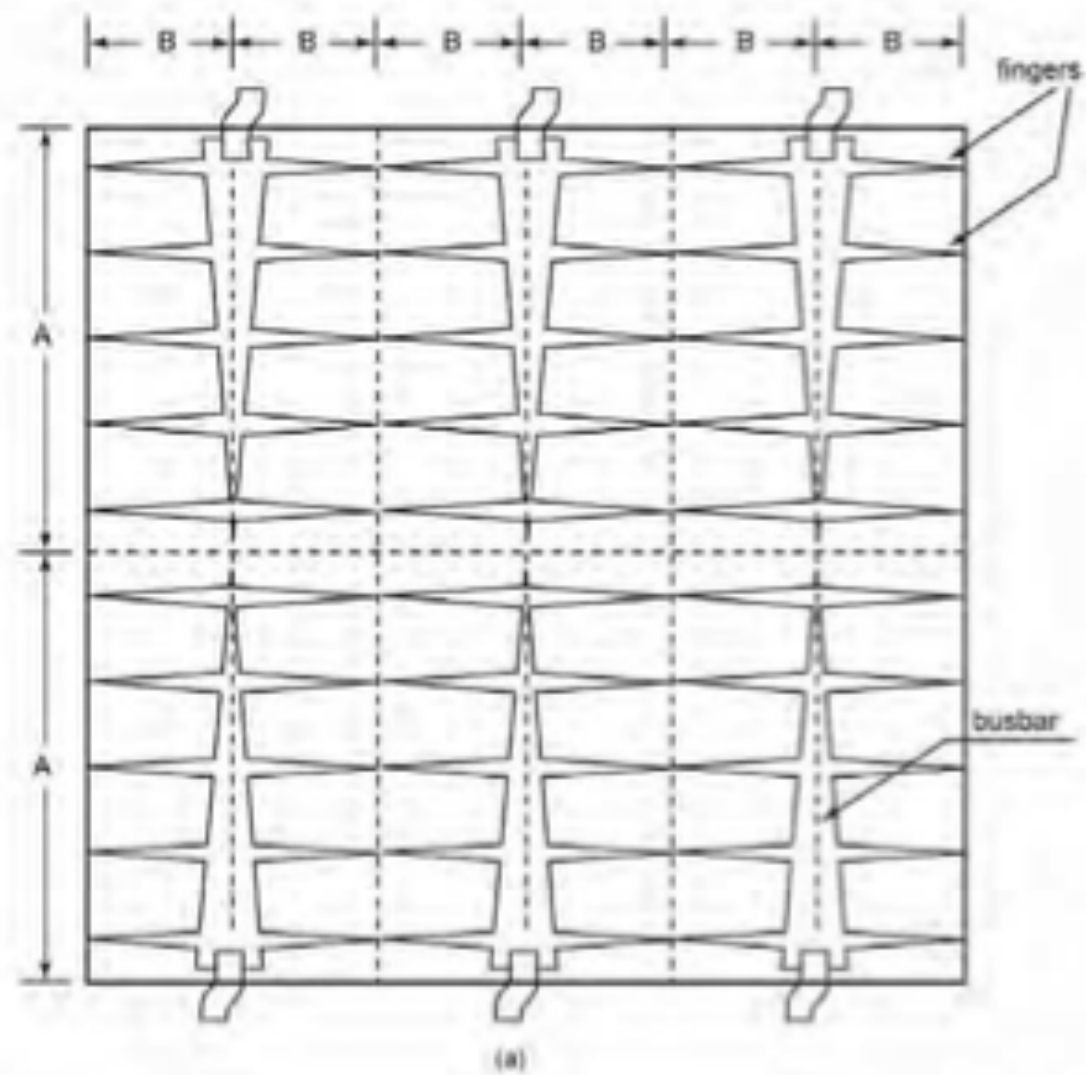


Figure 4.14. (a) Schematic of a top contact design showing busbars and fingers. (b) Important dimensions of a typical unit cell (©1978 IEEE, Serreze).

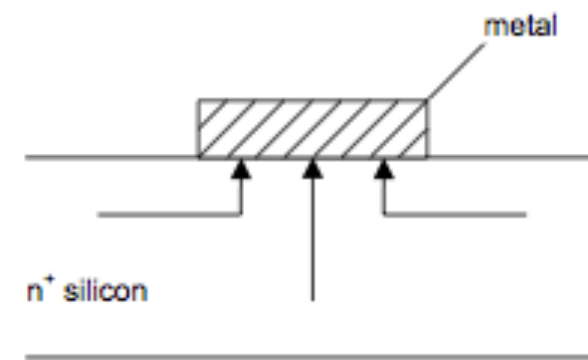


Figure 4.15. Points of contact resistance losses, at interface between grid lines and semiconductor.

Bulk & Sheet Resistivity

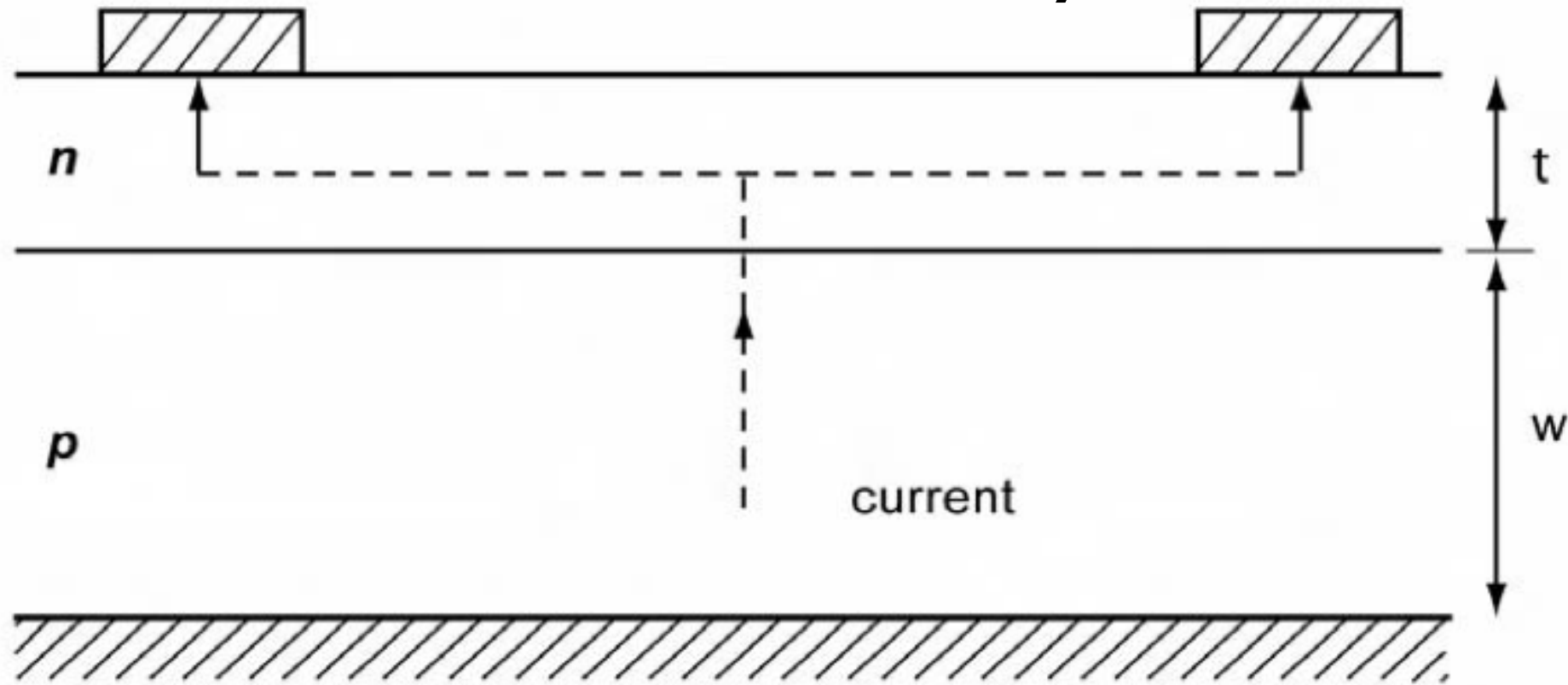


Figure 4.11. Current flow from point of generation to external contact in a solar cell.

Sheet Resistivity

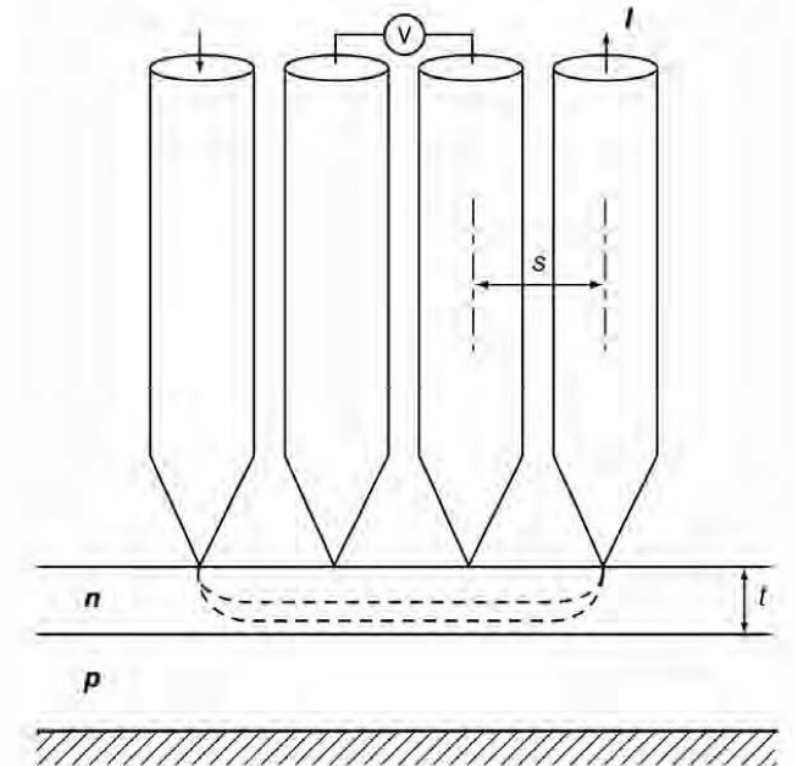
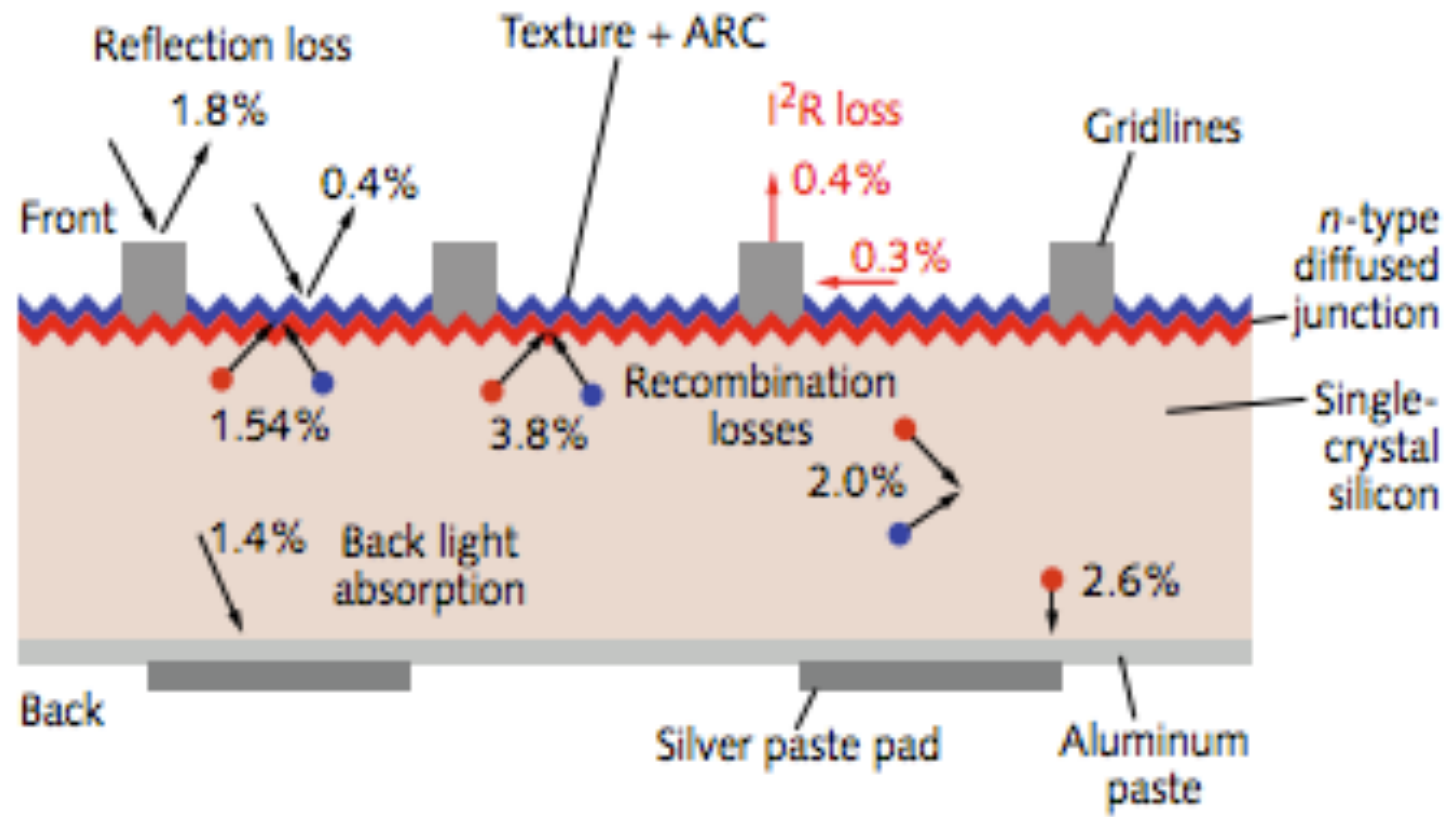


Figure 4.12. Use of a four point probe to measure the sheet resistivity of a solar cell.

Eglash, *Competition improves silicon-based solar cells*, *Photovoltaics* December, 38-41 (2009).

FIGURE 1. A generic solar cell has multiple loss mechanisms (losses shown are a percentage of the incident radiation). This device exhibits an efficiency of 14% to 15% and was the mainstay of the solar industry for several years. (Courtesy of SunPower)



Limit cell efficiency	29%
Total losses	-14.3%
Generic cell efficiency	14.7%

The highest efficiency

The conversion efficiency of a solar cell is limited by optical absorption, carrier transport, and carrier collection. For a silicon solar cell the maximum theoretical efficiency is 29%, limited by losses due to the excess energy of above-bandgap photons, transparency to photons below the bandgap, and radiative and Auger recombination. In practice, solar cells exhibit a much lower efficiency due to additional losses. It is only by understanding and reducing these losses that more-efficient solar cells can be developed.

SunPower San Jose, CA
20% efficiency from Czochralski silicon

Eglash, *Competition improves silicon-based solar cells*, *Photovoltaics* December, 38-41 (2009).

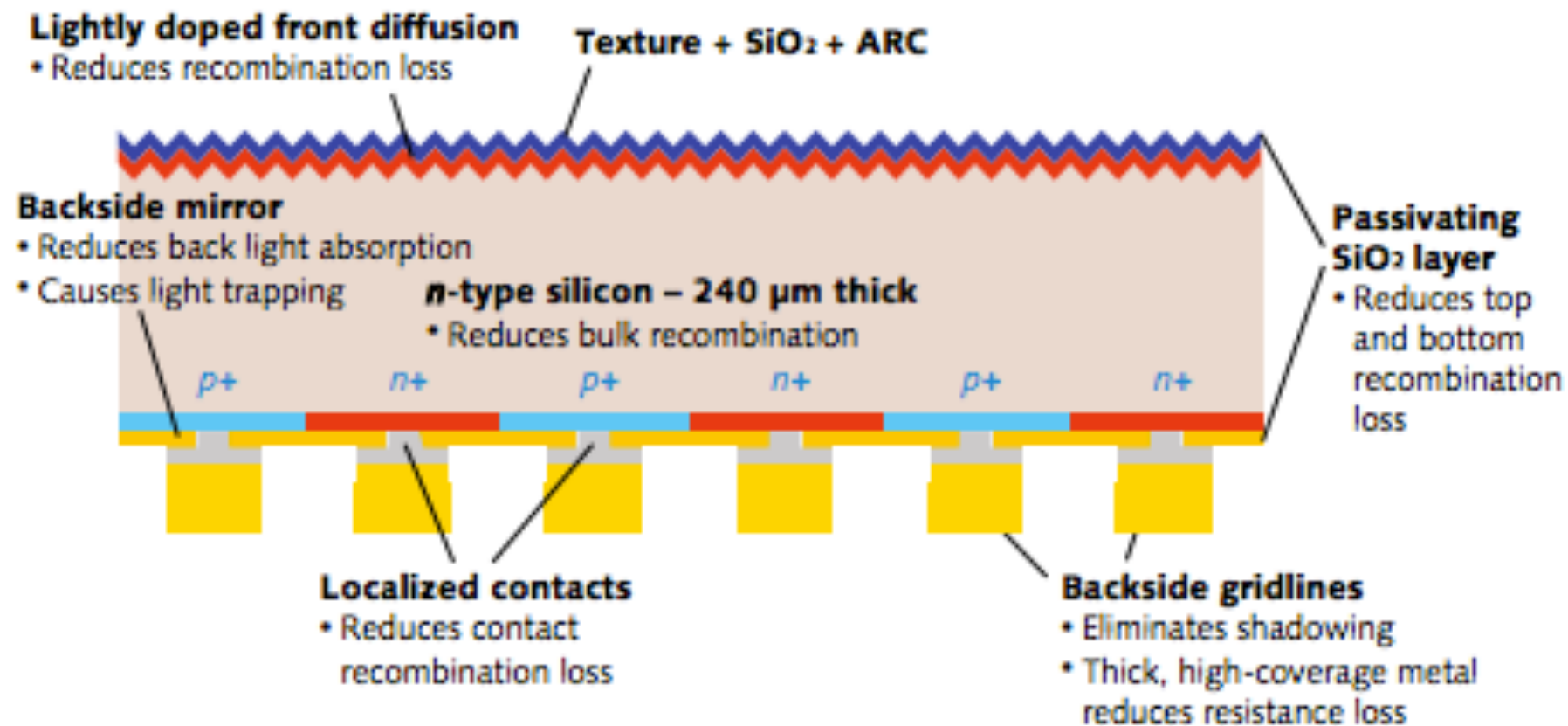


FIGURE 2. SunPower's backside contact cell is the result of implementing a wide range of high-efficiency concepts in a high-volume process to achieve a cell efficiency of 24%. (Courtesy of SunPower)

The lowest cost per watt

Suntech has taken a decidedly different approach. Historically Suntech has focused on achieving the lowest manufacturing cost per wafer by emphasizing process development, manufacturability, yield, uniformity, and reproducibility. But cost and efficiency must both be optimized to achieve the lowest cost per watt or cost per kilowatt-hour. Six years ago Suntech launched a collaboration with the University of New South Wales (UNSW; Sydney, Australia). The UNSW had achieved record efficiencies in laboratory-scale devices. Suntech wanted to know whether the high-efficiency concepts from UNSW could be applied to high-volume production at Suntech without adding significant cost.

Suntech, Wuxi, China
multi crystalline cast silicon
Efficiency 16.5%
Cost \$1.50 per watt

Eglash, *Competition improves silicon-based solar cells*, *Photovoltaics* December, 38-41 (2009).

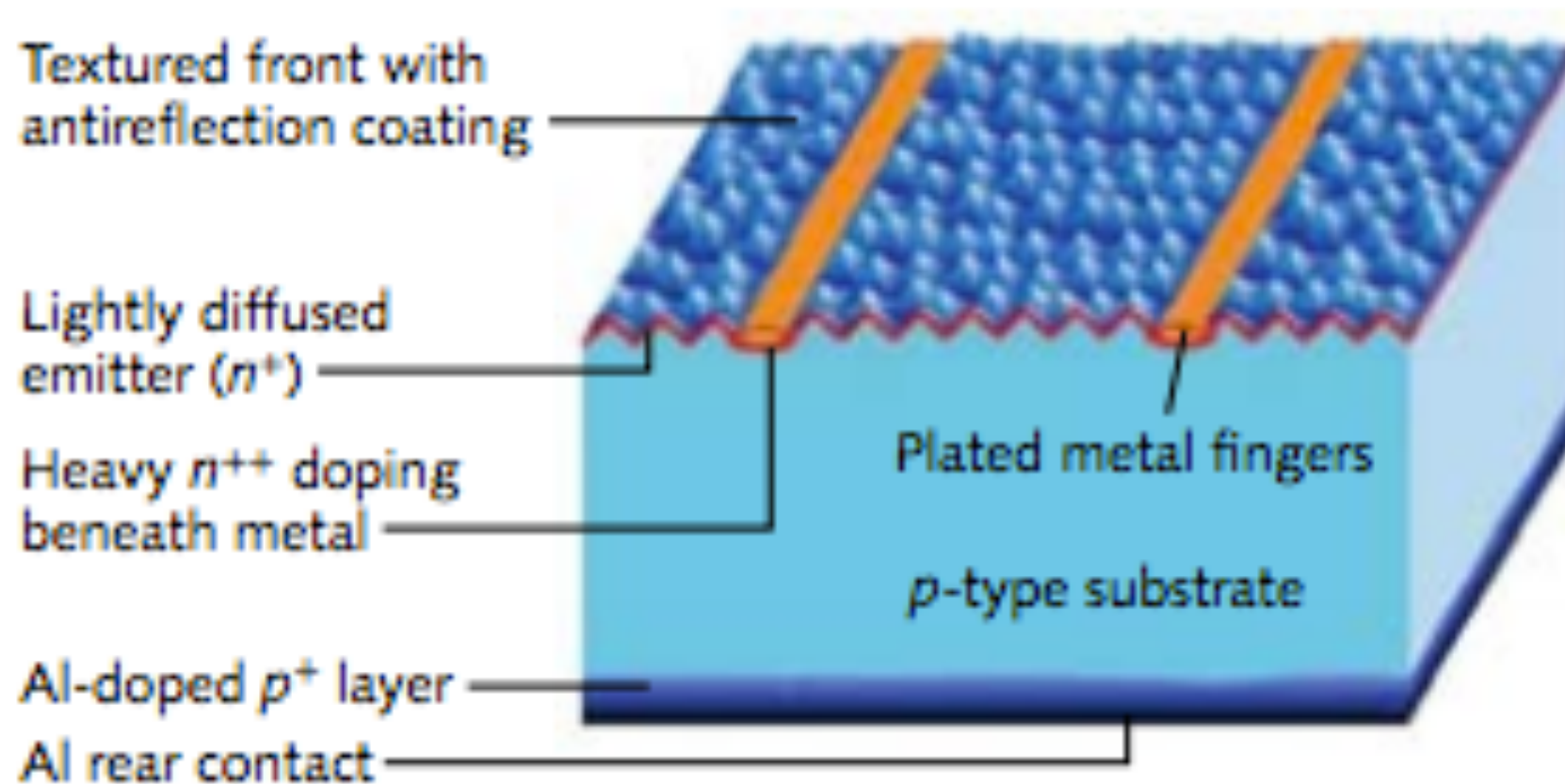


FIGURE 3. Suntech's high-efficiency and low-cost cell is based on the record-setting PERL cell developed at the University of New South Wales. This device incorporates front metal lines less than $25\ \mu\text{m}$ wide and screen-printed and fired rear aluminum contacts. (Courtesy of Suntech)

